VIRGINIA'S LAND-GRANT UNIVERSITY

VIRGINIA POLYTECHNIC INSTITUTE AND STATE UNIVERSITY

Blacksburg, Virginia 24061

GRADUATE SCHOOL

NOTE:

This dissertation does Not meet the required format as specified by the Graduate School. However, it is being accepted as an EXCEPTION to the general policy because of the complexity and neatness of the equations contained therein and the late date to demand a retype and duplication. This exception should not be construed by others that they should attempt a similar presentation prior to checking with their committee and the appropriate person(s) in the Graduate School office.

Fred W. Bull, Dean

Fred W. Bull

IN-PLANE VIBRATION OF A PLATE HAVING AN ELLIPTICAL HOLE OF ARBITRARY ECCENTRICITY

by

Robert F. Cooke

Dissertation submitted to the Graduate Faculty of the
Virginia Polytechnic Institute and State University
in partial fulfillment of the requirements for the degree of
DOCTOR OF PHILOSOPHY
in
Engineering Science and Mechanics

APPROVED:

Dr. H. Johnson, Chairman

Dr. R. Heller

Dr. E. G. Henneke

Dr. G. W. Swift

Dr. J. E. Kaiser

April, 1975

Blacksburg, Virginia

ACKNOWLEDGEMENTS

The author wishes to express his gratitude to Dr. Johnson for his advice and gentle coaching which contributed immeasurably to this thesis. The author also wishes to express his appreciation to the other members of the committee for their helpful suggestions and to the Department of Engineering Science and Mechanics for encouraging this investigation. The author thanks his wife Ronna, son Steven, and daughter Laura for their patience and encouragement in all his endeavors.

TABLE OF CONTENTS

LIST OF TABLES

LIST OF FIGURES

LIST OF SYMBOLS

C	C_R/C_S
C_P	dilatational wave speed
C_R	Rayleigh wave speed
C_S	shear wave speed
D	$1 - 2m\,\mathrm{Cos}(2\eta) + m^2$
L_1, L_2	differential operators
$\hat{R}$	mapping function scale factor
R_o	radius of remote boundary
U	$u + iv$
X, Y, t	space, time coordinates
Z	$x + iy = Re^{i\theta}$
$\overline{Z}$	denotes complex conjugate of Z
Re[Z]	denotes real part of Z
Imag[Z]	denotes imaginary part of Z
a	characteristic length, e.g., crack length
i	$\sqrt{-1}$
m	eccentricity parameter
u, v	x,y components of displacement
$w(\zeta)$	mapping function
x, y, τ	nondimensional space, time coordinates
α	separation constant (Chapter 2)
α	angle of normal (Chapter 3)
δ	$[C_S/C_P]^2$

γ	eigenvalue
λ	$\sqrt{\delta}\ \gamma$
λ	Lame' constant
μ	Lame' constant
ν	Poisson's ratio
ν	integer
ϕ	Lame' function
ψ	Lame' function
Φ	complex potential $\phi + i\psi$
$\sigma_{xx}, \sigma_{xy}, \sigma_{yy}$	stress components
ξ, η	coordinates in image plane
ζ	$\xi e^{i\eta}$
ξ, η	dummy parameter
$\doteq$	denotes approximately equal to

1. INTRODUCTION

1.1 Foreword

This thesis was motivated by the observations of many researchers [1]*, [2], [3] that microcracks often appear in the vicinity of a main crack and that coalescence of microcracks is one mechanism of crack growth.

> There are two modes of crack growth reported so far. One is the crack tip opening and closing and the other is the coalescence of microcracks or voids with the main crack. [4]

The origin or cause of these microcracks does not seem to be known, although it is widely supposed that they are a result of micro-flaws due to manufacture. This thesis will investigate an alternate possibility; that the microcracks are caused by standing waves whose wavelength is the same order of magnitude as the length of the main crack. As an analogy we have the Sommerfeld diffraction problem which shows concentrations of light intensity at discrete points away from the aperture [5, p. 576]. For our problem we anticipate analogous time varying stress concentrations which would cause fatigue and perhaps nucleate microcracks.

---

*Numbers in brackets [ ] refer to references at the end of each chapter and on pages 176 to 181

1.2 Mathematical Statement of the Problem

We consider the inplane vibration of a plate with an elliptic hole. It is assumed that the dimensions of the plate are large compared to the size of the hole. The boundary conditions at infinity are not prescribed a'priori but are a property of the solution in which we have some latitude of interpretation.

Let u, v denote the X, Y displacements respectively and introduce the Lame' wave potentials [6, p. 186] by

$$u(X,Y,t) = \left[\frac{\partial}{\partial x}\phi(x,y) + \frac{\partial}{\partial y}\psi(x,y)\right] \mathrm{Cos}(\tau) \qquad (1.1a,b)$$

$$v(X,Y,t) = \left[\frac{\partial}{\partial y}\phi(x,y) - \frac{\partial}{\partial x}\psi(x,y)\right] \mathrm{Cos}(\tau)$$

where x,y,τ are nondimensional space, time coordinates given by

$$x = X/a$$

$$y = Y/a$$

$$\tau = \frac{\gamma\, C_S}{a}\, t$$

where X,Y,t are dimensional coordinates

a = characteristic length, e.g., crack length

γ = separation constant or eigenvalue

C_S = shear wave speed

We will restrict our attention to symmetrical displacements of Mode I type, i.e.,

u = odd in x, even in y

v = even in x, odd in y

then

$$\phi = \text{even in both } x,y$$
$$\psi = \text{odd in both } x,y \qquad (1.2a,b)$$

Substitution for u,v into the equilibrium equation gives the field equations

$$[\nabla^2 + \delta\,\gamma^2]\phi = 0$$
$$[\nabla^2 + \gamma^2]\psi = 0 \qquad (1.3a,b)$$

where $$\delta = \left(\frac{C_S}{C_p}\right)^2 = \frac{\mu}{\lambda + 2\mu} = \frac{1 - 2\nu}{2 - 2\nu} \qquad (1.4)$$

C_S = shear wave speed [6, p. 186]

C_p = dilatational wave speed

λ,μ = Lame's constants [6, p. 129]

ν = Poisson's ratio

Since $\frac{1}{4} < \nu \leq \frac{1}{2}$ for most engineering materials, we find that

$$0 \leq \delta < \frac{1}{3}$$

It was found that δ in this range had only a small effect on the results. Results will be reported only for $\delta = \frac{1}{4}$ which corresponds to

$$\nu = \frac{1}{3}$$

$$C_p = 2\,C_S$$

It is interesting to note that the inverse of δ

$$\nu = \frac{1 - 2\delta}{2 - 2\delta}$$

has the same form as δ.

Introducing the complex variables

$$Z = x + iy$$

$$\Phi = \phi + \psi \quad = \text{Complex potential}$$

$$U = u + iv \quad = \text{Complex displacement}$$

$$= 2\frac{\partial \overline{\Phi}}{\partial \overline{Z}}$$

gives $$-\frac{1}{2\mu}[\sigma_{yy} + \sigma_{yy}] = (1 - \delta)\gamma^2 \operatorname{Re} \Phi$$

$$-\frac{1}{2\mu}[\sigma_{yy} - \sigma_{xx} + 2i\sigma_{xy}] = 4\frac{\partial^2}{\partial Z^2}\Phi$$

Using [7, p. 271]

$$2[N - iT] = \sigma_{xx} + \sigma_{yy} - [\sigma_{yy} - \sigma_{xx} + 2i\sigma_{xy}]e^{2i\alpha}$$

with

$$e^{2i\alpha} = -dZ/d\overline{Z}$$

gives the boundary condition

$$4\frac{\partial^2}{\partial Z^2}\Phi + (1 - \delta)\gamma^2 \operatorname{Re}[\Phi]\, d\overline{Z}/dZ = 0 \text{ on } S \qquad (1.5)$$

For the case of a slit $d\overline{Z}/dZ = 1$ on S

and

$$\frac{\partial^2\phi}{\partial x^2} + \frac{1}{2}\gamma^2\phi + \frac{\partial^2\psi}{\partial x\partial y} = 0$$

$$\frac{\partial^2\psi}{\partial x^2} + \frac{1}{2}\gamma^2\psi - \frac{\partial^2\psi}{\partial x\partial y} = 0 \qquad \text{on } S$$

The symmetry conditions (1.2), field equations (1.3), and boundary conditions (1.5) comprise the mathematical statement of the problem.

1.3 Thesis Outline

The thesis consists of three separate and independent analyses of the problem, each of which has certain advantages and disadvantages.

Chapter II is an analysis for the case of a slit by Dual Pair of integral equations.

Chapter III is analysis for arbitrary eccentricity. New techniques are presented for the analysis of wave equations with boundary conditions on an elliptical surface by perturbation and numerical methods. The results of Viktorov [8] for the circle case will be extended and the location of turning points determined. It will be shown that the tendency is to have repeated eigenvalues and multiple eigenvectors, and that the eigenvector is very sensitive to small changes in the eccentricity of the boundary ellipse. Contour plots of stresses, etc., are presented. A discussion of experimental methods to generate and detect standing surface waves of high frequency is included.

Chapter IV summarizes the results and conclusions of the previous chapters and the relative advantages of each method of analysis.

Appendix A contains a formulation of the problem analogous to the method of Muskhelishvili.

In summary, an explanation for the origin of microcracks is presented and the parametric dependence of the eigensolution is related to

1) void size

2) eccentricity

3) Poisson's ratio

4) crystal size

Also, new techniques for the representation and numerical solution of the wave equation with boundary conditions on an ellipse are presented.

Chapter 1 Literature Cited

1. Van Elst, H. C., "The Intermittent Propagation of Brittle Fracture," Personal Communication, Dynamic Crack Conf., Lehigh Univ., July, 1972.

2. Dvorak, G. J., Dynamic Crack Conf., Lehigh Univ., July, 1972.

3. Freudenthal, A. M., Columbia Univ. Tech. Report No. 28, June, 1965, Figures 2a, b.

4. Koterazawa, R., et al., "Fractographic Study of Fatigue Crack Propagation," ASME J. Eng. Mat. & Tech., Vol. 95, Series H, No. 4, Oct., 1973.

5. Born, M., and Wolf, E., Principles of Optics, Pergamon, 1970.

6. Fung, Y. C., Foundations of Solid Mechanics, Prentice-Hall, 1965.

7. Sokolnikoff, I. S., Mathematical Theory of Elasticity, Noordhoff, 1963.

8. Viktorov, I. A., "Rayleigh-Type Waves on a Cylindrical Surface," Soviet Physics Acoustics, V. 4, 1958, pp. 131-136.

CHAPTER 2

DUAL PAIR OF INTEGRAL EQUATIONS

Table of Contents

Introduction

For the case of a slit the boundary conditions are on the X-axis. Representation of the solutions of the reduced wave equation in Cartesian coordinates leads to three boundary conditions to be satisfied. Two of these are mixed in the sense that they only hold for a portion of the X-axis, and lead to a Dual Pair of integral equations of standard form. Integral transforms reduce the Dual Pair to a Fredholm integral equation of the second kind in which the kernel is nonlinear in the eigenvalue. The integral equation is studied numerically and some properties are obtained and conclusions reached.

2.1 Reduction to a Dual Pair of Integral Equations

The representation[1]

$$\phi(x,y) = \mathrm{Re}\int_C A(\alpha)\ \mathrm{Cos}(\alpha x)e^{-\sqrt{\alpha^2-\delta\gamma^2}\ y}\ d\alpha \tag{2.1}$$

$$\psi(x,y) = \mathrm{Re}\int_C B(\alpha)\ \sin(\alpha x)e^{-\sqrt{\alpha^2-\gamma^2}\ y}\ d\alpha \tag{2.2}$$

satisfies the field equations and Mode I symmetry conditions. The contour C is arbitrary and the unknown coefficients $A(\alpha)$ and $B(\alpha)$ are not necessarily real-valued. In order to continue this representation of the solution into the lower half plane ($y < 0$), it is necessary to satisfy the symmetry conditions that we require on the x-axis for $|x| > 1$. These are

$$v(x,0) = 0 \quad ; \quad |x| > 1 \tag{2.3}$$

$$\sigma_{yx}(x,0) = 0 \quad ; \quad |x| > 1 \tag{2.4}$$

As a consequence of (2.3) and (2.4)

$$\frac{\partial}{\partial y}\, u(x,0) = 0 \quad ; \quad |x| > 1$$

In explanation, we can cut the region (free body diagram) anywhere we

---

[1]Separation of variables in Cartesian coordinates, α = separation constant.

desire provided we apply to the cut surface the state of internal stress and displacement that exists there. The net result is that a Mode I representation in Cartesian coordinates requires the two additional symmetry conditions (2.3) and (2.4). The combined boundary conditions then read on $y = 0$

$$\frac{\sigma_{yy}}{-2\mu} = \frac{\partial^2\psi}{\partial x \partial y} + \frac{\partial^2\phi}{\partial x^2} + \frac{1}{2}\gamma^2\phi = 0 \quad ; \quad |x| < 1 \tag{I}$$

$$\frac{\sigma_{xy}}{-2\mu} = \frac{\partial^2\phi}{\partial x \partial y} - \frac{\partial^2\psi}{\partial x^2} - \frac{1}{2}\gamma^2\psi = 0 \quad ; \quad 0 \leq |x| < \infty \tag{II}$$

$$v = \frac{\partial\phi}{\partial y} - \frac{\partial\psi}{\partial x} = 0 \quad ; \quad |x| \geq 1 \tag{III}$$

Substitution for ϕ,ψ into boundary condition (III) gives

$$B(\alpha) = \frac{-2\alpha\sqrt{\alpha^2-\gamma^2}}{2\alpha^2-\gamma^2} A(\alpha) \tag{2.5}$$

$$\phi(x,y) = -\mathrm{Re}\int_0^\infty \frac{\alpha^2-\frac{1}{2}\gamma^2}{\sqrt{\alpha^2-\delta\gamma^2}} C(\alpha)\ \mathrm{Cos}(\alpha x) e^{-\sqrt{\alpha^2-\delta\gamma^2}\ y}\ d\alpha \tag{2.6}$$

$$\psi(x,y) = \mathrm{Re}\int_0^\infty \alpha\ C(\alpha)\ \sin(\alpha x) e^{-\sqrt{\alpha^2-\gamma^2}\ y}\ d\alpha \tag{2.7}$$

where $\alpha C(\alpha) = B(\alpha)$

and we have arbitrarily taken the contour C to be the real axis $(0,\infty)$.

Substitution for ϕ,ψ in the other two boundary conditions gives

$$\mathrm{Re}\int_0^\infty P\left(\frac{\alpha}{\gamma}\right) C(\alpha)\,\mathrm{Cos}(\alpha x)\,d\alpha = \sigma_{yy} \quad ; \quad |x| < 1 \text{ (I)}, \tag{2.8a}$$

$$\mathrm{Re}\int_0^\infty C(\alpha)\,\mathrm{Cos}(\alpha x)\,d\alpha = v(x) \qquad \text{(II)}, \tag{2.8b}$$

where $\sigma_{yy} = 0$

$$P(\alpha) = \frac{(2\alpha^2-1)^2}{\sqrt{\alpha^2-\delta}} - 4\alpha^2\sqrt{\alpha^2-1} \tag{2.9}$$

$$v(x) = \begin{cases} \text{Arbitrary} & ; \quad |x| < 1 \\ 0 & ; \quad |x| \geq 1 \end{cases}$$

The function $P(\alpha)$ is related to the Rayleigh equation [6, p. 180, equation (12)], [2]

$$R(s) = (2 - s^2)^2 - 4\sqrt{1 - s^2}\ \sqrt{1 - \delta s^2}$$

which (as shown by Lord Rayleigh) has three roots one of which is real [6, p. 181].

$$s = C_R/C_S = 0.934$$

and corresponds to the surface wave named in his honor. The role of this wave in the problem herein can be estimated by plotting the function $P(\alpha)$ vs. α.

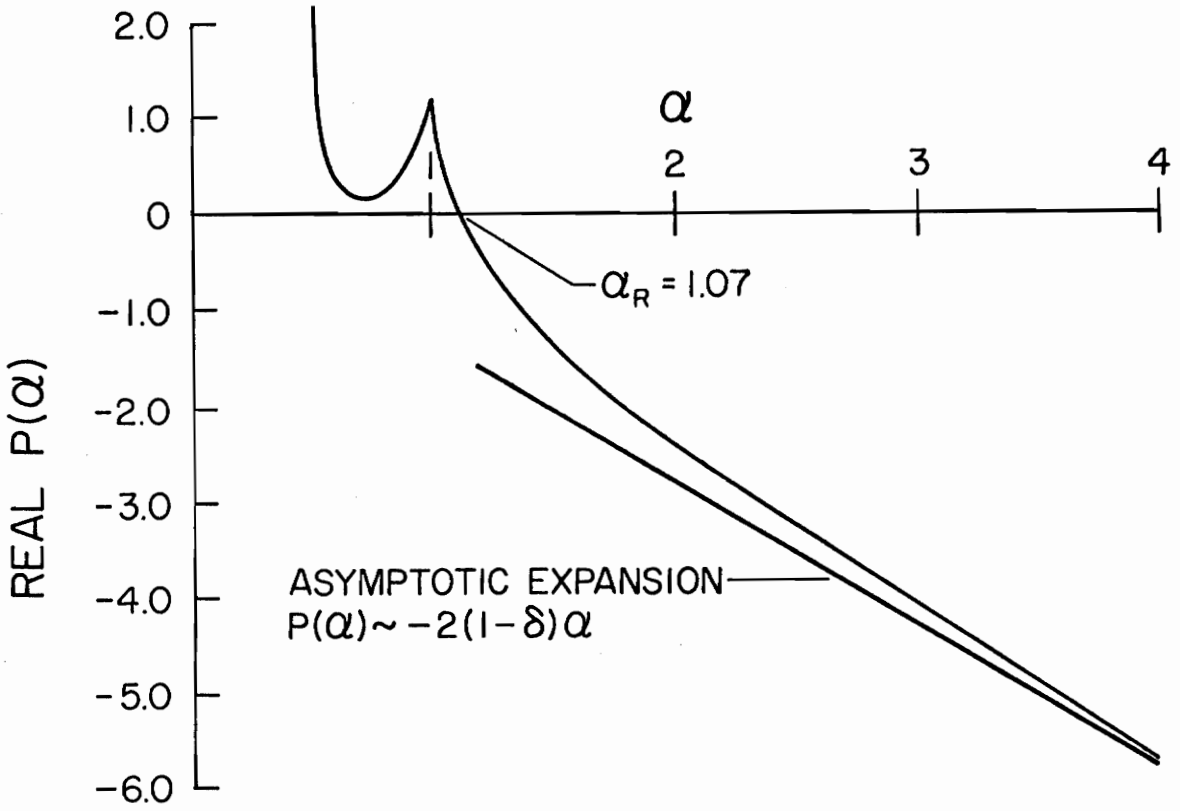

FIG.I. DUAL PAIR FUNCTION $P(\alpha)$

Certainly, the Rayleigh function and hence the Rayleigh wave must strongly influence our solution. Note that the Rayleigh root α_R of $P(\alpha)$ lies within the arbitrarily taken range on α, and that the proximity to $\alpha = 1$ suggests that the contribution due to $\alpha > 3$ is probably small. The asymptotic expansion of $P(\alpha)$ will suggest an appropriate integral transform.

The function $v(x)$ denotes the displacement $v(x,y)$ evaluated at $y = 0$ and must vanish for $|x| > 1$ for symmetry, and at $x = \pm 1$. Otherwise the material would tear at $x = \pm 1$ and the crack would extend. We will use

$$v(x,0) = v(x) = v(x,\gamma^2)$$

as equivalent functions.

The Dual Pair (2.8a,b) reduces to the Dual Pair studied by Yoffe [3] by letting $\gamma \to 0$ to get

$$\int_0^\infty \alpha\, C(\alpha)\, \mathrm{Cos}(\alpha x) d\alpha = T_0 \quad ; \quad |x| < 1$$

$$\int_0^\infty C(\alpha)\, \mathrm{Cos}(\alpha x) d\alpha = 0 \quad ; \quad |x| \geq 1$$

where $T_0 = \frac{\gamma}{2(1-\delta)} \sigma_{yy} = \text{Constant}$

Yoffe considered the case of a crack extending at constant speed subject to constant uniaxial tension T_0 at infinity by assuming that an observer riding on the tip of the crack would observe no motion (Lorentz transformation). The physics of the Yoffe problem and the problem here differ, but the mathematics is similar at this stage.

It is the opinion of this author that in a rigorous analysis the time independent boundary conditions should be satisfied by, and in turn, determine the static solution. This is in agreement with E. Sternberg [4]. Note however that if the crack length a is a function of time a(t) then nonhomogeneous terms due to differentiating the static solution with respect to time would appear in the dynamical field equations.

The Dual Pair here is similar to a form of the Rayleigh Integral Equation [5, p. 477] and the Sommerfeld formulation for the diffraction of light by an aperture [6, p. 564].

The Dual Pair which is the subject of this chapter differs from the Yoffe Dual Pair by the presence of the function $P(\alpha)$ and the absence of the nonhomogeneous constant term T_0. That is, we seek nontrivial eigensolutions of the Dual Pair (2.8a,b).

The main theme and contribution of this chapter is the question of existence of solutions of the Dual Pair (2.8a,b). Note that the presence of a zero of $P(\alpha)$, the Rayleigh root, strengthens the argument for the possibility of existence. The case $\gamma = 0$ which corresponds to rigid body motion does not however have a nontrivial solution of the homogeneous Dual Pair.

If solutions of the Dual Pair do exist in which $\text{Imag}(\gamma) = 0$, they imply the existence of standing surface waves: the crack surface experiences a periodic "breathing motion". The disturbance would decay rapidly away from the crack surface; faster than the Sommerfeld radiation condition [7] and hence there would be no radial emission of energy.[1] Once excited the energy would be conserved and the material near the crack would continue to vibrate indefinitely. The high frequency vibration (kilo Hz range) could quickly contribute to fatigue failure before crack extension.

Since the frequency is high, subcontinuum and rate effects could be expected to alter the character of the wave. In particular, random crystal orientation would tend to scatter the wave, cause emission of energy and reduce harmful effects. Also, for example, cold working

---

[1]Existence of solutions of the exterior Helmholtz problem are discussed in [8], [9].

of carbon steel aligns the crystal orientations rendering the steel harder and stronger. As an undesirable side effect the steel becomes more susceptible to fatigue and impact failure. It is conjectured here that the increase in fatigue sensitivity may be due in part to the increased crystal alignment which reduces scattering of standing waves of various classes. The presence of remote boundaries (see next chapter) increases greatly the number of possible classes of standing wave behavior.

The size of the subcontinuum particles could also alter[1] the character of the waves. Lord Kelvin [10]

> ...discussed periodic systems of discrete particles and concluded that waves of some frequencies would not propagate freely in them. [11, p. 3]

See also [12].

The technique for the solution of Dual Pair of integral equations seems to have originated with Titchmarsh [13] and Busbridge [14] in 1937. Improvements and extensions of the technique have been made by Tranter [15, p. 111], Williams [16], and Roberts [17]. Selected applications of the technique to problems in mechanics and optics can be found in [18], [19], [20], and [21]. Several of these references treat problems having an arbitrary function analogous to our $P(\alpha)$. Of special interest is [21] which deals with the diffraction of electromagnetic waves.

---

[1] We mean here an interaction between the continuum wave discussed herein and subcontinuum crystal lattice dynamics.

2.2 Reduction of Dual Pair to an Integral Equation of the Second Kind

The Dual Pair (2.8a,b) will be reduced to a Fredholm type integral equation of the second kind. This will permit numerical solution by successive substitution and by the Fredholm-Carleman theory for larger characteristic values.

2.2.1 The first step is to represent $C(\alpha)$ as an integral transform of some new function $G(\eta)$ such that (II) of the Dual Pair is satisfied automatically for arbitrary $G(\eta)$. In the solution of similar Dual Pair problems it is customary to employ the discontinuous integral [22]

$$\int_0^\infty J_0[at]\,\mathrm{Cos}[bt]dt = \begin{cases} \dfrac{1}{\sqrt{a^2 - b^2}} & a > b \\ \\ 0 & a < b \end{cases} \tag{2.11}$$

and the substitution

$$C(\alpha) = \int_0^\infty J_0[\alpha\eta]G[\eta]d\eta \tag{2.12}$$

to get

$$V(x) = \begin{cases} \displaystyle\int_x^1 \frac{G(\eta)}{\sqrt{\eta^2 - x^2}}\,d\eta & 0 \leq x < 1 \\ \\ 0 & 1 < x \end{cases}$$

If we find that $G(\eta)$ is continuous as $\eta \to 1$ then $V(x) \to 0$ as $x \to 1^-$ which is necessary for continuous displacements, and (2.8b) is

automatically satisfied.

2.2.2 The second step is to use (2.12) to transform (2.8a) from an integral equation of the first kind to an integral equation of the second kind. To do this, multiply (2.8a) by

$$\frac{2}{\pi}\frac{dx}{\sqrt{\xi^2 - x^2}}$$

and integrate $0 \leq x \leq \xi$ using [23, p. 21]

$$J_0[\alpha\xi] = \frac{2}{\pi}\int_0^{\xi}\frac{\cos(\alpha x)dx}{\sqrt{\xi^2 - x^2}}$$

to get

$$\mathrm{Re}\int_0^1 G(\eta)d\eta\int_0^{\infty} P\left(\frac{\alpha}{\gamma}\right) J_0(\alpha\xi)\, J_0(\alpha\eta)d\alpha = 0\ ;\ 0 \leq \xi \leq 1$$

Noting that $P(\alpha) \sim -2(1 - \delta)\alpha + O\left(\frac{1}{\alpha}\right)$ and using [24, p. 97]

$$\int_0^1 G(\eta)d\eta\int_0^{\infty}\alpha\, J_0(\alpha\xi)J_0(\alpha\eta)d\alpha = \frac{G(\xi^+) + G(\xi^-)}{2\xi}$$

gives

$$\mathrm{Re}\left[G(\xi) - \gamma\xi\int_0^1 H(\xi,\eta)G(\eta)d\eta\right] = 0\ ;\quad 0 \leq \xi \leq 1 \qquad (2.13a)$$

where

$$H(\xi,\eta) = \int_0^{\infty} Q\left(\frac{\alpha}{\gamma}\right) J_0(\alpha\xi)J_0(\alpha\eta)d\alpha \qquad (2.13b)$$

and

$$Q(\alpha) = \alpha + \frac{P(\alpha)}{2(1 - \delta)} \qquad (2.14)$$

The substitution (suggested by J. Cochran [27])

$$G(\eta) = \sqrt{\eta}\, g(\eta) \tag{2.15}$$

gives

$$\mathrm{Re}\left[g(\xi) - \gamma \int_0^1 K(\xi,\eta) g(\eta) d\eta\right] = 0 \tag{2.16a}$$

in which the kernel

$$K(\xi,\eta) = \sqrt{\xi\eta} \int_0^\infty Q\left(\frac{\alpha}{\gamma}\right) J_0(\alpha\xi) J_0(\alpha\eta) d\alpha \tag{2.16b}$$

is symmetric. This form has advantages for numerical purposes. However, results will be reported in terms of $G(\eta)$ which is advantageous for analytical purposes.

The kernel $K(\xi,\eta)$ is continuous since $Q(\alpha)$ has the asymptotic expansion

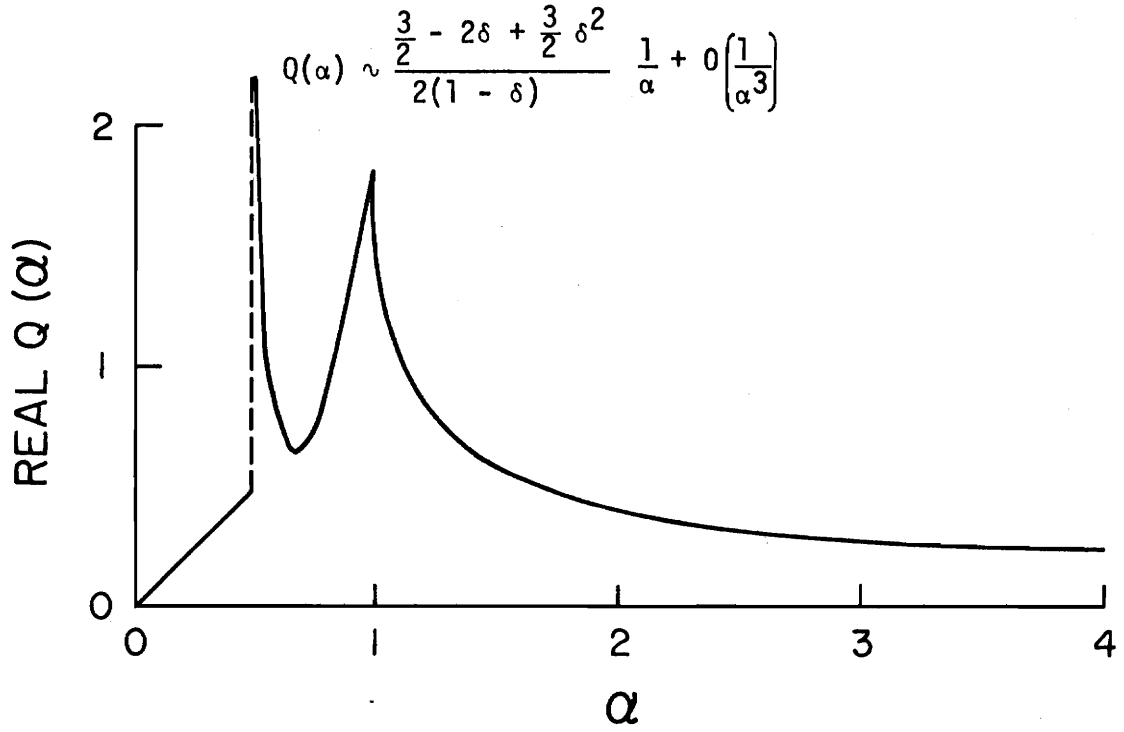

FIG. 2. DUAL PAIR FUNCTION $Q(\alpha)$

Before attempting a numerical solution of (2.16a,b) it should be pointed out that

i) $\mathrm{Im}[G(\eta)]$ is arbitrary as far as (2.8b) is concerned.

ii) The kernel is nonlinear in the eigenvalue. An example of the analysis of Fredholm's integral equation whose kernel is analytic in a parameter is given by Tamarkin [29].

iii) The kernel of the integral equation (both H and K forms) requires the α-integration which for numerical purposes must be approximated on a finite range

$$0 \leq \alpha \leq \alpha_{max}$$

with step size $\Delta\alpha$. It was found that the results to be discussed next were insensitive to the finite difference approximation of the α and η integrals provided

$$\Delta\alpha < \frac{\pi}{8}$$

$$\alpha_{max} > 8\gamma$$

$$\Delta\eta < .05$$

For large γ the numerical approximation becomes inefficient due to the large number of quadrature points required which is due to approximating the fast varying harmonic behavior of the Bessel functions. Filon [26], [15, p. 67] has devised a remedy for this type of problem.

The problem will now be restricted to real valued variables γ; $Q(\alpha)$, $g(\eta)$ and $K(\xi,\eta)$. This will enable a solution of (2.16a,b) to be

obtained and will dictate the behavior at infinity. It is supposed that other choices would permit solutions for specific remote boundaries.

2.3 Numerical Solution for Smallest Characteristic Value

Numerical solution of (2.16a,b) by successive substitution (power method) gave the following results:

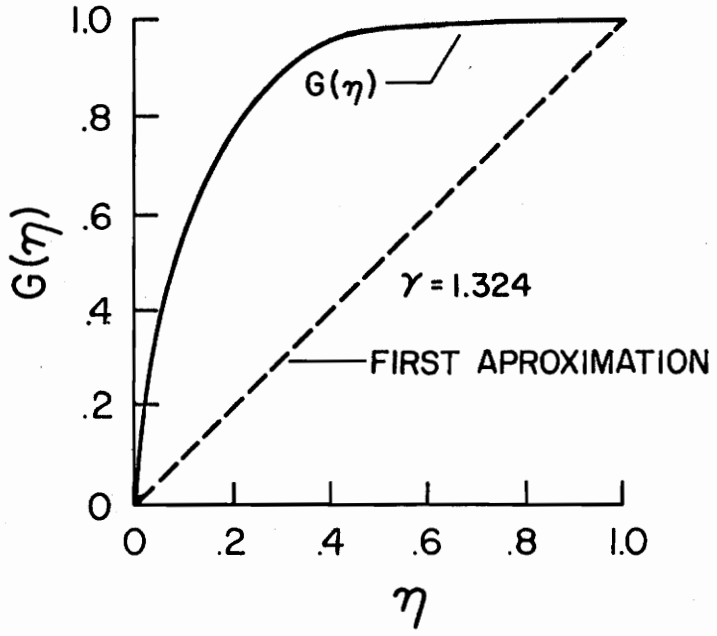

FIG.3 DUAL PAIR EIGENVECTOR

Expanding $G(\eta)$ in the series

$$G(\eta) = \eta \sum_{K=1}^{\infty} [1 - \eta^2]^{K-1} G_K \qquad (2.17)$$

gives $G_1 = 1.000$

$G_2 = 0.4\overline{98}$

$G_3 = 0.3\overline{75}$

and

$$C(\alpha) = \sum_{K=1}^{\infty} 2^{K-1}(K-1)! \frac{J_K(\alpha)}{\alpha^K} G_K \qquad (2.18)$$

Note that near $x = \pm 1$

$$V(x) = \mathrm{Re}[\sqrt{1 - x^2} + O(1 - x^2)^{3/2}] .$$

This term in the displacements leads (it would seem) to a square root singularity in the stresses at the crack tips which is of the same (or similar) character as the singularity in the Inglis solution of the analogous static problem.

The norm of the kernel (2.16b) can be used to give a lower bound on possible eigenvalues since [27, pp. 88, 214]

$$||K(\gamma)||^2 - \frac{1}{\gamma^2} = f(\gamma) \geq 0 \qquad (2.19)$$

By iteration of $\gamma = \dfrac{1}{||K(\gamma)||}$ it was found that $\gamma_{min} = 1.28$. We conclude that there are no small γ and in light of $\gamma_1 = 1.324$ and the formula [27, p. 214] valid for $K(\gamma)$ independent of γ

$$\sum_{\nu=1}^{\infty} \left[\frac{1}{\gamma_\nu}\right]^N = k_N \quad ; \quad N = 1,2,3,... \qquad (2.20)$$

we expect $\gamma_2 >> \gamma_1$.

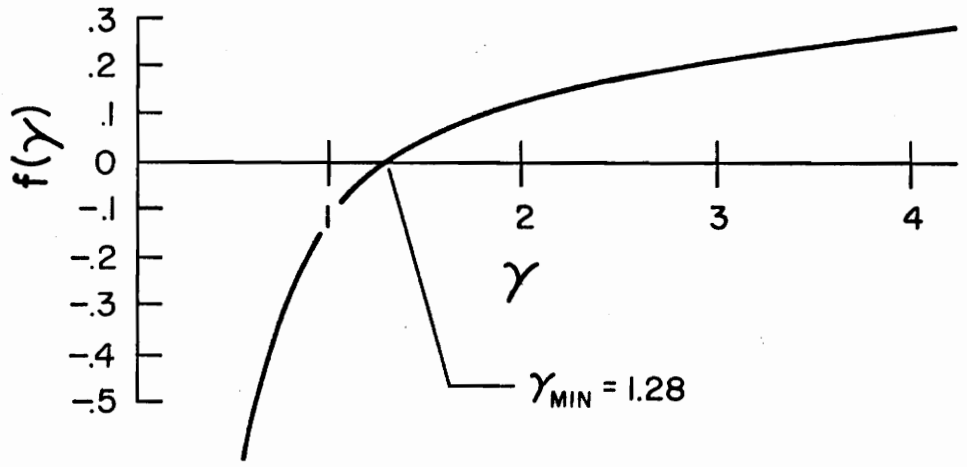

FIG. 4 LOWER BOUND ON POSSIBLE EIGENVALUES

2.4 Larger Characteristic Values

The symmetric kernel (2.16b) of the integral equation (2.16a) is nonlinear in the eigenvalue γ. In this case the coefficients d_N in the expansion of the Fredholm determinant [28, p. 25]

$$D(\gamma) = 1 + d_1\gamma + d_2\gamma^2 + d_3\gamma^3 + \ldots \qquad (2.21)$$

are likewise nonlinear in γ. Following the notation of Cochran [27, p. 91] trace relations

$$k_N = \sum_{\nu=1}^{\infty} \left[\frac{1}{\gamma_\nu}\right]^N \quad ; \quad N \geq 1$$

could be used to estimate the γ_ν ; $\nu = 1,2,\ldots$ Evaluating the k_N at $\gamma = 1.324$ gave

$$k_1 = 0.588 \qquad \gamma_1 \doteq 1.40$$
$$k_2 = 0.268 \qquad \gamma_2 \doteq 3.62$$

Since the k_N are nonlinear in γ these results must be considered questionable.

More accurate results were obtained by applying the Fredholm-Carleman theory [27, p. 46]

$$D(\gamma) = \sum_{m=0}^{N} d_m\gamma^m$$

$$D(\xi,\eta,\gamma) = \sum_{m=0}^{N} D_m(\xi,\eta)\gamma^m$$

where $d_0 = 1 \quad ; \quad D_0(\xi,\eta) = K(\xi,\eta)$

N = truncation number for numerical purposes.

$$D_m(\xi,\eta) = d_m\, K(\xi,\eta) + \int_0^1 K(\xi,\eta)\, D_{m-1}(\xi,\eta)d\eta \quad m \geq 1$$

$$d_m = -\int_0^1 \frac{D_{m-1}}{m}(x,x)\, dx$$

and the eigenvector $G(\xi)$ is given by

$$G(\xi) = D[\xi,\xi;\gamma]$$

The Fredholm determinant $D(\gamma)$ was plotted vs. γ to give estimates of the smaller characteristic values for N = 9.

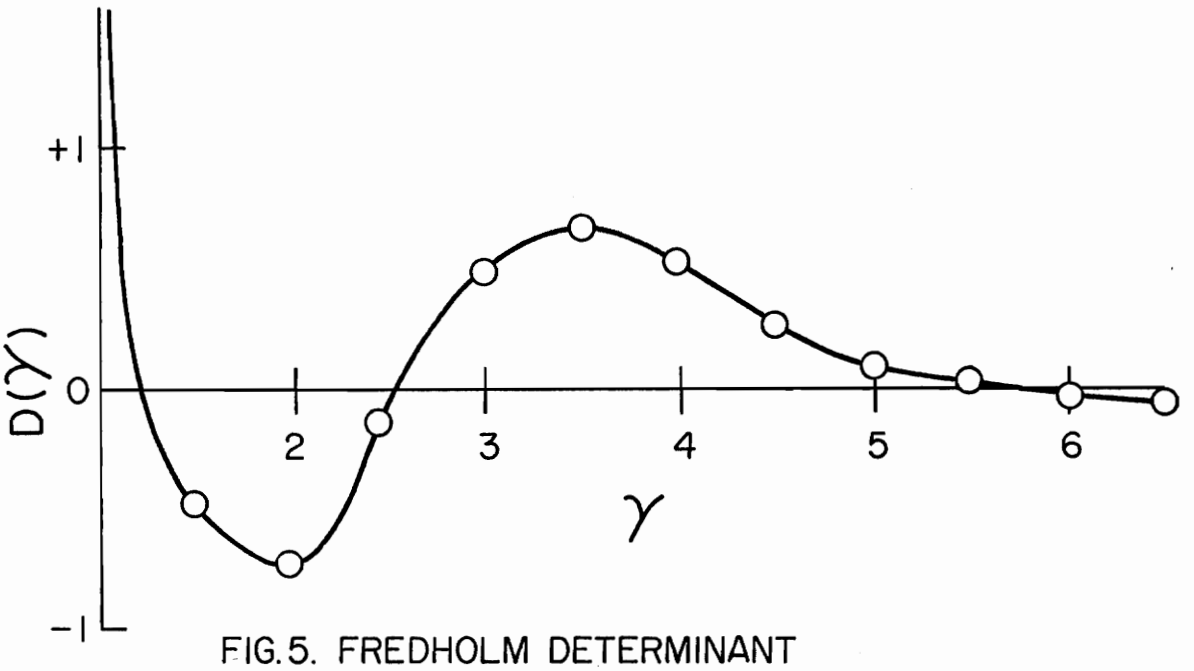

FIG. 5. FREDHOLM DETERMINANT

Using the graph to give initial estimates for the roots γ of $D(\gamma) = 0$ gave after iteration by Newton's method

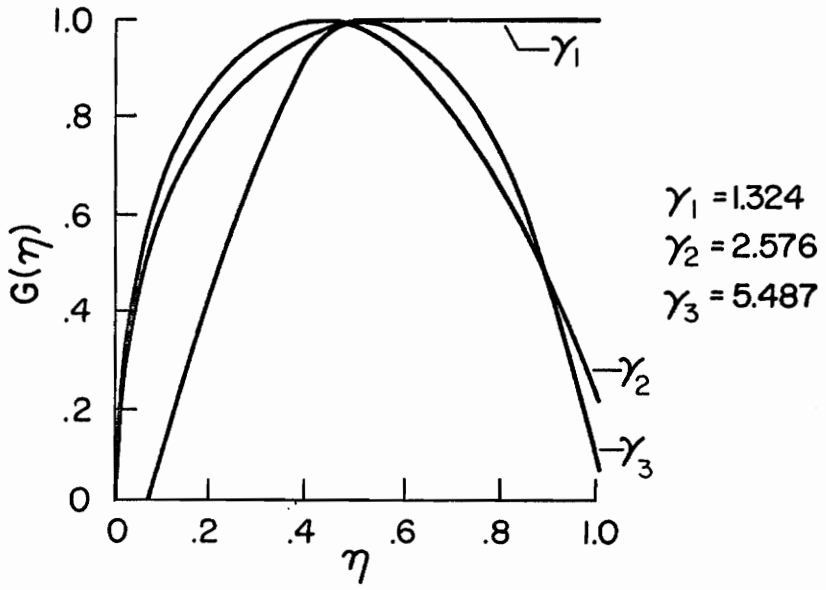

FIG. 6 EIGENVECTORS

It was found that γ was quite sensitive to errors resulting from the numerical approximation of the solution of

$$g(\xi) = \gamma \int_0^1 K[\xi,\eta;\gamma_0]g(\eta)d\eta$$

as can be seen from Fig. 7.

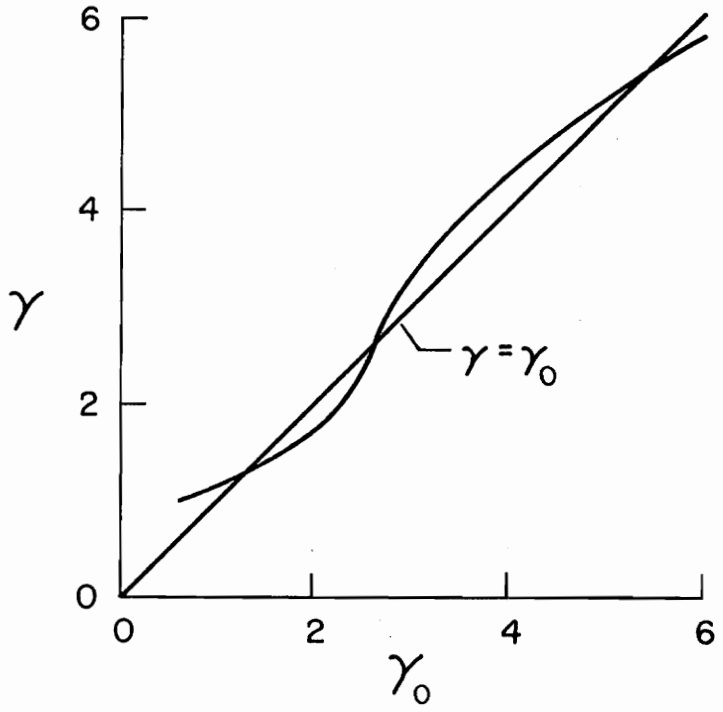

FIG. 7 γ vs. γ_0

2.5 An Observation on Terminal Crack Speed

It has been experimentally observed [29] [30] that the rate of crack propagation V_{max} is always less than about

$$V_{max} \doteq 0.50\ C_S \doteq 0.54\ C_R$$

The reason for this "magic number" of 0.5 does not seem to be known although several explanations have been offered [3], [31], [32], [33], [34], [35]. The observation here is that letting

$$\alpha = S^{-1/2}$$

in (2.9) gives:

$$S^{3/2}\ p[\alpha(S)] = R(S) = (2 - S)^2/\sqrt{1 - \delta S} - 4\sqrt{1 - S}$$

in which (see graph p. 29) R(S) has zero slope at

$$S_0 = 0.5344 - 0.064\delta + O(\delta^2)$$

This suggests that there may be a correlation between S_0 and V_{max} which would explain the "magic number." It would be of interest to study this correlation as a function of Poisson's ratio.

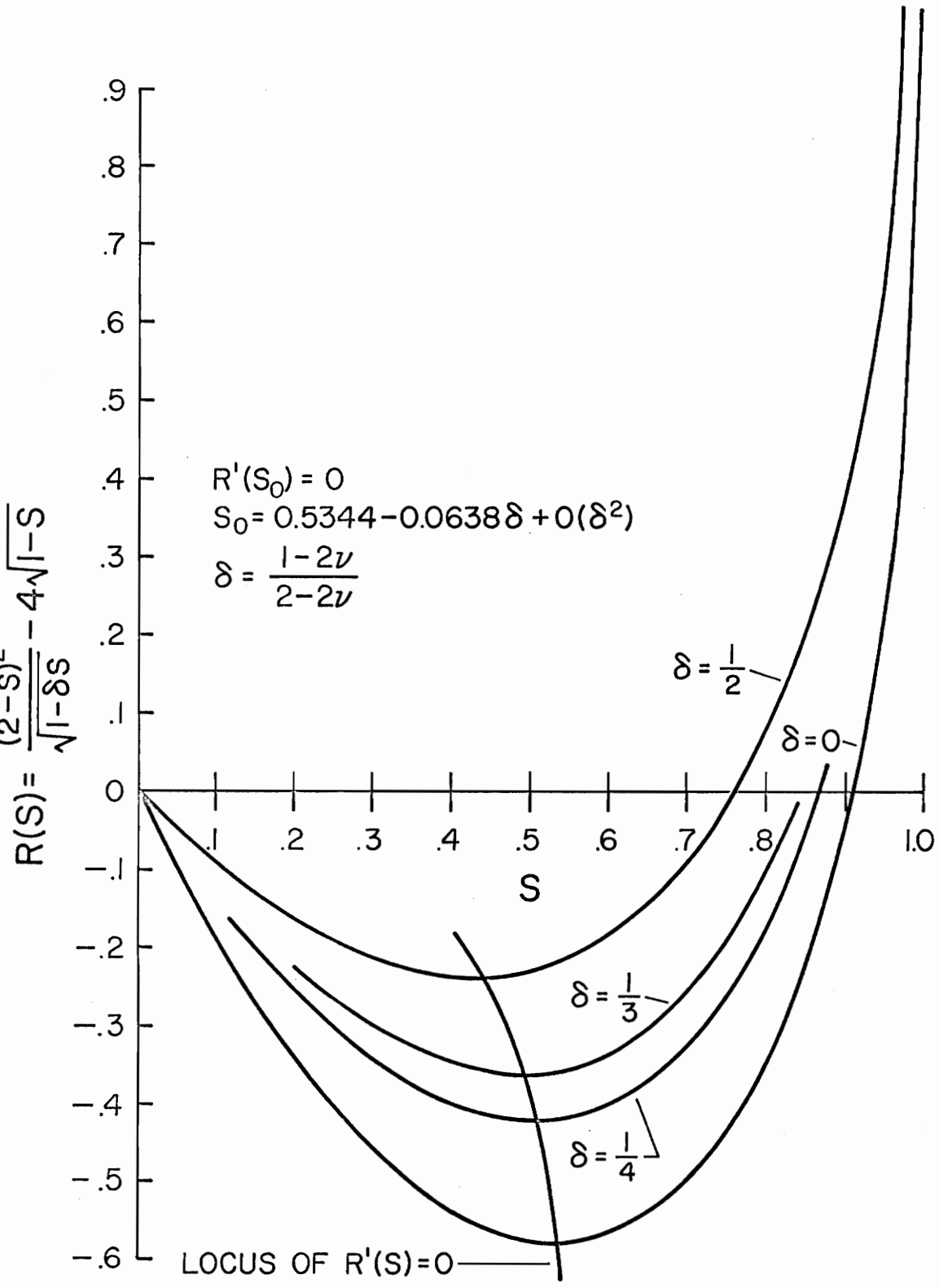

FIG. 8. DUAL PAIR FUNCTION R(S)

2.6 Summary

For the case of a slit the representation in Cartesian coordinates led naturally to the boundary conditions in the form of a homogeneous Dual Pair of integral equations. Properties of the function $P(\alpha)$ suggested that a solution might exist and that standard procedures could be used to reduce the problem to an integral equation of the second kind. Numerical solutions of the integral equation were found to exist which suggests the physical existence of standing waves having real valued eigenvalues. This seems to imply that energy is not radiated to infinity, except perhaps along the x-axis.

The analysis could be carried further if integrals of the form

$$\int_0^\infty J_\nu(\alpha\eta)\ \mathrm{Cos}(\alpha x)e^{-\sqrt{\alpha^2 - \gamma^2}y}\ d\alpha \quad ;\ \nu=1,2,\cdots$$

could be evaluated.

In closing this chapter it should be noted that the representations here do not rule out the possibility of other types of solutions. And, in fact, the results of the next chapter indicate that this is true. In particular there is a tendency towards multiple eigenvalues and multiple eigenvectors. In regard to the numerical results of this chapter, it should be again pointed out that small numerical errors can cause large changes in the eigenvalue as evidenced by Fig. 7. This raises the question as to the solubility, especially for large γ. Also, if $G(1) = 0$, then the stresses are not singular at the crack tip.

Chapter 2 Literature Cited

1. Fung, Y. C., Foundations of Solid Mechanics, Prentice-Hall, 1965.

2. Ewing, E., Jardetzky, W. S., and Press, F., Elastic Waves in Layered Media, McGraw-Hill (1957).

3. Yoffe , E. H., "The Moving Griffith Crack," Phil. Mag., 42, 739 (1951).

4. Sternberg, E. and Eubanks, R. A., "On Stress Functions for Elastokinetics and the Integration of the Repeated Wave Equation," Q. J. App. Math., 15 (1957) 149-153.

5. Mow, C. C., and Pao, Y. H., "The Diffraction of Elastic Waves and Dynamic Stress Concentrations," Rand Corp., R-482-PR, April, 1971.

6. Born, M. and Wolf, E., Principles of Optics, Pergamon, 1970.

7. Sommerfeld, A., Optics, Academic Press, 1967.

8. Smirnov, V. I., A Course of Higher Mathematics, Vol. IV, p 680, Addison Wesley, 1964.

9. Kleinman, R. E., and Roach, G. F., "Boundary Integral Equations for the Three-Dimensional Helmholtz Equation," SIAM Review, Vol. 16, No. 2, April, 1974, p 214.

10. Kelvin, Popular Lectures, Vol. I, Macmillan, 1891.

11. Musgrave, M. J. P., Crystal Acoustics, Holden-Day, 1970.

12. Born, M., and Huang, K., Dynamical Theory of Crystal Lattices, Oxford, 1954.

13. Titchmarsh, E. C., Theory of Fourier Integrals, Oxford, 1937.

14. Busbridge, I. W., "Dual Integral Equations," Proc. London Math. Soc., 44 (1938), 115.

15. Tranter, C. J., Integral Transforms in Mathematical Physics, Methuen & Co., 1951.

16. Williams, W. E., "The Reduction of Boundary Value Problems to Fredholm Integral Equations of the Second Kind," ZAMP, Vol. XIII, 1962, pp 133, 151.

17. Roberts, J. A., "Approximate Methods for the Solution of Certain Dual Fourier-Bessel Series Relations," North Carlina State Univ., Ph.D. Thesis, 1964; Univ. Microfilms, Ann Arbor, Mich., 65-2825.

18. Fichter, W., "Some Solutions for a Narrow Plate Containing a Central Longitudinal Crack," M. S. Thesis, V.P.I., 1966.

19. Hartranft, R. J. and Sih, G. C., "An Approx. Three-Dimensional Theory of Plates with an Application to Crack Problems," Lehigh Univ., 1972, unpublished.

20. Sneddon, I. N., Mixed Boundary Value Problems in Potential Theory, Interscience, 1966.

21. Tranter, C. J., "A Further Note on Dual Integral Equations and an Application to the Diffraction of Electromagnetic Waves," Q. J. Mech. and App. Math., Vol. VII, p 3 (1954).

22. Magnus, W. and Oberhettinger, F., "Formula and Theorems for the Functions of Mathematical Physics," Chelsea, 1949.

23. Watson, G. N., Theory of Bessel Functions.

24. Gray, A., Mathews and MacRobert, Bessel Functions, Macmillan & Co. (1931).

25. Tamarkin, J. D., "On Fredholm's Integral Equations Whose Kernel Are Analytic in a Parameter," Ann. of Math. 28 (1927), pp 122-152.

26. Filon, "On a Quadrature Formula for Trigonometric Integrals," Proc. Royal Soc. of Edinburgh, Vol. 49 (1928), pp 38-47.

27. Cochran, J., Analysis of Linear Integral Equations, McGraw-Hill, 1972.

28. Lovitt, W. V., Linear Integral Equations, Dover, 1950.

29. Kerkhof, F., Personal communication, Dynamic Crack Conf., July, 1972, Lehigh Univ.

30. Irwin, G. R., "Fracture Mechanics," Proc. First Symp. on Navel Struc. Mech., Pergamon, 1960.

31. Kolsky, H. and Rader, D., "Stress Waves and Fracture," Fracture, Vol. 1, Chap. 9, Academic Press, 1969.

32. Broberg, B., "On the Speed of a Brittle Crack," J. App. Mech., p 546, Sept., 1964.

33. Sih, G. C., "Dynamic Aspects of Crack Propagation," Inelastic Behavior of Solids, pp 607-639.

34. Mott, N. F., Engineering, Vol. 165, p 16, 1948.

35. Roberts, D. K., and Wells, A. A., "The Velocity of Brittle Fracture," Engineering, Vol. 178, p 820, 1954.

CHAPTER 3

GENERALIZED SEPARATION OF VARIABLES

Table of Contents

Introduction

It was suggested[1] that the question of existence and some properties of the Dual Pair solution for a slit could be resolved by a study of the case of an ellipse with small eccentricity.

This chapter presents an analysis for arbitrary eccentricity. The essence of the method is the observation that the appropriate conformal mapping function and the Bessel function addition formula have two similar groupings of variables which permit the separation of variables in the image plane.[2] The evaluation of the boundary conditions then gives an infinite system of algebraic equations to be solved numerically. The equations are analytic in both eigenvalue and eccentricity parameter, and are coupled due to the parametric resonance inherent in solutions of the Mathieu equation. For zero eccentricity the system reduces to two equations. This gives the zeroth order perturbation solution and serves as a check on the equations and computer code. A third order perturbation solution for small eccentricity was obtained. The results show that the first and third order perturbations in the eigenvalue are zero, and the first order perturbation in the eigenvector is comparatively large; i.e., the eigenvector is a fast varying function of the eccentricity parameter.

The perturbation solution gives accurate results for small eccentricity parameter m ($0 \leq m \leq 0.05$). The perturbation

---

[1] A. H. Nayfeh, personal communication.

[2] Unit circle.

method permits insight into the nature of the parametric resonance which causes the equations to be coupled. Contour plots of the results show stress concentrations away from the stress free boundary and for $m > 0$ suggest a more appropriate coordinate system in which to solve the problem.

The combined use of the Kutta conformal mapping function [2, p. 292], and the Bessel function addition formula [3, p. 359] to achieve a generalized separation of variables in the image plane (unit circle) is a new technique that provides a concise representation of solutions of the reduced wave equation for boundary conditions on an ellipse. This enables a single representation of the solution for all order[1] perturbations and permits a systematic procedure for each order. The order to which the solution can be carried is limited by computer precision. Each order loses about 3 to 4 significant figures. This is due to errors in finite difference approximation to the derivatives of the coefficient matrix and to the tendency of the coefficient matrix to have uncoupled, ill-conditioned subsystems. The loss of precision and restriction of the solution to $m << 1$ seem to be the primary disadvantages of the perturbation method. Results are presented accurate to order m^4.

Three numerical algorithms were used in attempts to get solutions for large eccentricity. In summary of the numerical results, it was found that for large eccentricity a large number of equations

---

[1]Each order perturbation refers to Taylor series coefficients in the eccentricity parameter m. See section 6 of this chapter.

are required and the eigenvector is such a rapidly varying function of the eccentricity parameter that numerical solution of this formulation is difficult by any algorithm. It is shown that the difficulty in obtaining a numerical solution is related to the nonlinear properties of the coefficient matrix.

Numerical results are presented for eigenvalue, eigenvector. Plots of stresses, displacements and invariant quantities are also presented.

3.1 Representation of Solution

The class of solutions to be studied can be represented in cylindrical R,θ coordinates by:

$$\phi[R,\theta] = \sum_{K=0}^{\infty} \phi_k \, J_{2k}[\lambda R] \, \mathrm{Cos}[2k\theta] \tag{3.1}$$

$$\psi[R,\theta] = \sum_{K=1}^{\infty} \psi_k \, J_{2k}[\gamma R] \, \sin[2k\theta] \tag{3.2}$$

where ϕ_k, ψ_k = arbitrary real valued constant (eigenvector)

$\lambda = \sqrt{\delta}\,\gamma$; γ = eigenvalue.

It can be shown that ϕ,ψ satisfy

$$[\nabla^2 + \lambda^2]\phi = 0 \quad ; \quad \phi = \text{even in both } x,y$$

$$[\nabla^2 + \gamma^2]\psi = 0 \quad ; \quad \psi = \text{odd in both } x,y$$

As a matter of convenience we can reject the Bessel function solutions of the second kind by considering special boundary conditions on the surface $R = R_0$ as $R_0 \to \infty$ so that the total energy of the system is constant.

The rate of increase of the energy in a region bounded by an arbitrary surface S is given by [1, p. 178]

$$\frac{d}{dt}[T + V] = \int\!\!\int_S \overset{\circ}{\vec{U}} \circ \overset{n}{\vec{T}} \, ds$$

In our case[1] for large R_o

$$U_R \sim \frac{\partial \phi}{\partial R} \quad , \quad \sigma_{RR} \sim -\mu\gamma^2\phi$$

$$U_\theta \sim \frac{\partial \psi}{\partial R} \quad , \quad \sigma_{R\theta} \sim \mu\gamma^2\psi$$

$$\overset{\circ}{\vec{U}} \circ \overset{n}{\vec{T}} \sim -\frac{\mu\gamma^2}{2} \frac{\partial}{\partial R} [\phi^2 + \psi^2]$$

$$\phi^2 \sim \frac{2}{\pi\lambda R} \left[\frac{1 + \sin 2\lambda R}{2}\right] \sum_K \sum_\ell \phi_k \phi_\ell (-1)^{k+\ell} \left[\frac{\text{Cos } 2(k+\ell)\theta + \text{Cos } 2(k-\ell)\theta}{2}\right]$$

Similarly for ψ^2.

Hence, taking S to be the circle $R = R_o$ we obtain

$$\frac{d}{dt}[T + V] = -\mu\gamma^2 \left[\cos 2\lambda R_o \sum_{K=0}^{\infty} \phi_k^2 + \text{Cos } 2\gamma R_o \sum_{K=1}^{\infty} \psi_k^2 + O\left(\frac{1}{R_o}\right)\right]$$

Therefore, if R_o is any root of

$$\text{Cos } 2\lambda R_o \sum_{K=0}^{\infty} \phi_k^2 + \text{Cos } 2\gamma R_o \sum_{K=1}^{\infty} \psi_k^2 = 0$$

then the total energy T + V is constant in time in the limit as $R_o \to \infty$. As a practical matter we can satisfy the remote boundary condition by allowing the remote boundary to be any of an infinite number of

---

[1] A multiplicative time function Cos(γt) is implied in both ϕ and ψ, see page 2.

discrete circles of radius $R = R_0$ as $R_0 \to \infty$; e.g.,

$$R_0 = \left[n - \frac{1}{2}\right] \frac{\pi}{2\gamma} \quad \text{as } n \to \infty$$

It would be of interest to consider linear combinations of solutions such that

$$\frac{d}{dt}[T + V] \sim O(R^{-N}) \quad ; \quad N \geq 1$$

independent of R. Even for the zero eccentricity case there are a doubly infinite number of eigensolutions. In addition for large eccentricity it is suspected that there may be repeated eigenvectors. If a solution can be found which attenuates to zero faster than the Sommerfeld radiation condition, then there is no energy reflected from the remote boundary ($R = R_0 \to \infty$), the location of R_0 would be arbitrary and such a solution would then be a surface wave.

By including the remote boundary $R = R_0 \to \infty$, the results for the interior and exterior regions are related by simple expressions as will be shown.

3.2 Separation of Variables

Introduce the conformal mapping function [2, p. 292]

$$Z = \hat{R}\left[\frac{1}{\zeta} + m\zeta\right] \quad ; \quad Z = x + iy = Re^{i\theta}$$

$$\zeta = \xi e^{i\eta}$$

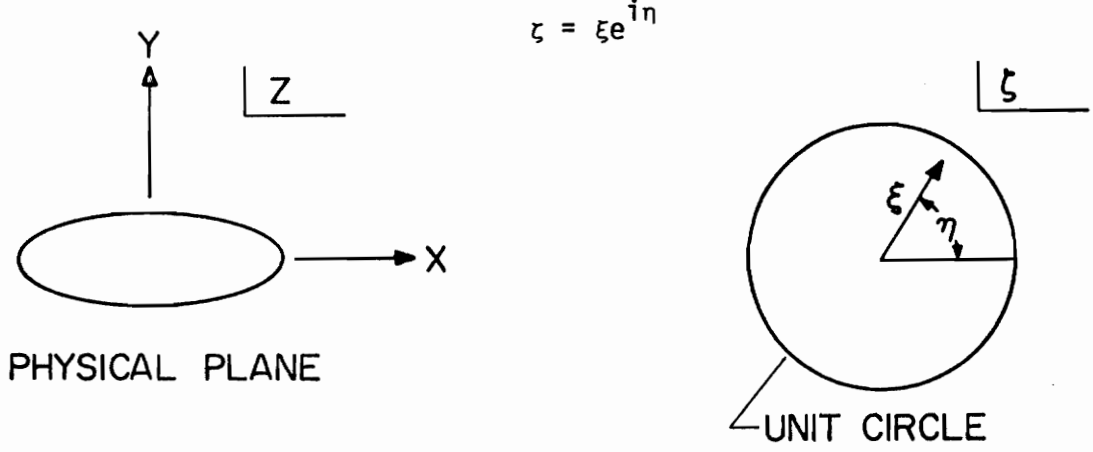

FIG.9 CONFORMAL MAPPING GEOMETRY

We will set $\hat{R} \equiv 1$ to get

$$a = 1 + m$$

$$b = 1 - m$$

$$e = \frac{2\sqrt{m}}{1 + m} = \text{eccentricity}$$

Choosing $0 \leq \xi \leq 1$ corresponds to the exterior ellipse problem

$1 \leq \xi < \infty$ corresponds to the interior ellipse problem

Note that

$$R = \sqrt{\frac{1}{\xi^2} + 2m \cos 2\eta + m^2\xi^2}$$

The use of the Bessel function addition formula (as suggested by the mapping function and solution of the wave equation) permits separation

of variables in the image plane. From [3, p. 359]

$$J_\nu[W] = \left[\frac{Z - ze^{i\alpha}}{Z - ze^{-i\alpha}}\right]^{\frac{\nu}{2}} \sum_{n=-\infty}^{\infty} J_{\nu+n}[Z]\, J_n[z] e^{in\alpha} \tag{3.4}$$

where

$$W = \sqrt{Z^2 - 2Z\, z\, \text{Cos}\ \alpha + z^2}$$

Choosing

$$Z = \frac{\lambda R}{\xi} \quad ; \quad z = m\xi\lambda R \quad ; \quad \alpha = 2\eta - \pi$$

gives

$$W = \lambda R$$

$$\frac{Z - ze^{i\alpha}}{Z - ze^{-i\alpha}} = e^{2i(\theta + \eta)}$$

and finally:

$$J_{2k}[\lambda R] e^{2ik\theta} = \sum_{n=-\infty}^{\infty} J_{k-n}[P]\, J_{k+n}[q] e^{2iN\eta}$$

where $P = \frac{\lambda R}{\xi}$; $q = m\xi\lambda R$

Hence, we can write ϕ, ψ in terms of ξ, η. For numerical purposes we truncate the infinite series (3.1), (3.2) and write

$$\phi = \sum_{j=0}^{N} A_j(\xi)\ \text{Cos}\ 2j\eta \tag{3.5}$$

$$\psi = \sum_{j=1}^{N} B_j(\xi) \sin 2j\eta \tag{3.6}$$

where

$$A_j(\xi) = \frac{1}{2} \varepsilon_j \sum_{k=0}^{\infty} \phi_k \left[J_{k-j}(P)\, J_{k+j}(q) + J_{k+j}(P)\, J_{k-j}(q)\right] \tag{3.7}$$

$$B_j(\xi) = \sum_{k=0}^{\infty} \psi_k \left[J_{k-j}(P)\, J_{k+j}(q) - J_{k+j}(P)\, J_{k-j}(q)\right] \tag{3.8}$$

ε_j = Neumann's Factor = $\begin{cases} 1 & ; \quad j = 0 \\ 2 & ; \quad j \geq 1 \end{cases}$
see [3, p. 22]

$$P = \frac{\lambda}{\xi} \quad , \quad q = m\lambda\xi$$

$$\lambda = \begin{cases} \sqrt{\delta}\,\gamma \text{ in } \phi \\ \gamma \text{ in } \psi \end{cases}$$

N = truncation number

For comparison with Mathieu functions it is interesting to note that if one introduced the mapping function

$$Z = \frac{1}{\zeta} + m\zeta$$

into the original partial differential equation and let

$$\phi = \sum_{k=0}^{\infty} A_k(\xi) \cos 2k\eta$$

one would then get the differential recurrence relations:

$$\left[\frac{d^2}{d\xi^2} + \frac{1}{\xi}\frac{d}{d\xi} + \lambda^2 - \frac{4k^2}{\xi^2} + \frac{\lambda^2 m^2}{\xi^4}\right] A_k(\xi)$$

$$= \frac{m\lambda^2}{\xi^2}\left[A_{k-1}(\xi) + A_{k+1}(\xi)\right]$$

This is a system of coupled Mathieu equations. See [4, p. 404] and [5, p. 405] in which solutions of the reduced wave equation in elliptic coordinates is discussed. For solutions of Mathieu's equation involving products of Bessel functions, see [6, p. 731].

The separation of variables by the method in [4] and [5] further compounds the difficulty since the turning points[1] then become functions of the separation constant. Also, one conclusion of this chapter is that separation of variables is not necessarily a computationly efficient technique for the case $m \to 1$.

One of the major difficulties in obtaining approximate solutions of Mathieu equations is not knowing where the turning points are. One of the results of this chapter is that the locations of the turning points are located for the circle case. It turns out that only for Rayleigh type eigenvalues do turning points not occur, and then only for the interior problem. Since it also turns out that the eigenvalue is a slowly varying function of the eccentricity parameter m, we may expect the locations of the turning points to be slowly varying functions of m.

It is hoped that sufficient numerical properties of the solution

---

[1] Turning points are discussed in [7, p. 335] and [8]. They correspond to transition points between wave type behavior and exponential growth decay behavior.

for m = 0 can be presented so as to enable the deduction of an approximate asymptotic solution for large m by the methods of the WKB approximation and the Langer transformation [8].

3.3 Boundary Condition

From [2, p. 271]

$$2[N - iT] = \sigma_{xx} + \sigma_{yy} - [\sigma_{yy} - \sigma_{xx} + 2i\sigma_{xy}]e^{2i\alpha}$$

N = normal stress

T = tangential stress

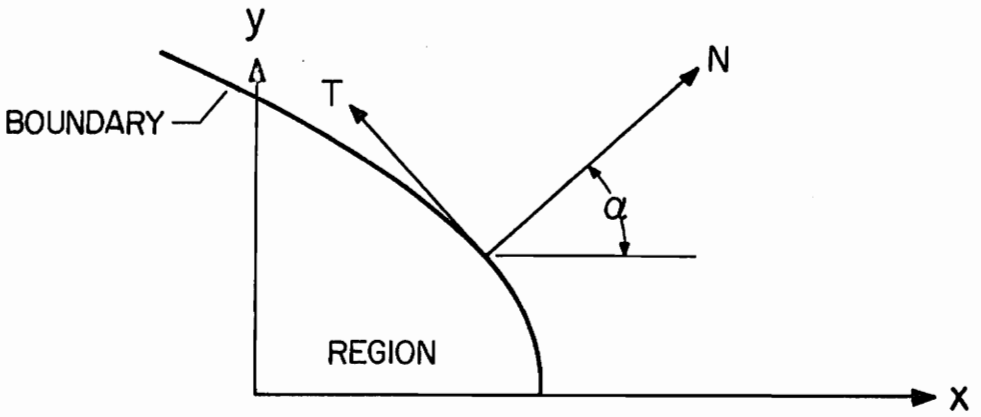

FIG. IO. SKETCH OF BOUNDARY CONDITION

For our case

$$\frac{\sigma_{xx} + \sigma_{yy}}{-8\mu} = \frac{1 - \delta}{4} \gamma^2 \phi \qquad (3.9a)$$

$$\frac{\sigma_{yy} - \sigma_{xx} + 2i\,\sigma_{xy}}{-8\mu} = \frac{\partial^2}{\partial Z^2} \Phi \quad ; \quad \begin{matrix} \Phi = \phi + i\psi \\ Z = x + iy \end{matrix} \qquad (3.9b)$$

From [2, footnote p. 276]

$$e^{2i\alpha} = e^{2i\eta}\, w'(\zeta)/\overline{w'(\zeta)} = -\frac{dZ}{d\bar{Z}}$$

$$= e^{-2i\eta} \quad ; \quad \text{circle case}$$

$$-1 \quad ; \quad \text{slit case}$$

where: $$w(\zeta) = \frac{1}{\zeta} + m\zeta = Z$$

After transforming the derivative from Z to ξ,η and using the field equation to avoid $\frac{\partial^2}{\partial \xi^2}$ we get

$$\begin{bmatrix} L_1 & -L_2 \\ L_2 & L_1 \end{bmatrix} \begin{Bmatrix} \phi \\ \psi \end{Bmatrix} = 0 \quad \text{on } \xi = 1 \tag{3.10}$$

where $$L_1 = (1 - m^2)\frac{\partial}{\partial \xi} - \frac{D\partial^2}{\partial \eta^2} + 2m \sin 2\eta \frac{\partial}{\partial \eta} - \frac{1}{2}\gamma^2 D^2$$

$$L_2 = 2m \sin(2\eta)\frac{\partial}{\partial \xi} - \frac{D\partial^2}{\partial \xi \partial \eta} - (1 - m^2)\frac{\partial}{\partial \eta}$$

$$D = 1 - 2m \cos(2\eta) + m^2$$

For the case m = 1, the ellipse degenerates to a slit, and

$$\frac{L_1}{-4 \sin^2\eta} = \sin(\eta)\frac{\partial}{\partial \eta}\frac{1}{\sin \eta}\frac{\partial}{\partial \eta} + \frac{1}{2}\gamma^2$$

$$\frac{L_2}{-4 \sin^2\eta} = \sin(\eta)\frac{\partial}{\partial \eta}\frac{1}{\sin \eta}\frac{\partial}{\partial \xi}$$

The following formulas were used in transforming the derivative

$$w'\bar{w}' = 1 - \frac{2m \cos(2\eta)}{\xi^2} + \frac{m^2}{\xi^4} = D \text{ on } \xi = 1$$

$$e^{2i\alpha}\frac{\partial^2}{\partial Z^2} = \frac{e^{2i\eta}}{D^2}\left[D\frac{\partial^2}{\partial \zeta^2} + 2e^{-2i\eta}\left\{e^{i\eta} - me^{-i\eta}\right\}\frac{\partial}{\partial \zeta}\right]$$

3.4 Circle Case: m = 0

In this case

$$\begin{bmatrix} \left\{\frac{1}{2}\gamma^2 - \frac{\partial}{\partial\xi} + \frac{\partial^2}{\partial\eta^2}\right\} & -\left\{1 + \frac{\partial}{\partial\xi}\right\}\frac{\partial}{\partial\eta} \\ \left\{1 + \frac{\partial}{\partial\xi}\right\}\frac{\partial}{\partial\eta} & \left\{\frac{1}{2}\gamma^2 - \frac{\partial}{\partial\xi} + \frac{\partial^2}{\partial\eta^2}\right\} \end{bmatrix} \begin{Bmatrix} \phi \\ \psi \end{Bmatrix} = 0$$

$$\phi = 2\,\phi_k\, J_{2k}\left[\frac{\lambda}{\xi}\right] \cos[2k\eta]$$

$$k = 1,2,3,\ldots$$

$$\psi = 2\,\psi_k\, J_{2k}\left[\frac{\gamma}{\xi}\right] \sin[2k\eta]$$

This agrees with [5, p. 219]. Note that the equations uncouple. In any nonlinear eigenvalue problem it is convenient to have a good first approximation to the eigenvalue. After some algebra we get (without approximation) the characteristic equation:

$$(4k^2 - 1)\,PQ - \frac{1}{2}\gamma^2[P + Q] + [4K^2 - \{\frac{1}{2}\gamma^2 - 4k^2\}^2] = 0 \quad (3.11)$$

where $$P = -\frac{\partial}{\partial\xi} \ln J_{2k}[\lambda/\xi]\Big|_{\xi = 1}$$

$$Q = -\frac{\partial}{\partial\xi} \ln J_{2k}[\gamma/\xi]\Big|_{\xi = 1}$$

The roots of this characteristic equation are the eigenvalues for the case of a circle. Note that this form of the characteristic equation requires only the derivative of the natural logarithm of the Bessel function and not the Bessel function itself. Since the asymptotic

expansion of the Bessel functions involve exponential terms this form is easier to work with. Numerical results showed that there are no eigenvalues in the range

$$0 \leq \gamma < \frac{9}{10} 2K$$

For $\gamma < 2K \equiv N$ and N large an approximation can be obtained using Debye's expansion [6, p. 366]

$$J_N[N \text{ sech } \alpha] = \frac{e^{N[\tanh \alpha - \alpha]}}{\sqrt{2\pi N \tanh \alpha}} \left[1 + O\left(\frac{1}{N \tanh \alpha}\right)\right]$$

Then

$$P = \left[\sqrt{N^2 - \lambda^2} + \frac{1}{2} \frac{\lambda^2}{N^2 - \lambda^2}\right] \left[1 + O\left(\frac{1}{N \tanh \alpha}\right)\right]$$

Substituting $x = \gamma/N$, $N = 2k$, $\lambda = \sqrt{\delta}\,\gamma$ in (3.11) gives

$$\left[2 - x^2\right]^2 - 4\left[1 - \frac{1}{N^2}\right] \frac{P}{N} \frac{Q}{N} - \frac{4}{N^2} + \frac{2x^2}{N} \left[\frac{P}{N} + \frac{Q}{N}\right] = 0 \qquad (3.12)$$

Substituting for P and Q using Debye's expansion gives:

$$\left[2 - x^2\right]^2 - 4\sqrt{1 - \delta x^2}\,\sqrt{1 - x^2}$$

$$= \frac{4x^2}{2N} \left[\frac{\sqrt{1 - \delta x^2}}{1 - x^2} + \frac{\delta\sqrt{1 - x^2}}{1 - \delta x^2} - \frac{1}{2}\left\{\sqrt{1 - x^2} + \sqrt{1 - x^2}\right\}\right] + O\left(\frac{1}{N^2}\right) \qquad (3.13)$$

As $N \to \infty$ this reduces to the Rayleigh equation:

$$(2 - x^2)^2 - 4\sqrt{1 - \delta x^2}\,\sqrt{1 - x^2} = 0$$

which has a real root[1] at x = C:

$$C = 0.934 \text{ if } \delta = \frac{1}{4}\ ,\ \nu = \frac{1}{3}$$

Expanding (3.13) in Taylor series about this root (x = C) gives a second approximation

$$\gamma = NC\left[1 + \frac{1}{2N\sqrt{1 - C^2}} + \frac{1}{N}\,O(\sqrt{1 - C^2}) + O\left[\frac{1}{N^2}\right]\right] \qquad (3.14)$$

Since C ≐ 1 this gives a useful approximation[2] to the order $\frac{1}{N}$ term, and the expression

$$\gamma \doteq NC\left[1 + \frac{1}{2N\sqrt{1 - C^2}}\right]$$

gives a good (four digit accuracy) first approximation to the lowest root for each N. For the case $\nu = 0.333$,

$$\gamma \doteq 0.934N\,[1 + 1.40/N]$$

It should be pointed out that if in the Debye expansion $N\alpha \to 0$ then the expansion is not valid. For the case here:

$$\text{Cosh } \alpha = \frac{N}{\gamma} \doteq \frac{1}{C}$$

and

$$\tanh \alpha \doteq \sqrt{1 - C^2} \doteq 0.357$$

---

[1] In the notation here, C is the quotient of the Rayleigh wave speed C_R to the shear wave C_S speed. See [20, p. 181].

[2] In the notation here, ≐ means approximately equal to.

in which case N tanh α is not small for large N, and the Debye expansion is valid.

The first term in (3.14) was obtained by Viktorov [22] in 1958. He also provided a complicated formula for the second term in (3.14). Here, noting that only the derivative of the logarithm of the Bessel functions is needed we give a simple formula for this second term which comes from the second term in P.

With the eigenvalues now known, it is interesting to locate the turning points of the governing differential equation

$$\left[\frac{d^2}{dR^2} + \frac{1}{R}\frac{d}{dR} - \frac{N^2}{R^2} + \lambda^2\right] \phi_N(R) = 0$$

The turning points separate the region of wave type behavior from exponential decay behavior and are located at

$$R = \frac{N}{\lambda} = \begin{cases} \dfrac{1}{\sqrt{\delta}\, C} \doteq 2.14 \text{ in } \phi \\ \\ \dfrac{1}{C} \doteq 1.07 \text{ in } \psi \end{cases}$$

We recall that the solution is valid for both interior and exterior problems with the agreement that in the exterior problem there is a remote circular boundary a large distance from the void.

A. Region interior to a circle $0 \leq R \leq 1$

We see that turning points do not occur (for the Rayleigh type root) and the solution has exponential decay everywhere. Hence the

disturbance is confined to a thin region near the surface R = 1. There are however other eigenvalues (as will be shown) that do not tend to the Rayleigh root as $N \to \infty$ and do produce turning points.

B. Region exterior to a circle $1 \leq R < \infty$

There are turning points at

$$R = \begin{cases} 2.14 & \text{in } \phi \\ 1.07 & \text{in } \psi \end{cases}$$

Hence, outside of a thin layer near the surface, the behavior is wave-like.

> Thus, a surface wave on a concave cylindrical surface will propagate with damping. This damping is connected with the radial emission of energy in the medium which conducts the surface wave. [22, p. 135]

We have constructed a remote circular boundary which reflects the radiated energy and the medium then vibrates without loss of energy.

If we do not have a remote circular boundary, then we must include Bessel functions of the second kind in the formulation. The eigenvalue can then be complex which gives the usual time dependent damping due to loss of energy by radiation. Viktorov has investigated this and showed that the imaginary part is small.

The five lowest eigenvalues for each N were obtained numerically and are plotted on the following graph. It is seen that the Rayleigh type roots are the fundamental frequencies and the higher eigenvalues tend to be separated from each other, but diverge from the fundamental

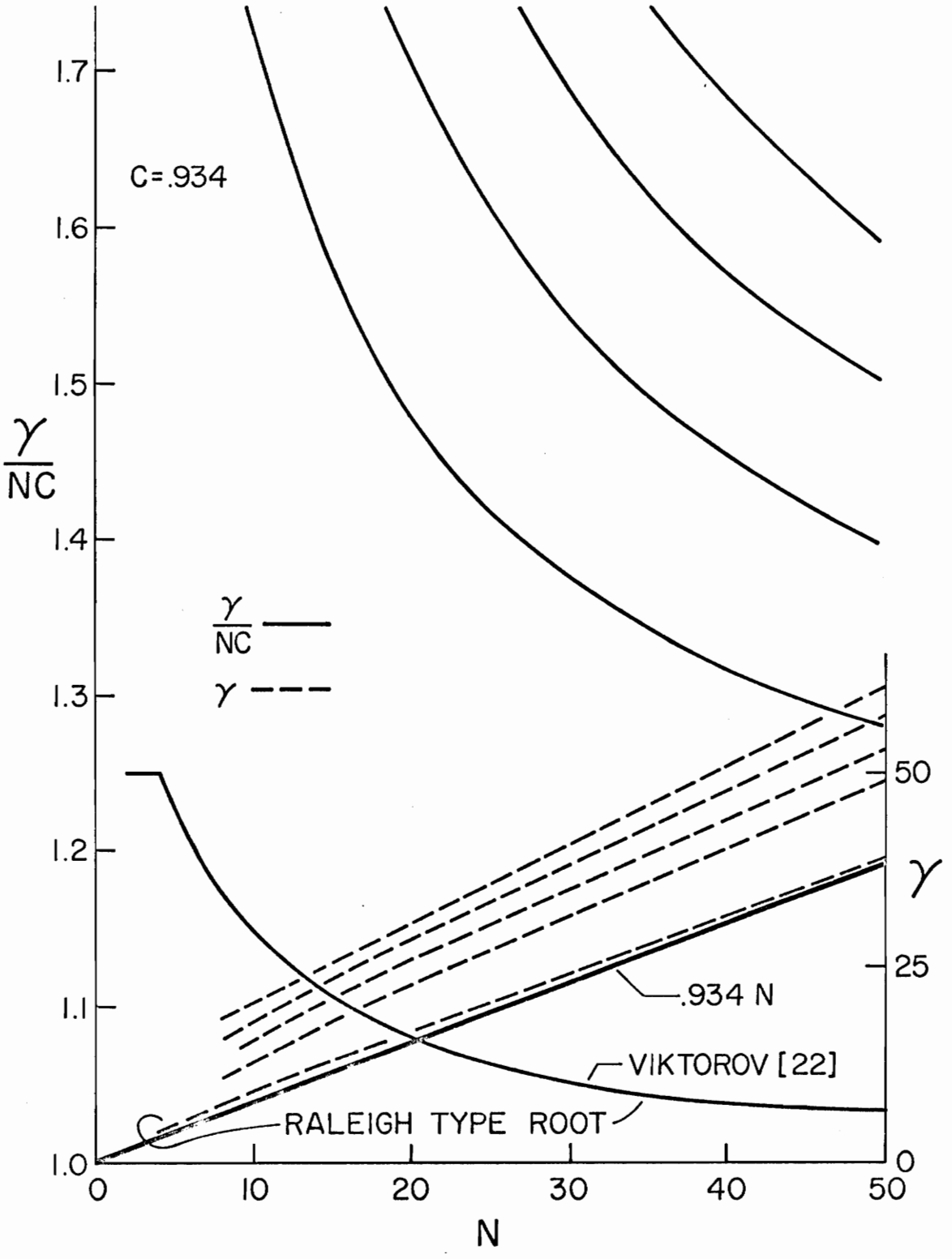

FIG. 11. EIGENVALUES FOR CIRCULAR BOUNDARY

root. (Note that both $\frac{\gamma}{NC}$ and γ are plotted vs. N.)

Note that from the graph of γ vs. N there are a few eigenvalues, which as a function of N, tend to be repeated. That is, with N as a variable the tendency is to have repeated or multiple eigenvalues.

Any of these roots could be used as a zeroth order solution for nonzero eccentricity. In the following, results for only the smallest eigenvalue will be presented:

$$\gamma = 2.349011$$

This corresponds to N = 2 or K = 1.

The results for the Rayleigh type root are in agreement with Viktorov for $N \geq 4$. Viktorov did not present results for N = 2. Apparently the knee in our curve is due to the order N^{-2} term which is not small for N = 2. Data was obtained and plotted only for even integer values of N.

A discussion of pertinent references may be found in [5, pp. 323-325].

3.5 The General Case; $0 \leq m \leq 1$

Performing the indicated differential operations (3.10) gives (3.15)

$$L_1\phi = (1-m^2) \sum_{j=0}^{\infty} A_j' \cos 2j\eta + \sum_{j=0}^{\infty} A_j \sum_{k=1}^{5} a_k(j) \cos 2(j-k+3)\eta$$

$$L_1\psi = (1-m^2) \sum_{j=1}^{\infty} B_j' \sin 2j\eta + \sum_{j=1}^{\infty} B_j \sum_{k=1}^{5} a_k(j) \sin 2(j-k+3)\eta$$

$$L_2\phi = (1-m^2) \sum_{j=1}^{\infty} 2jA_j \sin 2j\eta + \sum_{j=0}^{\infty} A_j' \sum_{k=1}^{3} b_k(j) \sin 2(j-k+2)\eta$$

$$-L_2\psi = (1-m^2) \sum_{j=1}^{\infty} 2jB_j \cos 2j\eta + \sum_{j=1}^{\infty} B_j' \sum_{k=1}^{3} b_k(j) \cos 2(j-k+2)\eta$$

where: $$( )' = \frac{\partial ( )}{\partial \xi} \Big|_{\xi = 1}$$

$$a_1(j) = -\frac{1}{2} m^2\gamma^2$$

$$a_2(j) = m[-(2j)^2 + 2j + \gamma^2(1 + m^2)]$$

$$a_3(j) = (2j)^2 (1 + m^2) - \frac{1}{2} \gamma^2[(1 + m^2)^2 + 2m^2]$$

$$a_4(j) = m[-(2j)^2 - 2j + \gamma^2(1 + m^2)]$$

$$a_5(j) = a_1(j)$$

$$b_1(j) = m[1 - 2j]$$

$$b_2(j) = (1 + m^2)\, 2j$$

$$b_3(j) = m[-1 - 2j]$$

It appears that the most efficient way to computer program this from the points of view of:

i) easiest coding, especially shift of indices

ii) easiest way to correct errors in FORTRAN

is to take advantage of certain patterns in the formulas by introducing the FORTRAN function subprogram:

$$C[i,j,k] = \frac{1}{2}\,\varepsilon_i\,[J_{j-i}(P)\,J_{j+i}(q) + (-1)^{k-1}\,J_{j+i}(P)\,J_{j-i}(q)]; \quad k = 1,2$$

$$= \frac{\partial}{\partial \xi}\,C[i,j,k-2] \qquad ; \quad k = 3,4$$

where $P = \frac{\lambda}{\xi}$; $q = m\lambda\xi$

$$\lambda \begin{cases} \sqrt{\delta}\,\gamma & ; \quad \text{if } k = 1,3 \\ \gamma & ; \quad \text{if } k = 2,4 \end{cases}$$

The differentiation indicated is performed analytically using the Bessel function differential recurrence relations after which, ξ is set equal to unity.

This leads to the partitioned matrix eigenvalue problem:

$$\left[\begin{array}{c|c} g^1 & g^4 \\ \hline g^2 & g^3 \end{array}\right] \left\{\begin{array}{c} \phi_k \\ \hline \psi_k \end{array}\right\} = 0 = [G]\,\{V\} \qquad (3.16)$$

in which: $N2 = N + 2$ and $\delta[j] = \begin{cases} 0 & j \neq 0 \\ 1 & j = 0 \end{cases}$

1. For: $1 \leq i,j \leq N + 1$

$$g^1_{ij} = (1 - m^2)\, C[i - 1, j - 1, 3]$$

$$+ \sum_{k=k_1}^{5} a_k\, C[i + k - 4, j - 1, 1]$$

$$+ a_5 \delta[i - 2]\, C[1, j - 1, 1]$$

$$+ a_2 \delta[i - 2]\, C[0, j - 1, 1]$$

$$+ a_5 \delta[i - 3]\, C[0, j - 1, 1]$$

$$k_1 = \begin{cases} 1 & i \geq 3 \\ 2 & i = 2 \\ 3 & i = 1 \end{cases}$$

$$a_1 = a_5 = -\frac{1}{2}\gamma^2 m^2$$

$$a_2 = m[-4(i - 2)^2 + 2(i - 2) + \gamma^2(1 + m^2)]$$

$$a_4 = m[-4(i)^2 - 2(i) + \gamma^2(1 + m^2)]$$

$$a_3 = 4(i - 1)^2\,(1 + m^2) - \frac{1}{2}\gamma^2[(1 + m^2)^2 + 2m^2]$$

2. For: $N + 2 \leq i \leq 2N + 1 \quad ; \quad 1 \leq j \leq N + 1$

$$g^2_{ij} = 2(i - 1 - N)\,(1 - m^2)\, C[i - 1 - N, j - 1, 1]$$

$$+ \sum_{k=1}^{3} b_k\, C[i - N + k - 3, j - 1, 3]$$

$$+ m\delta[i - N2]\, C[0, j - 1, 3]$$

$$b_1 = 3m - 2(i - 1 - N)\, m$$

$$b_2 = 2(i - 1 - N)\,(1 + m^2)$$

$$b_3 = -3m - 2(i - 1 - N)\, m$$

3. For: $N + 2 \leq i,j \leq 2N + 1$

$$g^3_{ij} = (1 - m^2)\, C[i - 1 - N,\ j - 1 - N,\ 4]$$

$$+ \sum_{k=k_1}^{5} a_k\, C[i - N + k - 4,\ j - 1 - N,\ 2]$$

$$- a_5\, \delta[i - N2]\, C[1,\ j - 1 - N,\ 2]$$

$$k_1 = \begin{cases} 1 & ;\quad i \geq N + 4 \\ 2 & ;\quad i = N + 3 \\ 3 & ;\quad i = N + 2 \end{cases}$$

$$a_1 = a_5 = -\frac{1}{2}\gamma^2 m^2$$

$$a_2 = m[-4(i - N - 2)^2 + 2(i - N - 2) + \gamma^2(1 + m^2)]$$

$$a_4 = m[-4(i - N)^2 - 2(i - N) + \gamma^2(1 + m^2)]$$

$$a_3 = 4(i - N - 1)^2\,(1 + m^2) - \frac{1}{2}\gamma^2[(1 + m^2) + 2m^2]$$

4. For: $1 \leq i \leq N + 1 \quad ; \quad N + 2 \leq j \leq 2N + 1$

$$g^4_{ij} = 2(i - 1)\,(1 - m^2)\, C[i - 1,\ j - 1 - N,\ 2]$$

$$+ \sum_{k=k_2}^{3} b_k\, C[i + k - 3,\ j - 1 - N,\ 4]$$

$$k_2 = \begin{cases} 1 & ; \quad i \geq 2 \\ 2 & ; \quad i = 1 \end{cases}$$

$$b_1 = 3m - 2(i - 1)\, m$$

$$b_2 = 2(i - 1)\,(1 + m^2)$$

$$b_3 = -3m - 2(i - 1)\, m$$

3.6 Perturbation Solution; ξ - η Coordinates

Insight into the nonlinear behavior of the coefficient matrix G and eigensolution γ,V can be obtained by considering a perturbation solution for small eccentricity parameter m. We have the matrix eigenvalue problem:

$$[G(\gamma,m)]\ \{V(m)\} = 0$$

in which G is nonlinear but analytic in both $\gamma(m)$ and m. Expanding in Taylor series gives:

$$G(\gamma,m) = \sum_{N=0}^{\infty} \frac{1}{N!} \left[(\gamma - \gamma_o) \frac{\partial}{\partial\gamma} + m \frac{\partial}{\partial m}\right]^N G(\gamma,m) \Bigg|_{\substack{m = 0 \\ \gamma = \gamma_o}}$$

$$= \sum_{N=0}^{\infty} \sum_{K=0}^{N} \frac{(\gamma - \gamma_o)^K}{K!} \frac{m^{N-k}}{(N - K)!} \frac{\partial^N G}{\partial\gamma^K \partial m^{N-K}} \Bigg|_{\substack{m = 0 \\ \gamma = \gamma_o}}$$

Now let

$$\gamma(m) = \gamma_o + m\gamma_1 + m^2\gamma_2 + m^3\gamma_3 + \ldots$$

$$V(m) = V_o + mV_1 + m^2V_2 + m^3V_3 + \ldots$$

$$\gamma_N = \frac{1}{N!} \frac{\partial^N \gamma}{\partial m^N}$$

$$V_N = \frac{1}{N!} \frac{\partial^N V}{\partial m^N}$$

$$G_N = \frac{1}{N!} \frac{\partial^N G}{\partial m^N}$$

$$H_N = \frac{1}{N!} \frac{\partial^N G}{\partial \gamma^N}$$

$$K = \frac{\partial^2 G}{\partial \gamma \partial m}$$

where derivatives are evaluated at $m = 0$ and $\gamma = \gamma_0$. Equating coefficients of powers of m to zero gives the sequence of equations:

$$G_0 V_0 = 0 \tag{3.17}$$

$$G_0 V_1 = L_1 V_0 \tag{3.18}$$

$$G_0 V_2 = L_1 V_1 + L_2 V_0 \tag{3.19}$$

$$G_0 V_3 = L_1 V_2 + L_2 V_1 + L_3 V_0 \tag{3.20}$$

$$\vdots$$

where: $L_1 = -G_1 - \gamma_1 H_1$

$$L_2 = -G_2 - \gamma_2 H_1 - \gamma_1 K - \gamma_1^2 H_2$$

$$L_3 = -G_3 - \gamma_3 H_1 - \gamma_2 K + O(\gamma_1)$$

The solution of $G_0 V_0 = 0$ is the solution for the unperturbed circle. As a numerical example we take the smallest eigenvalue: $\gamma_0 = 2.349011490$. Truncating the infinite system to seven equations and evaluating the partial derivatives numerically gives:

TABLE 1. TAYLOR SERIES COEFFICIENTS OF $G\{\gamma,m\}$.

$G_0 =$

-1.3096	0.0000	0.0000	0.0000	0.0000	0.0000	0.0000
0.0000	-0.0801	0.0000	0.0000	-0.0420	0.0000	0.0000
0.0000	0.0000	0.0434	0.0000	0.0000	0.5787	0.0000
0.0000	0.0000	0.0000	0.0015	0.0000	0.0000	0.0823
0.0000	-0.2342	0.0000	0.0000	-0.1229	0.0000	0.0000
0.0000	0.0000	-0.0529	0.0000	0.0000	-0.5870	0.0000
0.0000	0.0000	0.0000	-0.0016	0.0000	0.0000	-0.0826

$G_1 =$

-0.0008	-0.7647	-0.0000	-0.0000	-1.2045	-0.0001	-0.0000
6.6174	0.0003	-0.0776	-0.0000	0.0007	-0.9085	-0.0000
-0.0005	0.3324	0.0000	0.0010	-0.6290	0.0001	0.0578
0.0000	-0.0000	-0.0394	-0.0000	0.0001	-0.8756	-0.0000
-0.4233	-0.0000	0.0593	0.0000	0.0000	0.8690	0.0000
0.0000	0.3305	-0.0000	-0.0015	1.1714	-0.0001	-0.0593
-0.0000	-0.0000	0.0591	0.0000	-0.0002	0.9020	0.0000

$H_1 =$

-0.5264	0.0000	0.0000	0.0000	0.0000	0.0000	0.0000
0.0000	-0.3887	0.0000	0.0000	-0.8879	0.0000	0.0000
0.0000	0.0000	0.0610	0.0000	0.0000	0.7187	0.0000
0.0000	0.0000	0.0000	0.0036	0.0000	0.0000	0.1898
0.0000	-0.1120	0.0000	0.0000	0.5073	0.0000	0.0000
0.0000	0.0000	-0.0847	0.0000	0.0000	-0.7453	0.0000
0.0000	0.0000	0.0000	-0.0040	0.0000	0.0000	-0.1907

$G_2 =$

-7.8649	-0.0007	-0.0882	-0.0000	-0.0014	-0.8359	-0.0001
0.0031	2.6205	0.0001	-0.0053	7.2713	0.0011	-0.2704
-5.0910	-0.0003	0.0983	0.0000	-0.0023	1.0666	0.0001
0.0004	-0.2805	-0.0000	-0.0008	0.9399	-0.0000	-0.0983
-0.0000	-0.0264	-0.0000	0.0049	0.4543	0.0000	0.2664
0.4735	-0.0001	-0.0600	-0.0000	-0.0006	-0.9384	-0.0001
-0.0000	-0.1036	0.0000	0.0017	-1.5836	-0.0000	0.1030

$G_3 =$

-0.0009	-2.4071	-0.0001	-0.0040	-4.5361	-0.0012	-0.1757
10.4038	0.0008	0.2521	0.0000	0.0015	3.5156	0.0004
-0.0008	-0.8872	0.0000	0.0060	-7.7819	-0.0008	0.3334
1.1803	-0.0001	-0.0225	-0.0000	0.0022	-0.1477	-0.0001
-0.0022	0.0002	-0.0006	-0.0000	0.0007	0.1342	0.0000
-0.0003	-0.3159	0.0000	-0.0051	-1.9175	0.0005	-0.3205
-0.0523	0.0001	0.0006	0.0000	0.0012	-0.0010	0.0000

$K =$

-0.0006	-0.3972	-0.0000	-0.0000	0.8190	-0.0001	-0.0000
4.2307	0.0003	-0.1455	-0.0000	0.0005	-1.4798	-0.0001
-0.0005	0.8282	0.0000	0.0021	0.5654	0.0002	0.1108
0.0000	-0.0001	-0.0505	-0.0000	0.0001	-1.3732	-0.0000
-0.6782	-0.0000	0.1006	0.0000	0.0001	1.3534	0.0001
0.0001	0.2577	-0.0000	-0.0036	0.7292	-0.0002	-0.1167
-0.0000	-0.0000	0.1001	0.0000	-0.0002	1.4600	0.0000

Order m^0

$$G_0 V_0 = 0 \tag{3.17}$$

$$\gamma_0 = 2.349011490$$

$$\{V_0\} = \left\{ \begin{array}{r} 0.000 \\ -0.525 \\ 0.000 \\ 0.000 \\ \hline 1.000 \\ 0.000 \\ 0.000 \end{array} \right\} \leftarrow \text{line denotes partitioning between } \phi \text{ and } \psi \text{ coefficients}$$

Order m^1

$$G_0 V_0 = -G_1 V_0 - \gamma_1 H_1 V_0 \tag{3.18}$$

From the data for G_0, $-G_1 V_0$, $-H_1 V_0$ the first order perturbation equation (b) becomes:

$$\left[\begin{array}{rrrr|rrr} -1.309 & 0.000 & 0.000 & 0.000 & 0.000 & 0.000 & 0.000 \\ 0.000 & -0.080 & 0.000 & 0.000 & -0.042 & 0.000 & 0.000 \\ 0.000 & 0.000 & 0.043 & 0.000 & 0.000 & 0.579 & 0.000 \\ 0.000 & 0.000 & 0.000 & 0.001 & 0.000 & 0.000 & 0.082 \\ \hline 0.000 & -0.234 & 0.000 & 0.000 & -0.123 & 0.000 & 0.000 \\ 0.000 & 0.000 & -0.053 & 0.000 & 0.000 & -0.587 & 0.000 \\ 0.000 & 0.000 & 0.000 & -0.002 & 0.000 & 0.000 & -0.083 \end{array}\right] \left\{ V_1 \right\}$$

$$= \left\{ \begin{array}{r} 0.803 \\ -0.000 \\ 0.803 \\ -0.000 \\ \hline -0.000 \\ -0.998 \\ 0.000 \end{array} \right\} + \gamma_1 \left\{ \begin{array}{r} -0.000 \\ 0.684 \\ -0.000 \\ -0.000 \\ \hline -0.566 \\ -0.000 \\ -0.000 \end{array} \right\} = \{A\} + \gamma_1 \{B\}$$

This equation is written in full and the matrix G_0 repeated since it is the position of the nonzero elements that is now of importance. We cannot invert G_0 since it is singular. The usual procedure in this case is to determine γ_1 by the solvability condition [7, pp. 288, 302]. That is, choose γ_1 such that the right hand side of the equation

is orthogonal to the adjoint G_0^* of the left side operator G_0. That is:

$$G_0^*(A + \gamma_1 B) = 0$$

Due to the sparseness of the matrix G_0, a solution can be obtained by simply setting:

$$\gamma_1 = 0$$

$$\{V_1\} = 0 \quad ; \quad \text{except for rows 1, 3, 6}$$

That is $\{V_1\}$ has the same form as the right hand side with $\gamma_1 = 0$. The reduced coefficient matrix is then nonsingular and we get:

$$\{V_1\} = \begin{Bmatrix} -0.614 \\ 0.000 \\ 20.568 \\ 0.000 \\ \hline 0.000 \\ -0.153 \\ 0.000 \end{Bmatrix} + \{\tilde{V}\}$$

where $\{\tilde{V}\}$ is the homogeneous solution which can either be absorbed into $\{V_0\}$ or arbitrarily set equal to zero.

It is concluded that:

i) the perturbed eigenvalue γ_1 is zero

ii) the perturbed eigenvector V_1 is orthogonal to the unperturbed eigenvector V_0

iii) since: $||V_1|| \gg ||V_0||$ the result:

$$V(m) = V_0 + m\, V_1 + \ldots$$

is probably only valid for small m (about: $0 \leq m < 0.05$). See [10, p. 128] for a similar conclusion.

The property that $\gamma_1 = 0$ is due to the choice of the mapping function:

$$Z = \hat{R}\left[\frac{1}{\zeta} + m\,\zeta\right]$$

and to the condition that both geometry and solution have period π in η. In the solutions here, $\hat{R} \equiv 1$. If instead one held (for example) the semi-major axis (a) fixed then:

$$\hat{R} = \frac{a}{1 + m}$$

and

$$\gamma = 2.349\,\frac{1 + m}{a}$$

In which case $\gamma_1 \neq 0$.

The property that the perturbed eigenvector V_1 is large is characteristic of solutions of the wave equation with perturbed circle boundaries.[1] This is due to the tendency of the solution corresponding to different orders (N) of the Bessel functions to have at least a few nearly equal eigenvalues; see graph on page 53. Also, inspection of the coefficient matrix G_0 (p. 62) confirms that G_0 has many illconditioned[2] subsystems each of which render G_0 illconditioned.

---

[1] G. Birkhoff, colloquium talk, V.P.I. & S.U., Dec., 1974.

[2] By illconditioned we mean nearly zero determinant.

Furthermore, the eigenvectors of these subsystems tend to coalesce for large N. Therefore, the tendency is to have nearly repeated subsystem eigenvectors corresponding to a given eigenvalue which also tends to be repeated. The results and conclusions here agree with the statement by J. H. Wilkinson

> We expect the eigenvector corresponding to a simple eigenvalue λ_1 to be very sensitive to perturbations in G if λ_1 is close to any of the other eigenvalues and indeed this is true. [12, p. 70]

For an elementary example, see pages 113-4 on contour curves and stress invariants.

Order m^2

$$G_o V_2 = -G_1 V_1 - G_2 V_o - \gamma_2 H_1 V_o \qquad (3.19)$$

The vanishing of γ_1 simplifies the second order perturbation equation. From the data for $-G_1 V_1 - G_2 V_o$ and $-H_1 V_o$ the second order perturbation equation becomes:

$$\left[\begin{array}{ccccccc}
-1.309 & 0.000 & 0.000 & 0.000 & 0.000 & 0.000 & 0.000 \\
0.000 & -0.080 & 0.000 & 0.000 & -0.042 & 0.000 & 0.000 \\
0.000 & 0.000 & 0.043 & 0.000 & 0.000 & 0.579 & 0.000 \\
0.000 & 0.000 & 0.000 & 0.001 & 0.000 & 0.000 & 0.082 \\
\hline
0.000 & -0.234 & 0.000 & 0.000 & -0.123 & 0.000 & 0.000 \\
0.000 & 0.000 & -0.053 & 0.000 & 0.000 & -0.587 & 0.000 \\
0.000 & 0.000 & 0.000 & -0.002 & 0.000 & 0.000 & -0.083
\end{array}\right] \left\{ V_2 \right\}$$

$$= \left\{\begin{array}{c} 0.000 \\ -0.379 \\ 0.001 \\ \underline{-0.410} \\ -1.814 \\ 0.000 \\ 0.451 \end{array}\right\} + \gamma_2 \left\{\begin{array}{c} -0.000 \\ 0.684 \\ -0.000 \\ \underline{-0.000} \\ -0.566 \\ -0.000 \\ -0.000 \end{array}\right\} \equiv \{A\} + \gamma_2 \{B\}$$

The small nonzero rows on the right hand side were found to be proportional to the finite difference step size. They were attributed to finite difference error and neglected. This applies to all orders. Following the example of the order m^1 solution, set:

$$\{V_2\} = 0 \quad \text{except for rows } 2, 4, 5, 7$$

to get the two uncoupled subsystems:

$$\begin{bmatrix} G_{22} & G_{25} \\ G_{52} & G_{55} \end{bmatrix} \begin{Bmatrix} V_2 \\ V_5 \end{Bmatrix} = \begin{Bmatrix} A_2 \\ A_5 \end{Bmatrix} + \gamma_2 \begin{Bmatrix} B_2 \\ B_5 \end{Bmatrix}$$

$$\begin{bmatrix} G_{44} & G_{47} \\ G_{74} & G_{77} \end{bmatrix} \begin{Bmatrix} V_4 \\ V_7 \end{Bmatrix} = \begin{Bmatrix} A_4 \\ A_7 \end{Bmatrix}$$

The determinant of the coefficients of the first subsystem is zero. Applying the solvability condition:

$$\begin{vmatrix} G_{22} & A_2 + \gamma_2 B_2 \\ G_{52} & A_5 + \gamma_2 B_5 \end{vmatrix} = 0$$

to the first subsystem and inverting the coefficient matrix of the second subsystem gives:

$$\gamma_2 = -0.274516$$

$$\{V_2\} = \begin{Bmatrix} 0.000 \\ 7.081 \\ 0.000 \\ \underline{-372.143} \\ 0.000 \\ 0.000 \\ 1.718 \end{Bmatrix} + \tilde{\{V\}}$$

This value of γ_2 agrees with the results of the methods of Lanczo and Gauss-Jordan reduction to be discussed later.

Order m^3

$$G_o V_3 = -G_1 V_2 - (G_2 + \gamma_2 H_1) V_1 - (G_3 + \gamma_2 k) V_o - \gamma_3 H_1 V_o \qquad (3.20)$$

Again, the vanishing of γ_1 greatly simplifies the right hand side. The number of equations must now be increased from seven to nine for this order. Evaluation of the right hand side gives:

$$[G_o]\{V_3\} = \begin{Bmatrix} 5.919 \\ -0.002 \\ 0.617 \\ -0.001 \\ \underline{0.100} \\ -0.000 \\ 0.058 \\ -0.001 \\ -0.104 \end{Bmatrix} + \gamma_3 \begin{Bmatrix} -0.000 \\ 0.684 \\ -0.000 \\ -0.000 \\ \underline{-0.000} \\ -0.566 \\ -0.000 \\ -0.000 \\ -0.000 \end{Bmatrix}$$

$$\equiv \{A\} + \gamma_3\{B\}$$

As before, set:

$$\gamma_3 = 0$$

$$\{V_3\} = 0 \qquad \text{except for rows } 1, 3, 5, 7, 9$$

to get the following three uncoupled subsystems:

$$G_{11}\ V_1 = A_1$$

$$\begin{bmatrix} G_{33} & G_{37} \\ G_{73} & G_{77} \end{bmatrix} \begin{Bmatrix} V_3 \\ V_7 \end{Bmatrix} = \begin{Bmatrix} A_3 \\ A_7 \end{Bmatrix}$$

$$\begin{bmatrix} G_{55} & G_{59} \\ G_{95} & G_{99} \end{bmatrix} \begin{Bmatrix} V_5 \\ V_9 \end{Bmatrix} = \begin{Bmatrix} A_5 \\ A_9 \end{Bmatrix}$$

Inversion gives:

$$\{V_3\} = \begin{Bmatrix} -4.522 \\ 0.000 \\ -76.837 \\ 0.000 \\ \underline{6337.394} \\ 0.000 \\ 6.824 \\ 0.000 \\ -3.401 \end{Bmatrix}$$

Order m^4

Equating coefficients of m^4 with $\gamma_1 = 0 = \gamma_3$ gives:

$$G_o\ V_4 = -G_1\ V_3 - (G_2 + \gamma_2\ H_1)\ V_2$$

$$- (G_3 + \gamma_2 K)\ V_1$$

$$- (G_4 + \gamma_4\ H_1 + \gamma_2^{\,2}\ H_2 + \gamma_2\ L)\ V_o$$

where $$L \equiv \frac{1}{2} \frac{\partial^3 G}{\partial m^2 \partial \gamma}$$

Evaluation of the right hand side gives:

$$[G_0]\{V_4\} = \begin{Bmatrix} 2.690 \\ -1609.908 \\ 6.010 \\ -296.775 \\ 0.271 \\ \hline -130.979 \\ 1.433 \\ 418.254 \\ -0.510 \end{Bmatrix} + \gamma_4 \begin{Bmatrix} -0.000 \\ 0.684 \\ -0.000 \\ -0.000 \\ -0.000 \\ \hline -0.566 \\ -0.000 \\ -0.000 \\ -0.000 \end{Bmatrix}$$

Due to loss of precision the solution of this order gave drastically incorrect results. We can note however that the solution of this order probably has the same character as the order m^2 solution and that $\gamma_4 \neq 0$. The complete solution accurate through order m^3 reads:

$$\gamma = 2.3490115 - 0.274516\ m^2 + O(m^4)$$

$$\{V(m)\} = \begin{Bmatrix} 0.0000 \\ -0.5246 \\ 0.0000 \\ 0.0000 \\ 0.0000 \\ 0.0000 \\ \hline 1.0000 \\ 0.0000 \\ 0.0000 \\ 0.0000 \\ 0.0000 \end{Bmatrix} + m \begin{Bmatrix} -0.6136 \\ 0.0000 \\ 20.5676 \\ 0.0000 \\ 0.0000 \\ 0.0000 \\ \hline 0.0000 \\ -0.1532 \\ 0.0000 \\ 0.0000 \\ 0.0000 \end{Bmatrix} + m^2 \begin{Bmatrix} 0.0000 \\ 7.0817 \\ 0.0000 \\ -372.1439 \\ 0.0000 \\ 0.0000 \\ \hline 0.0000 \\ 0.0000 \\ 1.7189 \\ 0.0000 \\ 0.0000 \end{Bmatrix} + m^3 \begin{Bmatrix} -4.5224 \\ 0.0000 \\ -76.8375 \\ 0.0000 \\ 6337.3944 \\ 0.0000 \\ \hline 0.0000 \\ 6.8245 \\ 0.0000 \\ -3.4019 \\ 0.0000 \end{Bmatrix}$$

$$+ O(m^4) \qquad (3.21)$$

To clarify the notation, the first few terms of the solution read:

$$\phi(R,\theta) = -0.52\ J_2[\lambda R]\ \mathrm{Cos}(2\theta)$$

$$+ m[-0.61\ J_0(\lambda R) + 20.57\ J_4(\lambda R)\ \mathrm{Cos}(4\theta)] + \ldots$$

$$\psi(R,\theta) = 1.00\ J_2\ (\gamma R)\ \sin\ (2\theta)$$

$$- 0.15\ m\ J_4\ (\gamma R)\ \sin\ (4\theta) + \ldots$$

The procedure could theoretically be carried to higher orders. However, at each order about three or four digits of accuracy are lost due to:

i) finite difference approximation to the derivatives

ii) extensive cancellation in the computations

As a practical matter the procedure (per se) cannot be continued on a machine limited to sixteen digit precision. However, a modification of the procedure will be presented that will enable a fourth order solution.

It is concluded that this formulation permits a unified attack on all order perturbations but sacrifices accuracy in the result if finite differences are used to evaluate the derivatives. Analytical evaluation of the derivatives is possible but would lead to lengthy equations even for order m^2 for problems with Cauchy (mixed) type boundary conditions.

It is dangerous to extrapolate results for larger m; however the eigenvalue is certainly analytic in m and probably slowly varying in m. Since:

$$\gamma = \gamma_0 + m^2\gamma_2 + m^4\gamma_4 + O(m^5)$$

it is suggested that γ is a function of m^2 only. Also, γ appears in the final matrix formulation to even powers only. This suggests that:

$$\gamma = \frac{\gamma_o}{\hat{R}}\sqrt{1 + 2\,\frac{\gamma_2}{\gamma_o}\,m^2 + \frac{\gamma_2^2 + 2\gamma_4\gamma_o}{\gamma_o^2}\,m^4 + O(m^4)} \qquad (3.22)$$

where γ_o = eigenvalue for m = 0 (circle case), with $\hat{R} = 1$

$\hat{R} = \hat{R}(m) = \frac{a}{1+m}$ where a is the semi-major axis

It turns out that

$$2\,\frac{\gamma_2}{\gamma_o} = -0.233729$$

$$= -\frac{\gamma_o}{10} \text{ to three digit accuracy}$$

It would be interesting to have solutions for other orders of the Bessel functions in order to estimate the functional nature of the m^2 term in γ. A formula for large m which corresponds to the interior problem can be obtained by reinterpreting the mapping function:

$$Z = \hat{R}\left[\frac{1}{\zeta} + m\zeta\right] = m\hat{R}\left[\zeta + \frac{1}{m}\,\frac{1}{\zeta}\right]$$

and the property of the solution herein that the interior and exterior problems have the same eigenvalue. The result is:

$$\gamma = \frac{\gamma_o}{m\hat{R}}\sqrt{1 + 2\,\frac{\gamma_2}{\gamma_o}\,\frac{1}{m^2} + O(m^{-4})} \qquad (3.23)$$

See page 100 for numerical results of γ vs. m. It is suspected that $\gamma(m)$ is an elliptic integral function of m. It is also a function of the ratio of the wave speeds:

$$\left[\frac{C_S}{C_P}\right]^2 \equiv \delta \equiv \frac{1 - 2\nu}{2 - 2\nu}$$

or of the Poisson ratio ν.

It is interesting to note that as $m \to 1$ the ellipse degenerates into a slit. In this case the shear stress $\sigma_{\xi\eta}$ on the free surface is automatically zero by the symmetry conditions. Also, the coefficients of the Lame' ψ function are small compared to the coefficients of the Lame' ϕ function. This suggests that for the slit case, the ψ function drops out of the problem entirely. We would then have the simplified boundary value problem

$$\left[\frac{1}{\xi}\frac{\partial}{\partial\xi}\,\xi\,\frac{\partial}{\partial\xi} + \frac{1}{\xi^2}\frac{\partial^2}{\partial\eta^2} + \lambda^2\left\{\frac{1}{\xi^4} - \frac{2m}{\xi^2}\,\mathrm{Cos}\,2\eta + m^2\right\}\right]\phi(\xi,\eta) = 0$$

$$\left[\sin\eta\,\frac{\partial}{\partial\eta}\,\frac{1}{\sin\eta}\,\frac{\partial}{\partial\eta} + \frac{\gamma^2}{2}\right]\phi(1,\eta) = 0$$

If one interprets this standing wave solution as a combination of traveling waves, then this solution corresponds to dilatational waves striking the slit at grazing incidence and the remote circular boundary at normal incidence. It is shown in [25] that both dilatational (P) and shear (S) waves at grazing incidence to an elastic half space generate evanescent surface waves which are called PY and SY waves respectively. It is interesting to observe that these PY and SY waves are obtained as a limiting process in which the eigenvector (V) becomes large while the angle of incidence (e) becomes small such that:

$$\lim_{e \to 0} [Ve] = \text{finite constant}$$

Reflection and refraction of plane waves is discussed further in [26], [27].

Recall that in the solution here the ϕ part of the eigenvector became increasingly large as $m \to 1$. The question arises as to the nature of the limiting process of the solution here as $m \to 1$. For $m = 1$ (the slit case) the $\sigma_{\xi\eta}$ boundary condition is automatically satisfied by our symmetry conditions. That is, g^2 and g^3 of (3.16) are identically zero for $m = 1$. This results in the possibility of choosing the coefficient ϕ_k, ψ_k in a wide variety of ways. The one possibility discussed in detail here is that ψ_k tend to zero as $m \to 1$.

If either ϕ or ψ does not drop out of this formulation of the problem as $m \to 1$, then there is not necessarily a unique solution and perhaps a wealth of solutions. One possibility is Mode II deformation ($\phi \sim \sin 2k\theta$, $\psi \sim \text{Cos } 2k\theta$). In this case ϕ would perhaps drop out of the problem as $m \to 1$. One might then expect shear stress concentrations.

It is difficult at this point to enumerate and describe all of the possible types of behavior as $m \to 1$. This is because the formulation is nonlinear in both γ and m and because of the possibility of branching or bifurcation of the solution at each order or power of m.

Branching of both eigenvalue and eigenvector is most easily demonstrated by considering the transverse vibration of a nearly circular membrane with fixed edge boundary conditions. The presence of Dirichlet boundary conditions rather than the more complicated boundary conditions (3.9a,b) simplifies the analysis.

Since $\gamma_1 = 0$, the solution here does not bifurcate at the first order. It is however possible that the solution does bifurcate at the second order since $\gamma_2 \neq 0$. In any case, the solution here is a solution correct through order m^3 since it was found that the error:

$$\{E\} = [G]\{V\} \tag{3.24}$$

was proportional to m^4. Also, the quotient of the maximum boundary stress to the maximum field stress was less than 1.0% for all m in the range $0 \leq m \leq 1$. This tends to suggest that the solution is useful for all m. See graph, page 104, for further error analysis.

An approximate fourth order solution can be obtained by expanding (3.24) in Taylor series about some point m_0

$$E(m) = E(m_0) + (m - m_0)\left[\frac{\partial G}{\partial m} + \frac{\partial \gamma}{\partial m}\frac{\partial G}{\partial \gamma}\right] V(m_0)$$

$$+ (m - m_0)\, G(m_0)\frac{\partial V}{\partial m} + O[(m - m_0)^2]$$

The point m_0 must be chosen such that:

i) the order m^4 error dominates the order m^5 error (requires small m_0)

ii) m_0 must be sufficiently large to enable division by m_0^3.

To see this, set:

$$\Gamma \equiv \left.\frac{\partial \gamma}{\partial m}\right|_{m = m_o}$$

and:

$$\gamma = \gamma_o \sqrt{1 + am^2 + bm^4 + \ldots}$$

where:

$$\gamma_o = 2.3490$$

$$a = -0.2337$$

$$b = \text{unknown}$$

Solving for b gives:

$$b \doteq [\Gamma/\gamma_o - am_o + a^2 m_o{}^3/2]/2/m_o{}^3 + O(m_o)$$

3.7 Numerical Solution for Arbitrary Eccentricity

The perturbation method provides a solution for small eccentricity ($0 \leq m < .5$ for eigenvalue, $0 \leq m < .05$ for eigenvector). The object here is to obtain a solution for larger eccentricity. The results of the perturbation method show that the eigenvector and number of equations required are fast varying functions of m. This suggests difficulty in obtaining numerical solutions for large m by any method.

Four numerical algorithms and several modifications thereof were used in attempts to obtain solutions for m in the range $0 \leq m < 1.0$. The relative merits of these algorithms will be discussed in some detail for comparison with each other and to clarify why the algorithm breaks down for large m. Numerical results by two methods will be presented. It is concluded that the separation of variables in the image plane may lead to an intractable matrix eigenvalue problem for large eccentricity ($0.6 < m \leq 1.0$). It is also concluded that the perturbation method gives more information than the numerical methods described next.

The nonlinear matrix eigenvalue problem to be considered:

$$[G_{ij}]\{V_j\} = 0 \quad ; \quad i,j = 1,2,\ldots,N$$

has the following properties:

a) the order (N) is small; 5 to 50 equations

b) G_{ij} is analytic but nonlinear in both the eigenvalue[1] (γ) and eccentricity parameter (m)

c) each G_{ij} is a quadratic combination of as many as ten Bessel functions

d) the eigenvalues tend to coalesce

e) the solution for small m is known

f) G_{ij} is nonsymmetric

g) only one eigensolution is required, not the complete eigenspectrum.

As a consequence of statements a), b) and c) above, most of the computer time will be consumed in evaluating Bessel functions rather than solving the system of N equations. Therefore, the algorithm should require as few iterations (in the nonlinear sense) as possible for computational efficiency.

As a consequence of d) an algorithm that depends on the eigenvalues being well separated, i.e., power method [17, p. 474] cannot be expected to work well. An exception to this is if one has a very good estimate (γ_0) of the eigenvalue (γ) and then shifts or translates it ($\gamma = \gamma_0 + \varepsilon$) so that one is then seeking an ε close to zero.

As a consequence of e), iterative methods such as Newton or Lanczo [17, p. 500] are suggested. However, since the eigenvector is fast-varying in m, small steps (0.1) in m are required to ensure

---

[1]The eigenvalue γ appears only in the combination γ^2 and numerically γ^2 is taken as the eigenvalue. Doing this accelerates convergence [17, p. 344].

stability.

As a consequence of the perturbation solution it should not be surprising to find that any method does not work as well as one would like in pursuit of the eigenvector.

The following algorithms were tried:

a) Power method

b) QR transformation

c) Lanczos' method

d) Gauss-Jordan reduction

Each method and certain modifications thereof will now be summarized, after which their relative merits will be compared. Consult [17, p. 521] for "biographical notes" on the origins of these and other methods.

3.7.1 Power Method

It is convenient to introduce the notation

$$G(\gamma) = A + \varepsilon B + \varepsilon^2 C + \ldots$$

where $\varepsilon = \gamma - \gamma_o$

$A = G(\gamma_o)$

$$B = \left.\frac{\partial G}{\partial \gamma}\right|_{\gamma=\gamma_o} \qquad C = \frac{1}{2!}\left.\frac{\partial^2 G}{\partial \gamma^2}\right|_{\gamma=\gamma_o}$$

to get

$$[A]\{V\} = -\varepsilon[B]\{V\} - \varepsilon^2[C]\{V\}.$$

If a = adjoint of A

α = determinant of A

$K = -aB$

$\varepsilon = \alpha\mu$

then

$$\{V\} = \mu[K]\{V\} \tag{3.25}$$

Equation (3.25) can be solved by the power method [17, p. 474] and is guaranteed to converge to the smallest eigenvalue μ provided μ is real valued [17, p. 477]. In the case here μ approaches zero as α approaches zero. Note that division by α was not required and that μ is not necessarily small even though it is the smallest eigenvalue. This method gives second order (quadratic) convergence, but does require iteration to get the eigenvector. This is a form of inverse iteration [15] in which the equivalent of the inverse of A is required.

Advantages of this method:

a) quadratic convergence

b) conceptually simple to implement

c) does not require division by the determinant

Disadvantages of this method:

a) requires calculation of the adjoint

b) requires iteration to get eigenvector

3.7.2 Gaussian-Elimination vs. Gauss-Jordan Reduction

In considering other methods it turns out to be important to distinguish between the methods of Gaussian elimination and Gauss-

Jordan reduction [17, p. 400]. Both methods are used to effect matrix inversion and use the transformation:

$$A_{ij} \leftarrow A_{ij} - A_{i\beta}\, A_{\alpha i}/A_{\alpha\beta} \quad ; \quad i \neq \alpha,\ j \neq \beta$$

where $A \leftarrow B$ means replace A by B

α = pivot row

β = pivot column.

This transformation puts zeros in either (or both) the α-row and/or the β-column except for the pivot element (α,β). By Gaussian elimination either rows or columns (not both) are eliminated which reduces A_{ij} to triangular form. By Gauss-Jordan reduction both rows and columns are eliminated which reduces A_{ij} to diagonal form. Both of these methods are very stable provided one uses complete or at least partial pivoting [17, p. 405]. In comparison:

> At first glance it might seem that Gauss-Jordan reduction is to be preferred to Gaussian elimination, but.... for large N (order) the Gauss-Jordan reduction requires about 50 percent more operations than Gaussian elimination. [17, p. 401]

However, for problems of the type here, the order is small and the number of operations by either version is small compared to the number of operations required to calculate the G_{ij} (due to the Bessel functions). A disadvantage with Gaussian elimination is that the subsequent calculation of the eigenvector requires back substitution [17, p. 400] which can be unstable [13]. We recall that it is primarily the eigenvector we seek and with which we expect difficulty.

Wilkinson [13] has devised a procedure by which back substitution can be rendered stable by employing an elimination scheme using maximum pivots. This however requires further coding and computation which tends to nullify the above advantage of Gaussian elimination over Gauss-Jordan reduction.

An advantage of Gauss-Jordan reduction is that it can be coded just as easily as Gaussian elimination. It is concluded, for problems of the type considered here, that Gauss-Jordan reduction is preferred to Gaussian elimination. This is an important conclusion since it precludes the utility of the QR method (since it employs Gaussian elimination) which will nevertheless be discussed next.

3.7.3 The QR Transformation

The basis of this method [17, p. 516] is to decompose G_0 into the product QU where Q is orthogonal and U is upper triangular such that

$$A = QU \quad ; \quad Q^TQ = I$$

to get

$$[U]\{V\} = -\varepsilon[Q]^T[B]\{V\}.$$

Since U is upper triangular its inverse P exists (for $\varepsilon \neq 0$) and can be calculated by back substitution to get:

$$\{V\} = [P]\{X\}$$

$$\{X\} = -[a^T][B][P]\{X\}$$

This form could be arrived at directly with fewer calculations by using Gauss-Jordan reduction.

Advantages of this method:

a) all eigenvalues (eigenspectrum) are obtained if and only if B is diagonalized

Disadvantages of this method:

a) the calculation of Q,U is lengthy if Gaussian elimination is not first used to reduce G_0 to triangular form [17, p. 517]

b) requires more computer coding than Gauss-Jordan reduction (50%)

c) requires back substitution (unstable)

3.7.4 Lanczos' Method

We have seen that any method for nonlinear eigenvalue problems involves iteration to find the eigenvalue. Iteration of the Lanczos method seems ideally suited for problems in which a good initial estimate of the eigenvector is available; especially if the order (N) is large. There are further advantages for problems of the type considered here.

Consider the linearized matrix eigenvalue problem:

$$AV + \varepsilon BV = O(\varepsilon^2) \tag{3.26}$$

The method of Lanczos for nonsymmetric matrices is to construct a similarity transformation

$$p = Y^T A X \tag{3.27}$$

such that: p = symmetric tridiagonal (codiagonal) matrix

$Y^T X$ = identity matrix (the X,Y are biorthogonal sequences of vectors)

Then, the adjoint p* of p can economically be computed to get

$$Z = \mu Q Z \tag{3.28}$$

where $Q = -p^* Y^T B X$

Equation (3.28) can be solved by the power method for μ, Z. After which

$$\varepsilon = \mu \rho \quad ; \quad \rho = \text{determinant of } p$$

$$V = XZ$$

If A is symmetric, then Y = X. The column vectors X_i, Y_i of X,Y are constructed according to the recurrence relations [17, p. 500]

$$\begin{aligned} X_{i+1} &= A X_i - b_i X_i - C_i X_{i-1} \\ Y_{i+1} &= A^T Y_i - b_i Y_i - C_i Y_{i-1} \end{aligned} \quad ; \quad i = 1,2,\ldots,N-1$$

where

X_o, Y_o = zero

X_1, Y_1 = arbitrary

$b_i = Y_i^T A X_i / d_i$

$C_i = d_i / d_{i-1}$; $C_1 = 0$

$d_i = Y_i^T X_i$

The algorithm proceeds as follows

$$X_1,\ Y_1 = \text{arbitrary}$$

$$d_1 = Y_1^T X_1$$

$$b_1 = Y_1^T A X_1 / d_1$$

$$X_2 = AX_1 - b_1 X_1$$

$$Y_2 = A^T Y_1 - b_1 Y_1$$

$$d_2 = Y_2^T X_2$$

$$b_2 = Y_2^T A X_2$$

$$C_2 = d_2/d_1$$

$$\vdots$$

It is seen that if X_1 is close to an eigenvector of A then AX_1 is nearly null, and hence X_2, X_3,... are nearly null. Thus in an actual numerical application, the Lanczos method may break down due to loss of precision when $\sqrt{d_i/d_1} < 10^{-NP}$ where NP = number of significant digits available (NP = 16 for the numerical results here).

> A vital aspect of the calculation of the eigenvalues of nonsymmetric matrices is the stability of the calculation with respect to roundoff errors. [17, p. 500]

Note that the method provides a fairly precise estimate or criterion of when the procedure can no longer be continued and that normalization [14] does not significantly alter the loss of precision.[1]

---

[1] Normalization can reduce the loss of precision to a small extent depending on how the machine performs roundoff.

This situation can be exploited by observing that the d_i tend to zero while the b_i tend to an indeterminant quotient. Suppose, for example, that $\sqrt{d_3/d_1} < 10^{-NP}$. The p matrix reads:

$$[p] = \begin{bmatrix} b_1 & d_2 & 0 & 0 & \cdots & 0 \\ d_2 & b_2 & d_3 & 0 & \cdots & 0 \\ 0 & d_3 & b_3 & d_4 & \cdots & 0 \\ 0 & 0 & d_4 & b_4 & \cdots & 0 \\ \vdots & \vdots & \vdots & \vdots & \ddots & d_N \\ 0 & 0 & 0 & 0 & d_N & b_N \end{bmatrix}$$

If d_3 can be considered zero, then the p matrix uncouples [14, p. 149] into two separate portions, and the rank is reduced from N to 2. This is of considerable significance for large N. Wilkinson [14, p. 149] states that "Vanishing of a d_i is a simplifying factor rather than a complication."

Several modifications of Lanczos' method have been proposed [14]

a) Re-orthogonalization

Since the error in X_i is due in part to the accumulation of errors in each previous X_j, some improvement can be achieved by reorthogonalization such that Y_i^T is "orthogonal to all previous X_j to the full number of working figures." [14, p. 149] It was found however that the improvement (2 or 3 working figures) was not sufficient to warrant the increased coding required. The method

(without re-orthogonalization) converged rapidly until only two equations could be retained, in which case there is little opportunity for roundoff errors to propagate.

b) Normalization (scaling)

This does not alter loss of precision more than one significant figure.

The adjoint p* of the symmetric tridiagonal matrix p can be computed quite simply (especially for small order N) and is given by

$$p^*_{ij} = (-1)^{i+j} E_{i-1} D_{j+1} \prod_{m=i}^{j} d_m/d_i \quad ; \quad j \geq i$$

where p* is symmetric

D_N = determinant of lower right N x N portion of p

E_N = determinant of upper left N x N portion of p,

i.e., the determinant of p truncated to N equation

$E_0 = 1$

$E_1 = b_1$

$E_K = b_k E_{k-1} - d_k^2 E_{k-2} \quad ; \quad k = 2,3,\ldots,N$

$D_{N+1} = 1$

$D_N = bN$

$D_{N-K} = b_{N-K} D_{N-K+1} - d^2_{N-K+1} D_{N-K+2} \quad ; \quad k = 1,2,\ldots,N-1$

The b_k and d_k are computed by the Lanczo process. If any D_K is zero, the matrix can be partitional.

An alternative to computing the adjoint is some form of back substitution which as shown by Wilkinson can be either unstable or

not straightforward.

> ...the straightforward use of the recursions (back substitution) often gives vectors which are catastrophically in error. [13, p. 90]
>
> It can not be too strongly emphasized that the eigenvectors of the codiagonal forms cannot be calculated reliably from the recursions, or, from what amounts to the same thing, from the determinants of the principal minors (of the reduced form: $I-\mu Q$). [14, p. 151]

Therefore, according to Wilkinson, the adjoint cannot be calculated reliably by our procedure above. If however a good approximation p_a^* to the adjoint p^* can be obtained such that the error matrix E defined by

$$E = I - \frac{1}{\rho} p_a^* p$$

$$\rho = \text{determinant of } p$$

satisfies

$$||E|| < 1$$

then the correct adjoint is given by

$$p^* = [I + E + E^2 + \ldots] p_a^* .$$

Note that as a result of shifting the eigenvalue $\gamma = \gamma_0 + \varepsilon$ there results:

$$\varepsilon \to 0$$

$$\rho \to 0$$

Hence it may be impossible to improve the accuracy of the adjoint.

Proposed Modification of Lanczos' Method

A proposed modification of Lanczos' method will now be presented. This apparently new method avoids the problem of having to calculate the adjoint matrix and minimizes the sum of the squares of the errors while retaining the desirable features of the Lanczos method. The basis of this method is the construction of an orthogonality transformation E from the recursion formula (Gram-Schmidt orthogonalization process), [19, p. 216]

$$X_k = E_{k-1} - \sum_{j=1}^{k-1} C_j^{k-1} X_j \quad ; \quad k = 2,3,\ldots,N \qquad (3.29)$$

where X_1 = arbitrary

$E_k = AX_k$; $k = 1,\ldots,N$

subscripts on E,X denote column vector

By induction, if for arbitrary k $E_i^T E_j = 0$; $i \neq j$; $i,j < k$

then pre-multiplication of (3.29) by $E_i^T A$ gives

$$E_i^T AX_k^{(i)} = E_i^T AE_{k-1} - \sum_{j=1}^{k-1} C_j^{k-1} E_i^T E_j$$

$$= E_i^T AE_{k-1} - C_i^{k-1} E_i^T E_i$$

then $E_i^T AX_k = 0$; $i = 1,2,\ldots,k-1$

provided $C_i^{k-1} = E_i^T AE_{k-1} | E_i^T E_i$

That is $E_i^T E_k = 0$; $i < k$

provided $E_i^T E_j = 0$; $i,j < k$ and $i \neq j$

Since k is arbitrary the sequence $\{E_k\}$ are orthoginal and

$$E^TE = \text{Diagonal}$$

This transformation reduces

$$AV + \varepsilon BV + {}^2CV = E$$

to the form

$$DZ = \varepsilon PZ + \varepsilon^2 QZ + O(\varepsilon^3)$$

where D = diagonalized

$$-P = X^T(A^TB + B^TA)X = E^TB + B^TE$$

$$-Q = X^T(B^TB + A^TC + C^TA)X$$

$$= X^TB^TBX + E^TCX + X^TC^TE$$

By comparison with the results of Lanczos' method

a) D is diagonal rather than tridiagonal

b) P is tridiagonal if B is diagonal

c) the sum of the square of the errors is minimized (least squares sense)

d) the equation is now nonlinear in the eigenvalue ε, but P, Q are symmetric

It is suggested (incorrectly) that the nonlinear problem be linearized after transformation rather than before transformation. However, this leads to problems since $P = O(\varepsilon)$. This formulation was arrived at by minimizing the sum of squares of the errors E

$$[A + \varepsilon B + \varepsilon^2 C]V = E$$

This gives:

$$Z^TDZ + \epsilon Z^TPZ + \epsilon^2 Z^TQZ = I = \text{MINIMUM}$$

which is a positive definite quadratic form.

Setting $\frac{\partial I}{\partial \epsilon} = 0$

gives

$$\epsilon = \frac{1}{2} Z^TPZ/Z^TQZ$$

Advantages of this method are:

a) uses estimate of the eigenvector to reduce order from N to 2 or 1. (Of value for large N)

b) gives precise criterion of onset of instability due to loss of precision (before which the transformation process must be terminated).

c) as the iteration converges fewer computations are required due to reduction in order. This is important for stability as well as computational efficiency

d) quadratic convergence. This is important if considerable computation is required to calculate the matrices A, B, C

e) if B is diagonal and C is null, then p is tridiagonal and Q is diagonal

f) the coefficient matrix D is diagonal

g) to the extent that G is symmetric, the X_k tend to be orthogonal

Disadvantages of this method:

a) requires iteration

b) the reduced form is nonlinear in the eigenvalue ε even if the original form is linear in ε. This is a minor problem for small order N since the substitution

$$Z_1 = \varepsilon QZ$$

gives:

$$\begin{bmatrix} D & 0 \\ 0 & I \end{bmatrix} \begin{Bmatrix} Z \\ Z_1 \end{Bmatrix} = \varepsilon \begin{bmatrix} P & I \\ 0 & Q \end{bmatrix} \begin{Bmatrix} Z \\ Z_1 \end{Bmatrix}$$

in which the order is doubled.

c) since loss of precision can be dependent on the order of computation, it is important that P be computed as follows.

1) $E = AX$

2) $-P = E^T B + B^T E$

Results of this method are presented in comparison to the perturbation results and the results of Gauss-Jordan reduction to be discussed next.

3.7.5 Gauss-Jordan Reduction

As already shown, the methods of QR, Lanczos, and Gauss-Jordan reduction all reduce the general eigenvalue problem:

$$AV + \varepsilon BV = O(\varepsilon^2) \tag{3.26}$$

to the form

$$V = \mu KV + \varepsilon O(\mu) \tag{3.27}$$

where

$$\varepsilon = \mu\alpha \quad ; \quad \alpha = \text{determinant of A}$$

$$K = -A^*B \quad ; \quad A^* = \text{adjoint of A}$$

Note that $\mu = \varepsilon/\alpha$ is an indeterminant quotient since both ε and α tend to zero.

This equation can be solved iteratively by the power method with quadratic convergence. An alternative method, or first approximation to the power method can be devised which has certain advantages. This entails a detailed study of Gauss-Jordan reduction.

The transformation $A_{ij} \leftarrow A_{ij} - A_{i\beta}A_{\alpha j}/A_{\alpha\beta}$ can be interpreted as

$$A^M = T^M A^{M-1} S^M$$

in which

T^M = row operations, combine equations

S^M = column operations, coordinate transformation

It will be shown that the eigenvector V is the product of the S-transformations provided $\varepsilon = 0$. That is, the information necessary to calculate the eigenvector is available without iteration or further computation.

The T^M, S^M matrices are given by

$$T^M_{ij} = \delta_{ij} - \delta_{i\beta}[A^M_{\alpha j}/A^M_{\alpha\beta} - \delta_{\beta i}]$$

$$S^M_{ij} = \delta_{ij} - [A^M_{i\beta}/A^M_{\alpha\beta} - \delta_{i\alpha}]\delta_{\alpha j}$$

where α = pivot row

β = pivot column

$i,j = 1,2,3,\ldots,N-M+1$

δ_{ij} = Kronecker delta

Now, for $M = 1,2,3,\ldots,N$; $X^{\circ} = V$, $A^{\circ} = A$

let $$A^{M}_{ij} = A^{M-1}_{IJ} - A^{M-1}_{I\beta} A^{M-1}_{\alpha J}/A^{M}_{\alpha\beta}$$

$$S^{M}_{ij} = \delta_{ij} - \delta_{i\beta}[A^{M-1}_{\alpha J}/A^{M-1}_{\alpha\beta} - \delta_{\beta J}]$$

the T^{M}_{ij} does not need to be computed

where:
$$I = \begin{cases} i & ; \quad i < \alpha \\ i+1 & ; \quad i \geq \alpha \end{cases}$$

$$J = \begin{cases} j & ; \quad j < \beta \\ j+1 & ; \quad j \geq \beta \end{cases}$$

This interchanges the α and M rows, and the β and M columns. Then irrespective of the pivot choice, there are zeros in the M-row and M-column except for the (M,M) element. For $A^{1}X^{1} = 0$

$$\begin{bmatrix} & & & 0 \\ & A^{1}_{ij} & & \vdots \\ & & & 0 \\ 0 \ \ldots\ 0 & & & A^{\circ}_{\alpha\beta} \end{bmatrix} \begin{Bmatrix} X^{1}_{1} \\ X^{1}_{2} \\ \vdots \\ X^{1}_{N-1} \\ X^{1}_{N} \end{Bmatrix} = 0$$

Now in the last equation there are two possibilities:

a) $A^{\circ}_{\alpha\beta} = 0$ in which case X^{1}_{N} = arbitrary

b) $X^{1}_{N} = 0$ in which case A° = arbitrary

If the reduction used complete pivoting then

$$|A^{\circ}_{ij}| \leq |A^{\circ}_{\alpha\beta}|$$

Therefore $X^{1}_{N} = 0$ and the order is reduced.

If, however, after several stages of reduction

$$|A^{M}_{ij}| \leq |A^{M}_{\alpha\beta}| < 10^{-NP}$$

then division by $A^{M}_{\alpha\beta}$ is not allowed and the process must be terminated. The pivots $A^{M}_{\alpha\beta}$ tend to zero due to cancellation in the Gaussian elimination. This causes loss of precision. If the matrix is initially scaled to unity, and Np is the machine precision, and $|A^{M}_{\alpha\beta}| < 10^{-NP}$ then $A^{M}_{\alpha\beta}$ does not have any significant digits. Division by $A^{M}_{\alpha\beta}$ in this case would result in an apparent loss of stability in the results. In this case A^{M} must be considered null, X^{M} arbitrary, and the rank is equal to M.

If M = N then there is only one equation

$$A_{11}{}^{N} X_{1}{}^{N} = 0$$

in which $A^{N}_{11} = 0$ if A is singular.

If M = N and $\varepsilon \neq 0$ we would get a scaler equation of the form

$$A_{11}{}^{N} X_{1}{}^{N} = \varepsilon B_{11}{}^{N} X_{1}{}^{N}$$

Hence: X_1^N = arbitrary

$$\varepsilon = \frac{A_{11}^N}{B_{11}^N}$$

This permits a workable test on the solvability of the problem. As the nonlinear eigenvalue problem is iterated and the eigenvalue shifted: $\gamma = \gamma_0 + \varepsilon$

it is necessary that

$$\varepsilon \to 0$$

$$A_{11}^N \to 0$$

Hence $|A_{11}^N| << |B_{11}^N|$

Note that if $A*B \equiv 0$, the problem is not solvable unless $\det[A] \equiv 0$. In reality it may be difficult to decide the solvability and the rank due to loss of precision.

The eigenvector is given by:

$$V = X^\circ = s^1 X^1 = s^1 s^2 X^2 = s^1 s^2 \ldots s^M X^M$$

Let $S = s^1 s^2 \ldots s^M$

to get $V_i = S_{ij} X_j^M \quad ; \quad i = 1,N, j=1,N-M+1$

Each of the X_j^M is arbitrary and so there are N-M+1 eigenvectors. Note that the magnitude of the determinant is the product of the pivot elements.

There are several possibilities for the choice of the pivot at each stage. Several of these will now be discussed. Each choice of pivot attempts to exploit some property of the algorithm to achieve increased stability and reduce error due to loss of precision.

a) Choice of pivot column. In order that the s^M and the eigenvector $V = s^1 s^2 s^3 \ldots$ be stable, it is necessary that

$$|A^M_{\alpha j}| \leq |A^M_{\alpha\beta}| \quad ; \quad j=1,\ N-M+1$$

and as a result we have the property

$$|s^M_{ij} - \delta_{ij}| \leq 1$$

which is desirable for stability.

b) Choice of pivot row.

1) The system of equations here is the result of truncation of an infinite set of equations. This suggests choosing the pivot rows in the sequence 1,2,3,....

2) Since the determinant is the product of the pivot elements, choosing the pivot row whose largest element is smaller than any other row

$$|A_{\alpha,\beta(\alpha)}| \leq |A_{i,\beta(i)}| \text{ and } |A_{ij}| \leq |A_{i,\beta(i)}|$$

would tend to drive the determinant to zero.

3) One could seek two rows which are most nearly parallel. This is suggested by our case for m = 0.

4) Complete pivoting (maximum pivots):

$$|A_{ij}| \leq |A_{\alpha\beta}| \qquad \text{for all } i,j$$

This will work and is to be preferred in lieu of demonstration of a better strategy. All other strategies require more computer coding.

Each of these strategies was tried and worked. But in comparing the accuracy of the resulting eigenvector there was no conclusive preference except that complete pivoting worked as well as or better than the others for arbitrary m. In agreement with Wilkinson:

> We do not claim that selecting the largest elements as pivots is the best strategy and indeed this will often be far from true. We do claim that no alternative practical procedure has yet been proposed. [12, p. 217]

The possibility of an alternative practical procedure was suggested by the observation that

$$\{V\} = [s^1 s^2 s^3 \ldots s^M]\{X^M\}$$

$$s_{ij}^{M+1} = \delta_{ij} - \delta_{i\beta}[A_{\alpha J}^M / A_{\alpha\beta}^M - \delta_{\beta J}]$$

It would seem that loss of precision could be held to a minimum if the number of computations could be held to a minimum. This would suggest choosing pivots such that

$$s^M \to I$$

as fast as possible with respect to M. Note that the only variable

in this respect is the pivot row α.

Advantages of Gauss-Jordan reduction:

a) reveals repeated eigenvectors, rank

b) efficient computationly

c) stable if use complete pivoting

d) provides a criterion on the solvability

e) gives determinant, forms a basis for iteration of the eigenvalue by Newton's method

Disadvantages:

a) requires good estimate of the eigenvalues

3.7.6 Numerical Results

The graph of γ vs. m on page 100 was obtained by the methods of Gauss-Jordan Reduction and Modified Lanczos. In comparison of these two methods it was found that both worked. The Modified Lanczos method required about twice as many iterations to converge[1] but the accuracy was slightly better. It was concluded that the Modified Lanczos method is a good technique to improve the accuracy of Gauss-Jordan Reduction, if so desired.

Note from the graph that the approximate formulas (3.22) and (3.23) obtained by the perturbation method give good approximations to $\gamma(m)$ for $m < 0.3$ and $m > 3.0$ respectively. Also, the fourth order perturbed eigenvalue γ_4 (see page 70) is negative and is approximately

$$\gamma_4 = -8. \pm 1$$

---

[1]Until the determinant could not be reduced in magnitude.

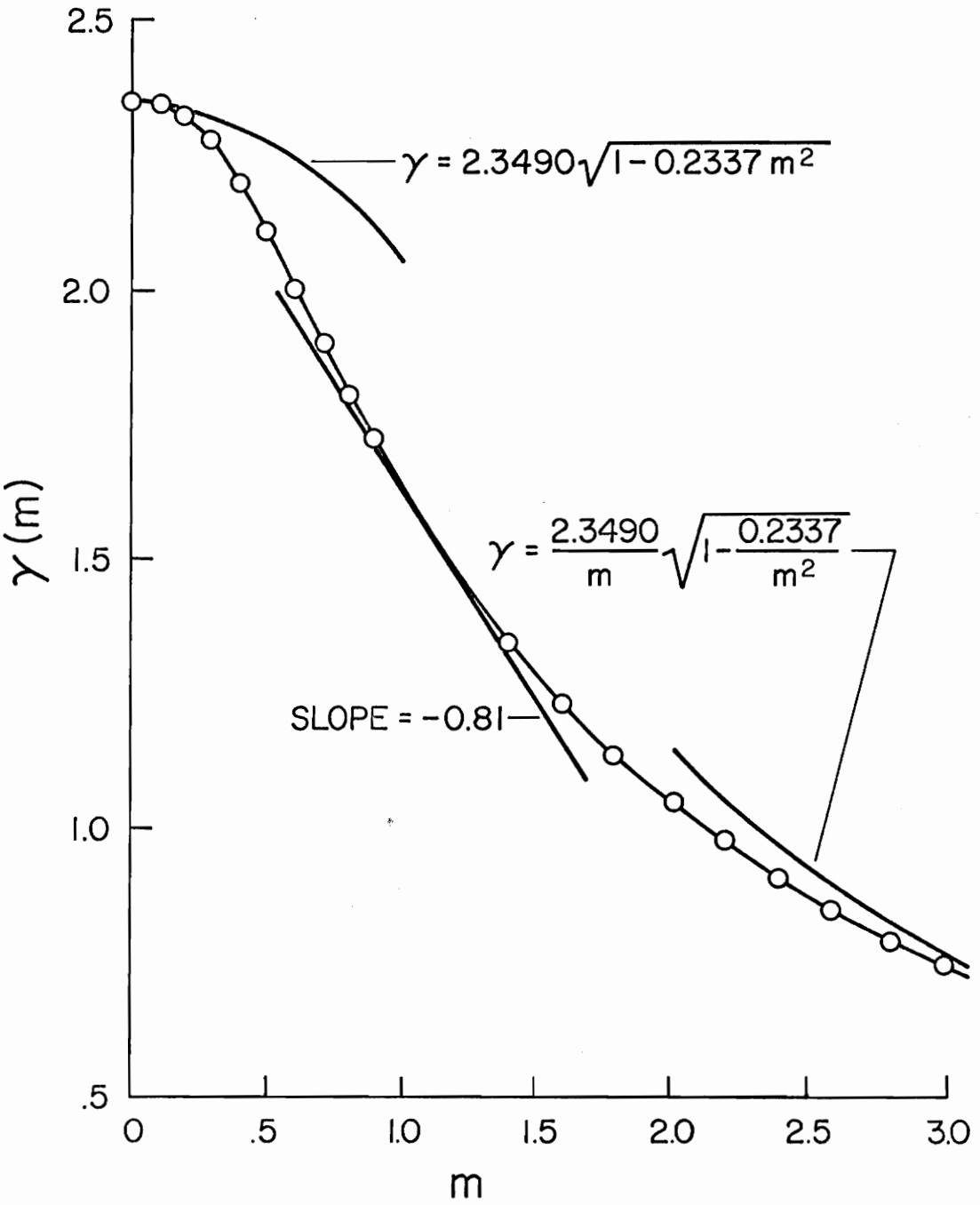

FIG. 12. EIGENVALUE vs. ECCENTRICITY PARAMETER

This gives

$$\gamma(m) = 2.3490\sqrt{1 - 0.23373\ m^2 - \overline{6}.5\ m^4} + O(m^4)$$

Thus the relationship

$$\gamma(m) = \frac{1}{m}\,\gamma\left(\frac{1}{m}\right)$$

is verified for large and small m. At m = 1 it is an identity. Evaluating the derivatives at m = 1 gives

$$\frac{d\gamma}{dm}(m)\Big|_{m=1} = -\frac{1}{2}\,\gamma(1)$$

$$\frac{d^2}{dm^2}\left[\gamma(m) - \frac{1}{m}\,\gamma\left(\frac{1}{m}\right)\right]\Big|_{m=1} \equiv 0 \text{ if } \gamma'(1) = -\frac{1}{2}\,\gamma(1)$$

From the numerical results

$$-\frac{1}{2}\,\gamma(1) = -0.8\overline{13}$$

$$\text{slope} = -0.8\overline{08}$$

This agreement in the data supports the conclusion that

$$\gamma(m) = \frac{1}{m}\,\gamma\left(\frac{1}{m}\right)$$

and that the numerical results for $\gamma(m)$ are accurate to at least two digits for all m, including m = 1.

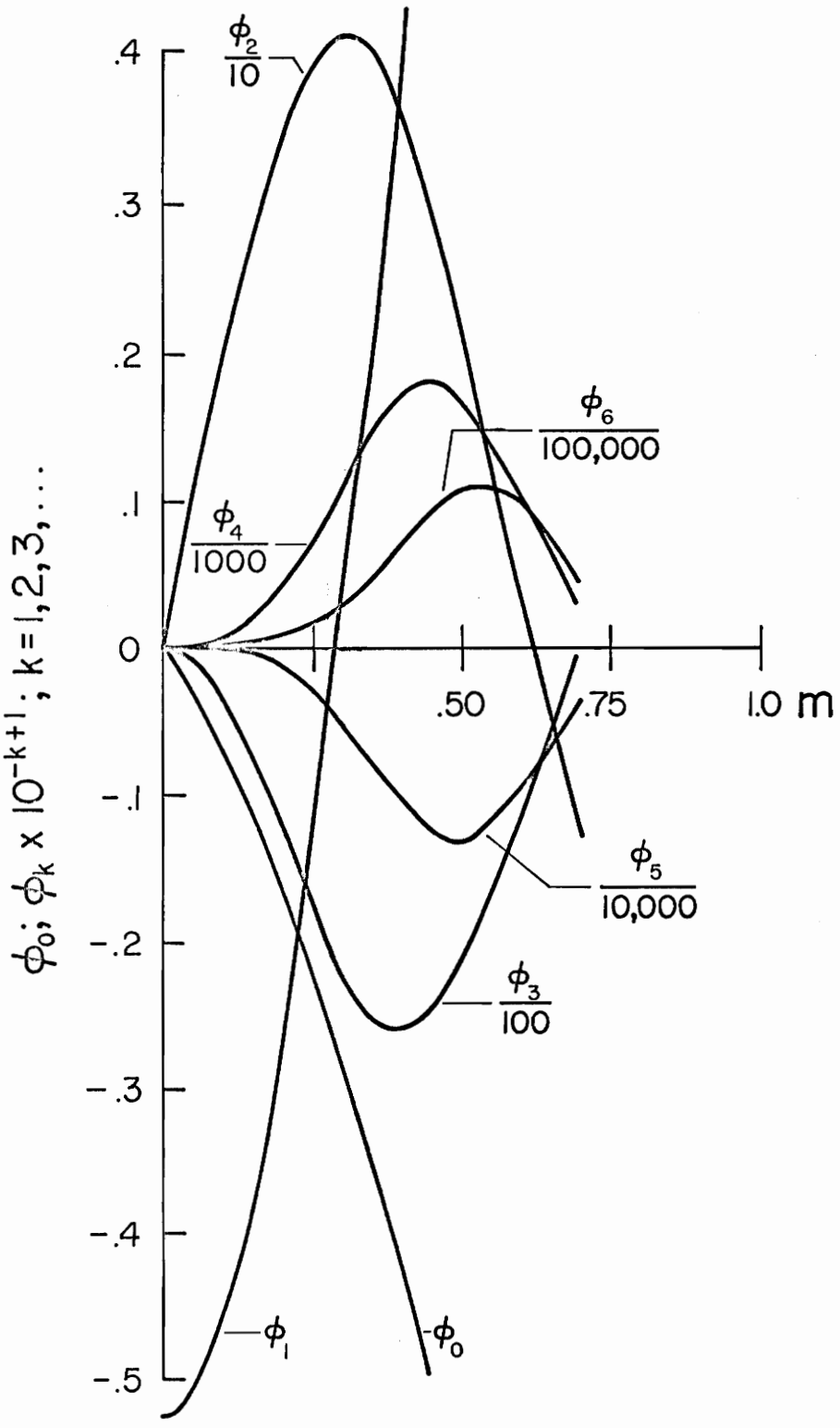

FIG. 13. EIGENVECTOR vs. ECCENTRICITY PARAMETER

In order to estimate the effect of the truncation parameter N, results were obtained for N in the range $4 \leq N \leq 8$. It was found that γ was insensitive to N for $N \geq 6$. For $N = 4$ and $.5 < m < 1.5$ there resulted a small error in γ due to truncation of the infinite system of equations. The results for the ϕ-part of the eigenvector are plotted on page 102. Recall that in our notation

$$\{v\} = \left\{ \begin{array}{c} \phi_0 \\ \phi_1 \\ \phi_2 \\ \vdots \\ \phi_N \\ \hline \psi_1 \\ \psi_2 \\ \vdots \\ \psi_N \end{array} \right\} \leftarrow \text{partition}$$

The tendency is for the ϕ_j; $j = 0,N$ to be increasingly large. It was found that the results for the eigenvector were accurate provided

$$m \leq .45 \text{ for } N = 5$$

$$m \leq .70 \text{ for } N = 7$$

In order to estimate the error in the perturbation solution the logarithm of the error vs. m was plotted on page 104 where

$$\text{ERROR} = E^T E$$

$$E = Gv$$

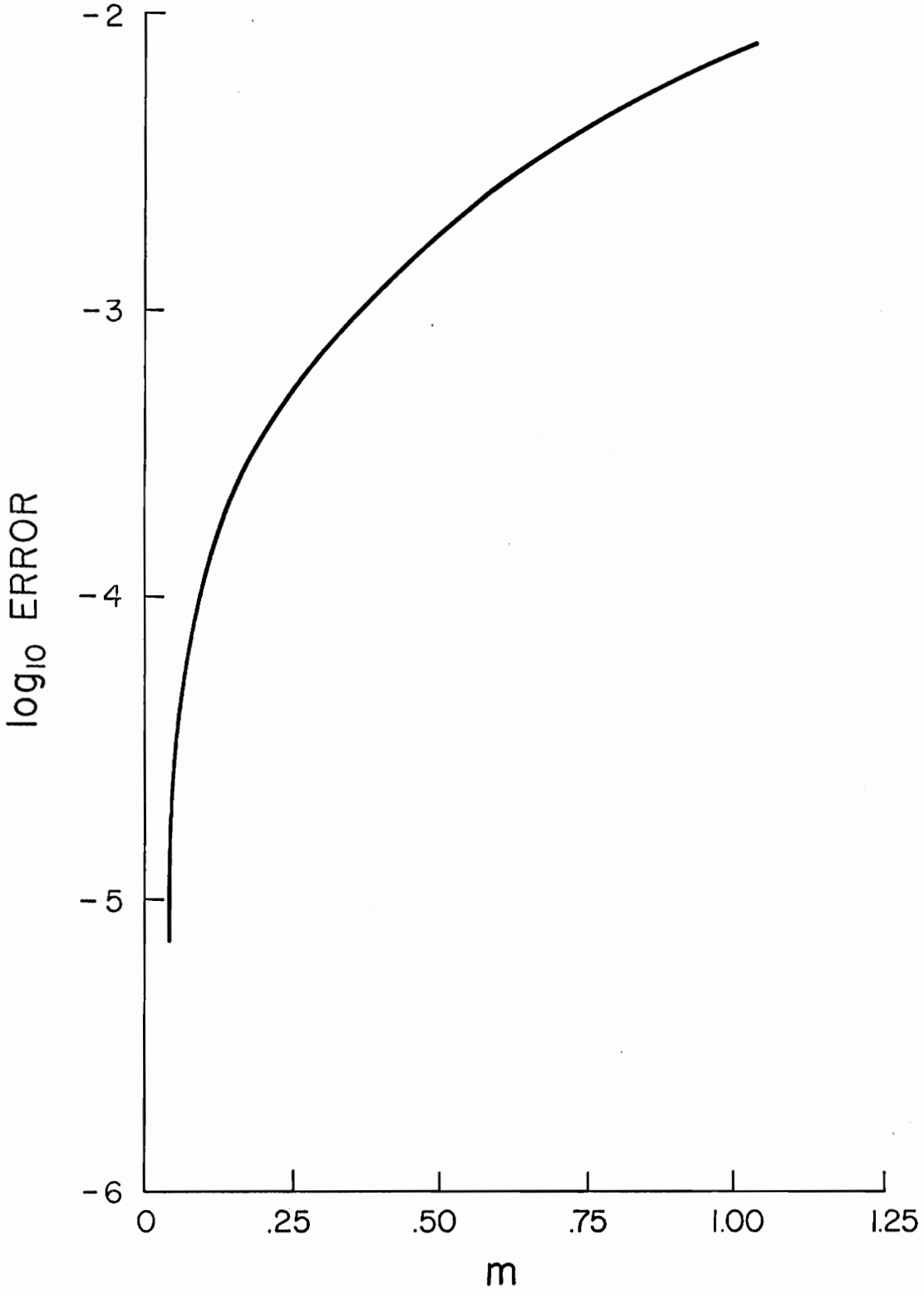

FIG. 14. ERROR vs. ECCENTRICITY PARAMETER

It can be seen that

$$\text{ERROR} \propto m^4$$

and hence that the $O(m^3)$ perturbation solution is correct.

3.8 Checking the Boundary Conditions: Error Analysis

Due to the complexity of the formulation it was felt desirable to have an independent check of the boundary conditions. This will verify the range of eccentricity parameter m for which the solution is correct to a given error.

The boundary condition to be evaluated reads

$$\frac{\partial^2 \Phi}{\partial Z^2} \frac{dZ}{ds} + \frac{1 - \delta}{4} \gamma^2 \phi \frac{d\overline{Z}}{ds} = 0 \text{ on } S$$

where

S is the boundary of the ellipse

$$\left(\frac{X}{a}\right)^2 + \left(\frac{Y}{b}\right)^2 = 1$$

$a = 1 + m$ = semi-major axis

$b = 1 - m$ = semi-minor axis

ds = differential arc length along ellipse

$$\Phi = \phi + i\psi, \quad Z = X + iY = Re^{i\theta}$$

$$\phi(R,\theta) = \sum_{j=0}^{\infty} \phi_j \, J_{2j}(\lambda R) \, \text{Cos}(2j\theta)$$

$$\psi(R,\theta) = \sum_{j=1}^{\infty} \psi_j \, J_{2j}(\gamma R) \, \sin(2j\theta)$$

$$\lambda = \sqrt{\delta}\,\gamma \quad ; \quad \delta = \frac{1 - 2\nu}{2 - 2\nu} \doteq \frac{1}{4}$$

γ = eigenvalue

ϕ_j, ψ_j = eigenvector

It is convenient to introduce the differential operators L_1, L_2 defined by

$$\frac{\partial^2}{\partial Z^2} = \frac{e^{-2i\theta}}{2}\left[L_1 + iL_2\right]$$

to get

$$L_1 = \frac{1}{2}\left\{\frac{\partial^2}{\partial R^2} - \frac{1}{R}\frac{\partial}{\partial R} - \frac{1}{R^2}\frac{\partial^2}{\partial \theta^2}\right\}$$

$$L_2 = \frac{1}{R}\left\{\frac{1}{R} - \frac{\partial}{\partial R}\ \frac{\partial}{\partial \theta}\right\}$$

Using $\quad [\nabla^2 + \lambda^2]\phi = 0 \quad ; \quad [\nabla^2 + \gamma^2]\psi = 0$

and $\quad J_\nu'(X) = J_{\nu-1}(X) - \frac{\nu}{X} J_\nu(X)$

gives

$$L_1\phi = -\sum_{k=0}^{\infty}\left[\left\{\frac{1}{2}\lambda^2 - \frac{2k(2k+1)}{R^2}\right\} J_{2k}(\lambda R) + \frac{\lambda}{R} J_{2k-1}(\lambda R)\right]\phi_k \cos(2k\theta)$$

$$L_1\psi = -\sum_{k=1}^{\infty}\left[\left\{\frac{1}{2}\gamma^2 - \frac{2k(2k+1)}{R^2}\right\} J_{2k}(\gamma R) + \frac{\gamma}{R} J_{2k-1}(\gamma R)\right]\psi_k \sin(2k\theta)$$

$$L_2\phi = \sum_{k=0}^{\infty}\frac{-2k}{R}\left[\frac{1+2k}{R} J_{2k}(\lambda R) - \lambda J_{2k-1}(\lambda R)\right]\phi_k \sin(2k\theta)$$

$$L_2\psi = \sum_{k=1}^{\infty} \frac{2k}{R}\left[\frac{1+2k}{R} J_{2k}(\gamma R) - \gamma J_{2k-1}(\gamma R)\right]\psi_k \cos(2k\theta)$$

The results of the perturbation solution thru order m^3 showed that the error in the boundary conditions was proportional to m^4. The magnitude of the error after normalizing so that the largest stresses are unity suggests three digit accuracy for all m. It was concluded that the perturbation solution was a correct solution thru order m^3 and that the results should yield useful qualitative information for even large m. This information will be displayed in contour plots.

3.9 Contour Maps

Contour maps of several quantities are presented. They show that there are dynamic stress concentrations far removed from the boundary. This evidence supports the conclusion that these standing waves may cause microcracks away from a boundary. Note that the solution has an arbitrary multiplicative constant and hence does not have a concentration factor in the usual sense.

Each quantity is plotted on one quadrant of the X,Y Cartesian axes. For example,

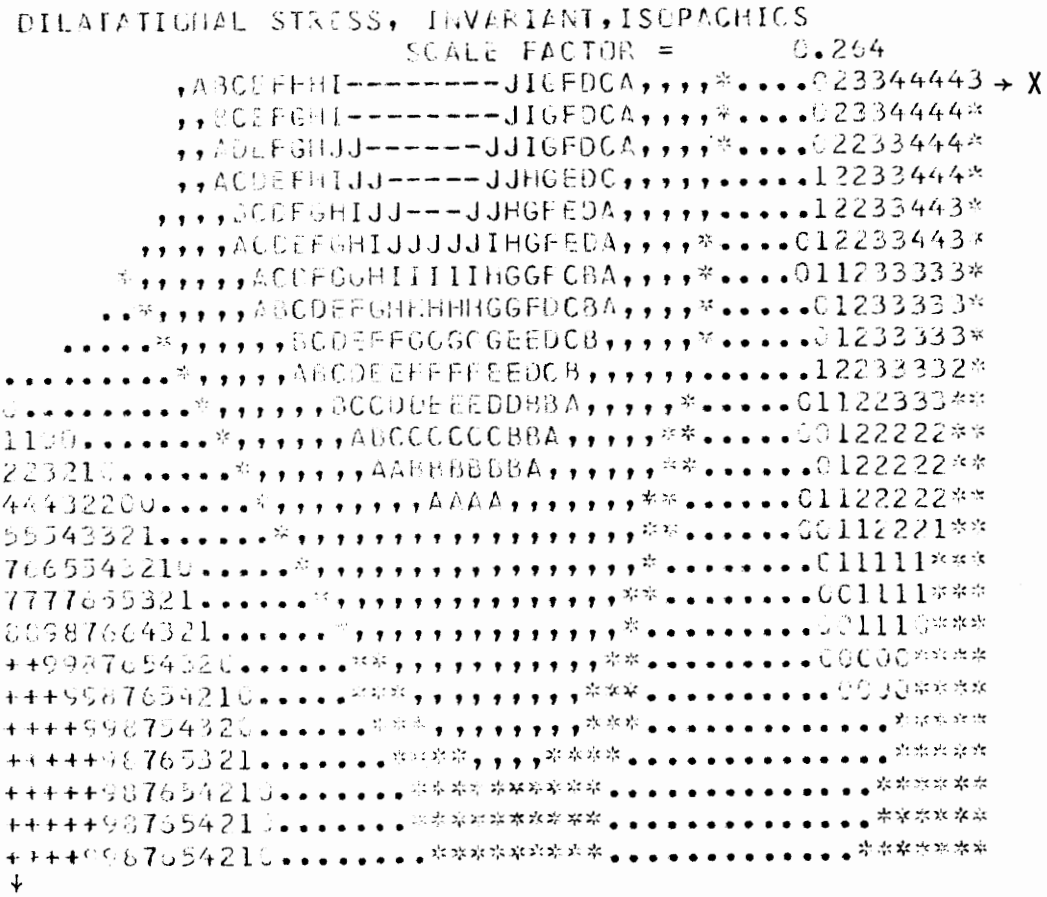

The quantity (Q) is first scaled such that

$$-20 \leq Q \leq +20$$

The symbols then have the following values (to the nearest integer):

+ = 20	A = -10
9 = 19	B = -11
8 = 18	C = -12
7 = 17	D = -13
6 = 16	E = -14
5 = 15	F = -15
4 = 14	G = -16
3 = 13	H = -17
2 = 12	I = -18
1 = 11	J = -19
0 = 10	- = -20
. = 1 to 9	, = -1 to -9

* = 0

Contour curves can be constructed by drawing lines through like symbols. This has been done in certain instances in order to highlight the behavior being discussed. The blank area is the elliptical void with semi-major axis: a = 1 + m inch or (1 + m)*10 characters. The axes are distorted since the computer prints 10 characters/inch and 6 lines/inch. However, each character represents a spatial separation (Δs) of either 0.10 or 0.20 inch in both X and Y directions. For large $R = \sqrt{X^2 + Y^2}$, the results attenuate like $R^{-1/2}$. It is convenient to define s_1, s_2, s_3 as follows:

$$s_1 = -\left[\frac{\sigma_{xx} + \sigma_{yy}}{2\mu}\right] = + \frac{1 - \delta}{4} \nabla^2 \phi$$

$$s_2 + i s_3 = -\left[\frac{\sigma_{yy} - \sigma_{xx} + 2i\sigma_{xy}}{2\mu}\right] = + 4 \frac{\partial^2}{\partial Z^2} \Phi; \quad \Phi = \phi + i\psi, \quad Z = X + iY$$

From the values of s_i we can compute stresses in any coordinate system, and in particular:

a) Cartesian coordinates X, Y

b) Elliptic coordinates ξ, η (polar if m = 0)

c) Principal stresses

Maps 1, 2, 3 are the stresses σ_{xx}, σ_{xy}, σ_{yy}.

Note large shear stress σ_{xy} at angles of $\pi/8$, $3\pi/8$.

Maps 4, 5, 6 are the stresses $\sigma_{\xi\xi}$, $\sigma_{\xi,\eta}$, $\sigma_{\eta\eta}$. These were obtained using [2, p. 271].

$$\sigma_{\xi\xi} - i\sigma_{\xi\eta} = \frac{\sigma_{xx} + \sigma_{yy}}{2} - \left[\frac{\sigma_{yy} - \sigma_{xx}}{2} + i\sigma_{xy}\right]e^{2i\alpha}$$

$$\sigma_{\xi\xi} + \sigma_{\eta\eta} = \sigma_{xx} + \sigma_{yy}$$

Maps 7 through 12 are invariant quantities. It was hoped that knowledge of the principal stresses would suggest a more favorable coordinate system in which to solve the problem. To this end special attention is given to the nature of the invariant quantities. The principal normal stresses σ_{MAX}, σ_{MIN} are the roots (λ) of the eigenvalue problem [20, p. 73]

$$\begin{bmatrix} \sigma_{xx} - \lambda & \sigma_{xy} \\ \sigma_{xy} & \sigma_{yy} - \lambda \end{bmatrix} \begin{Bmatrix} \nu_1 \\ \nu_2 \end{Bmatrix} = 0$$

in which the ν_i are the direction cosines. This gives the characteristic equation:

$$\lambda^2 - I_1\lambda + I_2 = 0$$

where I_1, I_2 are invariant:

$$I_1 = \sigma_{xx} + \sigma_{yy} \qquad \text{(plot 7)}$$

$$I_2 = \sigma_{xx}\sigma_{yy} - \sigma_{xy}^2 \qquad \text{(plot 8)}$$

Since: $I_1 \propto \nabla^2\phi = -\delta\gamma^2\phi$

$$= \nabla \cdot \vec{u} = \text{dilatation}$$

The stress invariant I_1 serves as an excellent example of the stress concentrations located some distance from the boundary, and are typical of several of the quantities plotted for $m \neq 0$. For the circle case ($m = 0$) with $\delta = \frac{1}{4}$ ($\nu = \frac{1}{3}$) we have:

$$I_1 \propto \phi = J_2[1.175\ R]\ \text{Cos}[2\theta]$$

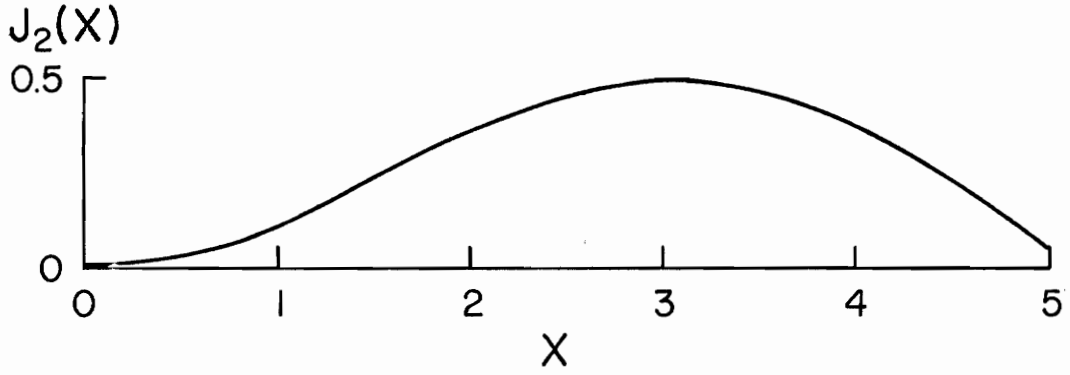

Therefore, the I_1 stress concentrations for $m = 0$ at (2.4, 0) and (0, 2.4) correspond to the maximum value of $J_2[X]$ at $X = 3.1$. The dilatational stress is of interest for materials that fail in tension. In the language of photoelasticity lines of constant I_1 are termed isopachics [21].

Solving for the roots of the characteristic equation gives the principal normal stresses σ_{MAX}, σ_{MIN}

$$\lambda = \frac{\sigma_{xx} + \sigma_{yy}}{2} \pm \sqrt{\left(\frac{\sigma_{yy} - \sigma_{xx}}{2}\right)^2 + (\sigma_{xy})^2}$$

$$= \sigma_{MAX}, \sigma_{MIN} \text{ (see plots 9, 10)}$$

and the maximum shear stress:

$$T_{MAX} = \frac{\sigma_{MAX} - \sigma_{MIN}}{2} \qquad \text{(see plot 11)}$$

Lines of constant T_{MAX} are called isochromatics.

The principal direction θ_P is given by (see plot 12)

$$\tan 2\theta_P = \frac{\sigma_{xy}}{\frac{1}{2}(\sigma_{yy} - \sigma_{xx})}$$

Lines of constant θ_P are called isoclinics.

Note that if at some point $\sigma_{yy} = \sigma_{xx}$ and $\sigma_{xy} = 0$ then any direction is a principal direction. This corresponds to hydrostatic stress in which the roots of the characteristic equation are repeated. Such points are isotropic points. A special case of isotropic points are singular points which are unstressed. The isotropic points are of special interest since: "Isoclinics of all parameters must pass through isotropic or singular points" [21, p. 228].

The isotropic points are of further interest since the principal directions can be discontinuous in the neighborhood of an isotropic point. To see this, consider the example (Taylor series in x, y about

an isotropic point):

$$\sigma_{xx} = \sigma_o + \varepsilon[f_1 X + f_2 Y] + \ldots$$

$$\sigma_{yy} = \sigma_o + \varepsilon[g_1 X + g_2 Y] + \ldots$$

$$\sigma_{xy} = \varepsilon[s_1 X + s_2 Y] + \ldots$$

where σ_o = stress at the isotropic point (X, Y = 0)

ε = small parameter

f,g,s = Taylor coefficients

Letting $X = r \cos \theta$

$Y = r \sin \theta$

leads to:

$$\tan 2\theta_p = \frac{2[s_1 \tan \theta + s_2]}{(g_1 - f_1) \tan \theta - (g_2 - f_2)} + O(r)$$

$$\lambda = 1 + O(\varepsilon)$$

This shows that if the stresses σ_{ij} are analytic in ε then λ is analytic in ε but the eigenvector and principal directions are not necessarily analytic in ε near an isotropic point. That is, θ_p is discontinuous as a function of two variables r,θ at the origin (isotropic point) r = 0. Recall that this phenomena was encountered in efforts to obtain eigenvectors numerically. It was found that the perturbed eigenvector can be large if the eigenvalues are nearly repeated. The relationship between the direction cosines ν_i and the principal direction θ_i can be obtained by considering:

$$\tan \theta_{1,2} = \left(\frac{\nu_1}{\nu_2}\right)_{1,2} = a \pm \sqrt{a^2 + 1} \qquad (1),(2)$$

where: $a \equiv \text{Cot } 2\,\theta_p$

The product of (1), (2) gives:

$$\tan\theta_1 \tan\theta_2 = -1$$

which implies: $\theta_2 - \theta_1 = \pm \frac{\pi}{2}$

and that directions $\left(\frac{\nu_1}{\nu_2}\right)_1$ and $\left(\frac{\nu_1}{\nu_2}\right)_2$ are orthogonal.

Using the identity $\frac{\tan\theta_1 + \tan\theta_2}{1 - \tan\theta_1 \tan\theta_2} = \tan(\theta_1 + \theta_2)$

and summing (1) and (2) gives:

$$\tan(\theta_1 + \theta_2) = \tan 2\theta_p$$

Hence: $\theta_1 = \theta_p = \text{atan}(\nu_1/\nu_2)_1$

$\theta_2 = \theta_p + \frac{\pi}{2} = \text{atan}(\nu_1/\nu_2)_2$

The location of the isotropic points can be obtained from the zeros of the maximum shear stress.

$$T_{MAX} = \sqrt{\left(\frac{\sigma_{yy} - \sigma_{xx}}{2}\right)^2 + (\sigma_{xy})^2}$$

and are denoted by asterisks (*) on plot 11.

One conclusion of this chapter is that separation of variables in the image plane (unit circle) is not a computationally efficient way to represent the solution. Perhaps knowledge of the location of the isotropic points would suggest a more appropriate coordinate system (principal coordinates) in which to construct an approximate

solution.

The displacements in Cartesian coordinates are presented in maps 13, 14, 15.

LISTING OF CONTOUR MAPS AND CURVES

A. Various Quantities for Circle; m = 0; Δs = 0.10 inch

B. Dilatational Stress for Various Values of Eccentricity Parameter m; Δs = 0.20 inch

SIGMA XX

MAP NO. 1

M = 0.0 SCALE FACTOR = 0.697

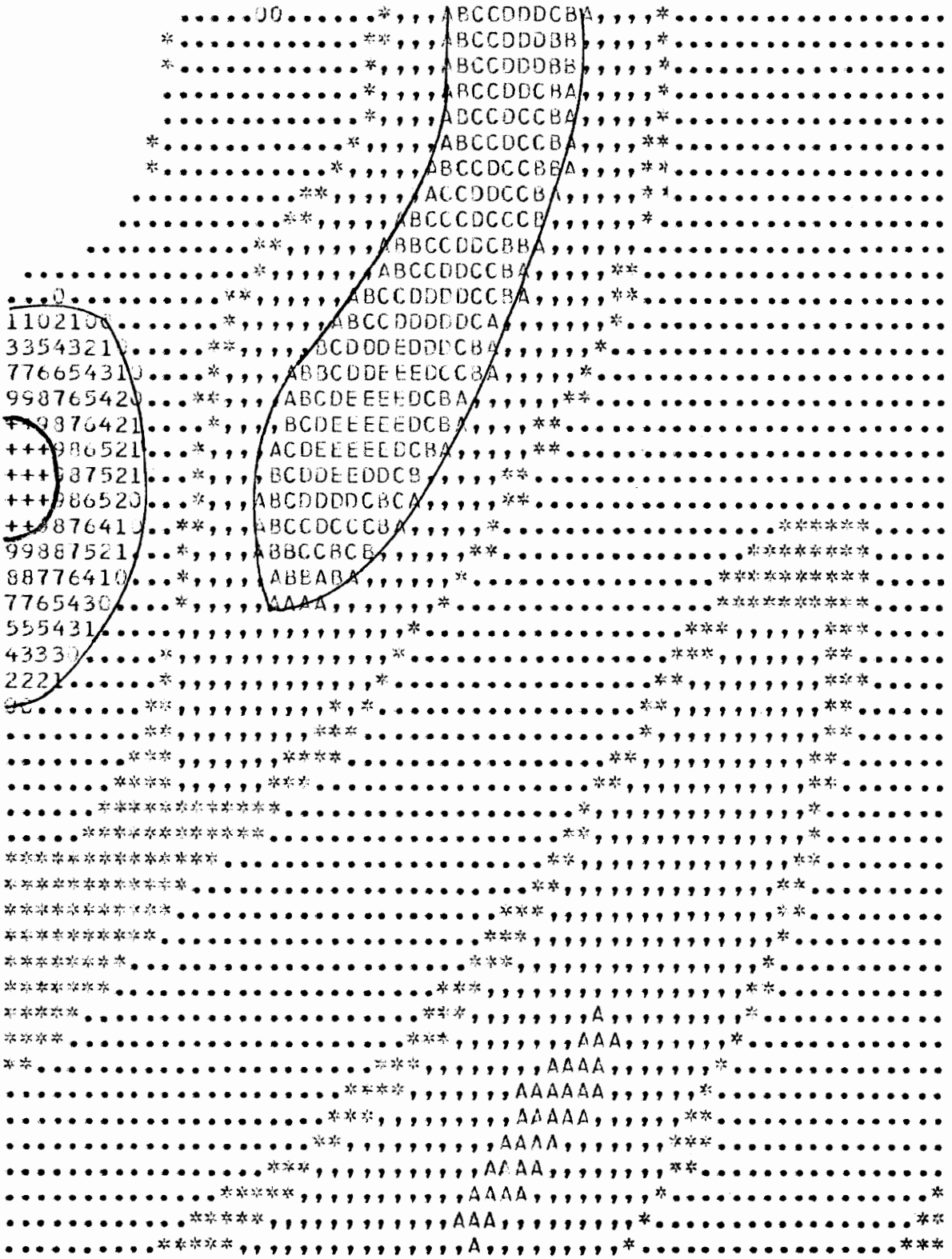

SIGMA XY

MAP NO. 2

M = 0.0 SCALE FACTOR = 0.283

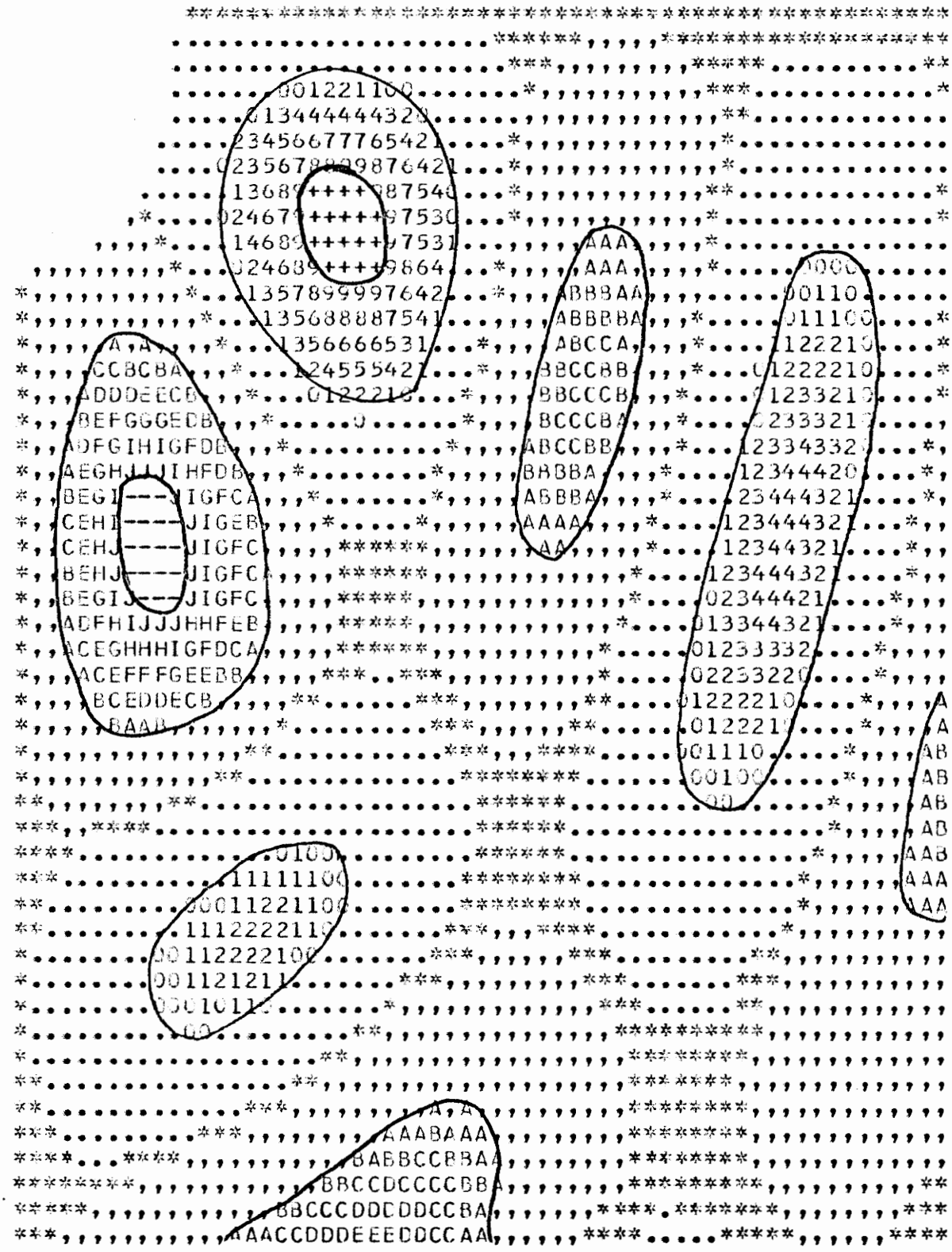

SIGMA YY

MAP NO. 3

M = 0.0 SCALE FACTOR = 0.697

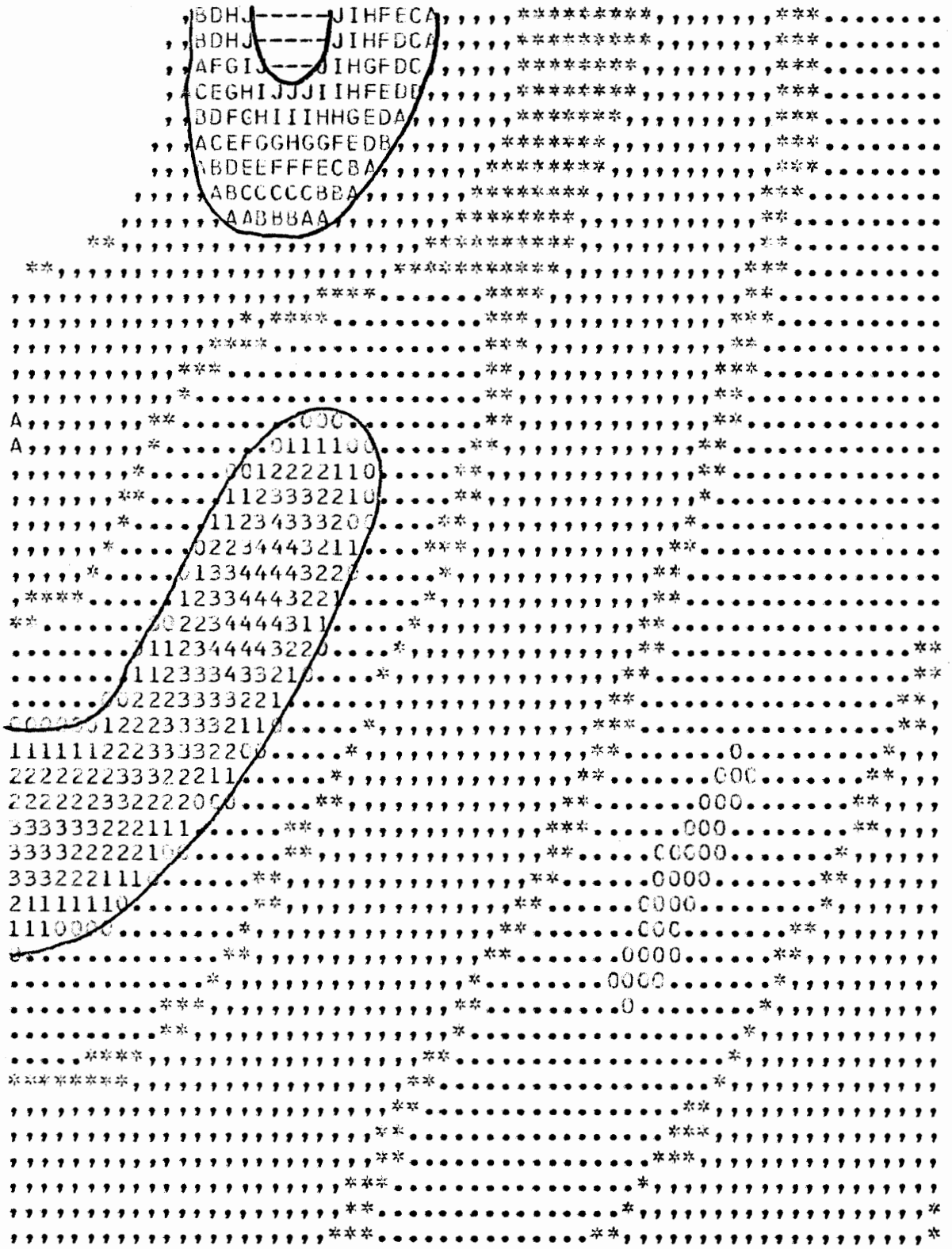

SIGMA XI,XI MAP NO. 4

M = 0.0 SCALE FACTOR = 0.485

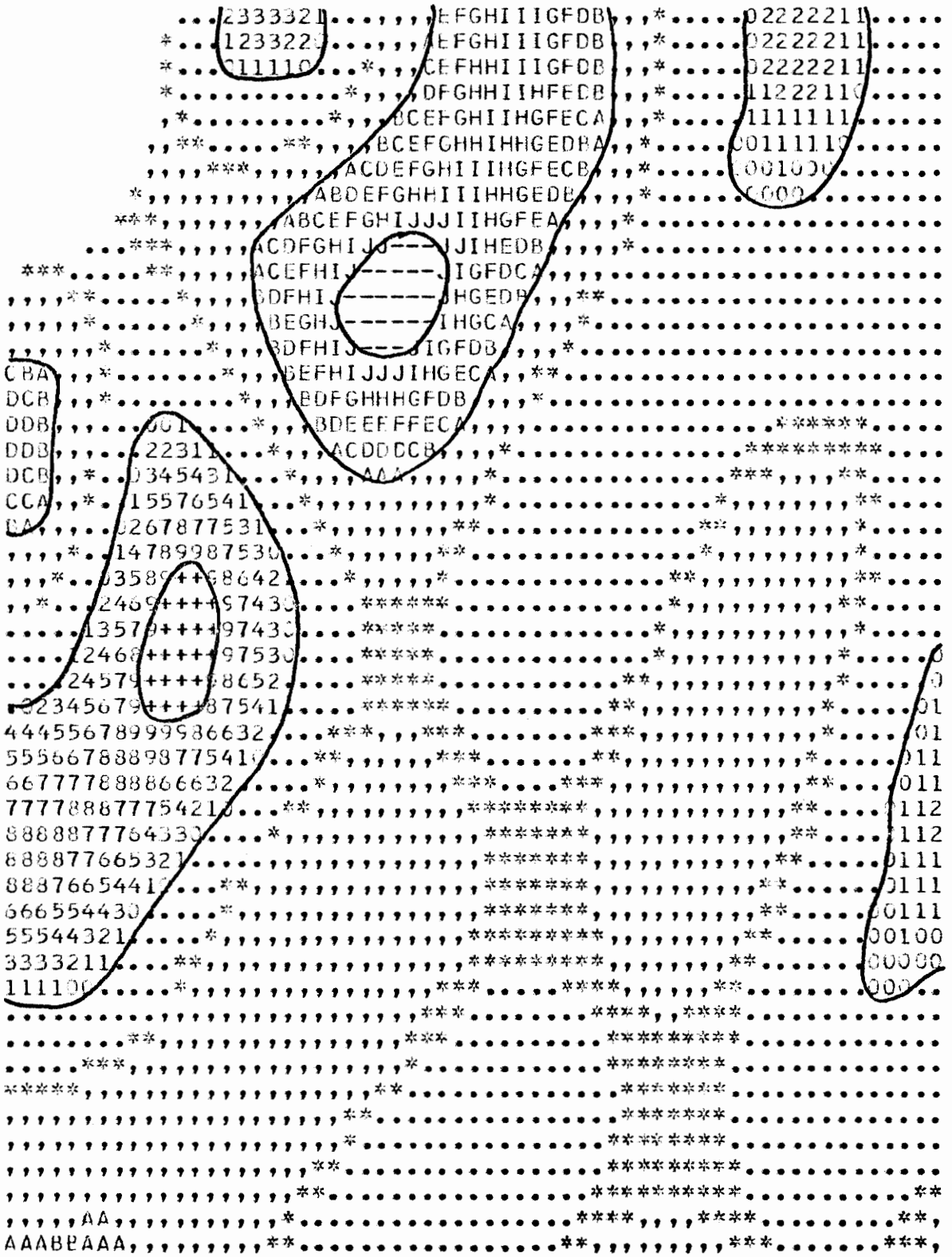

SIGMA XI,ETA

MAP NO. 5

M = 0.0 SCALE FACTOR = 0.412

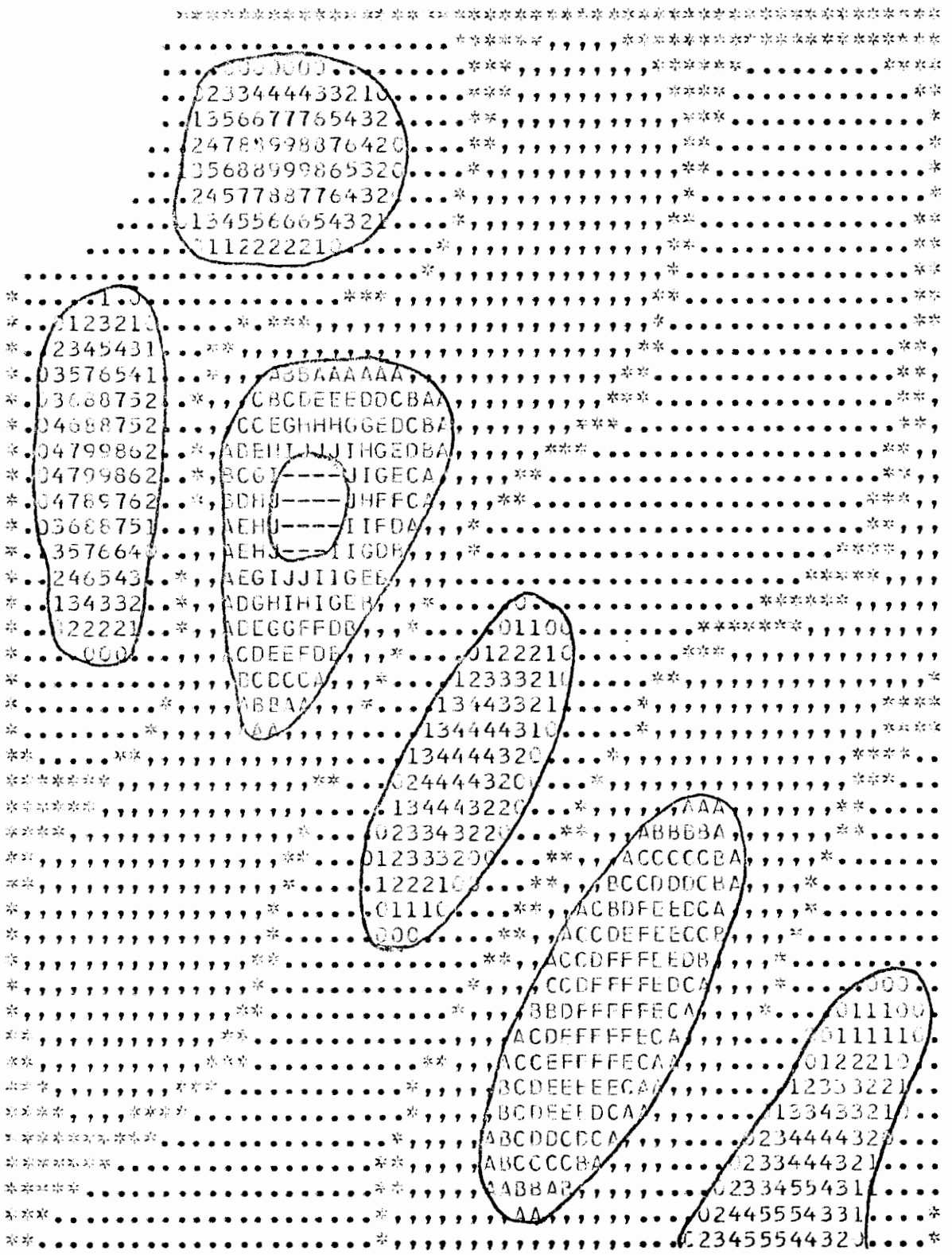

SIGMA ETA,ETA

MAP NO. 6

M = 0.0 SCALE FACTOR = 0.697

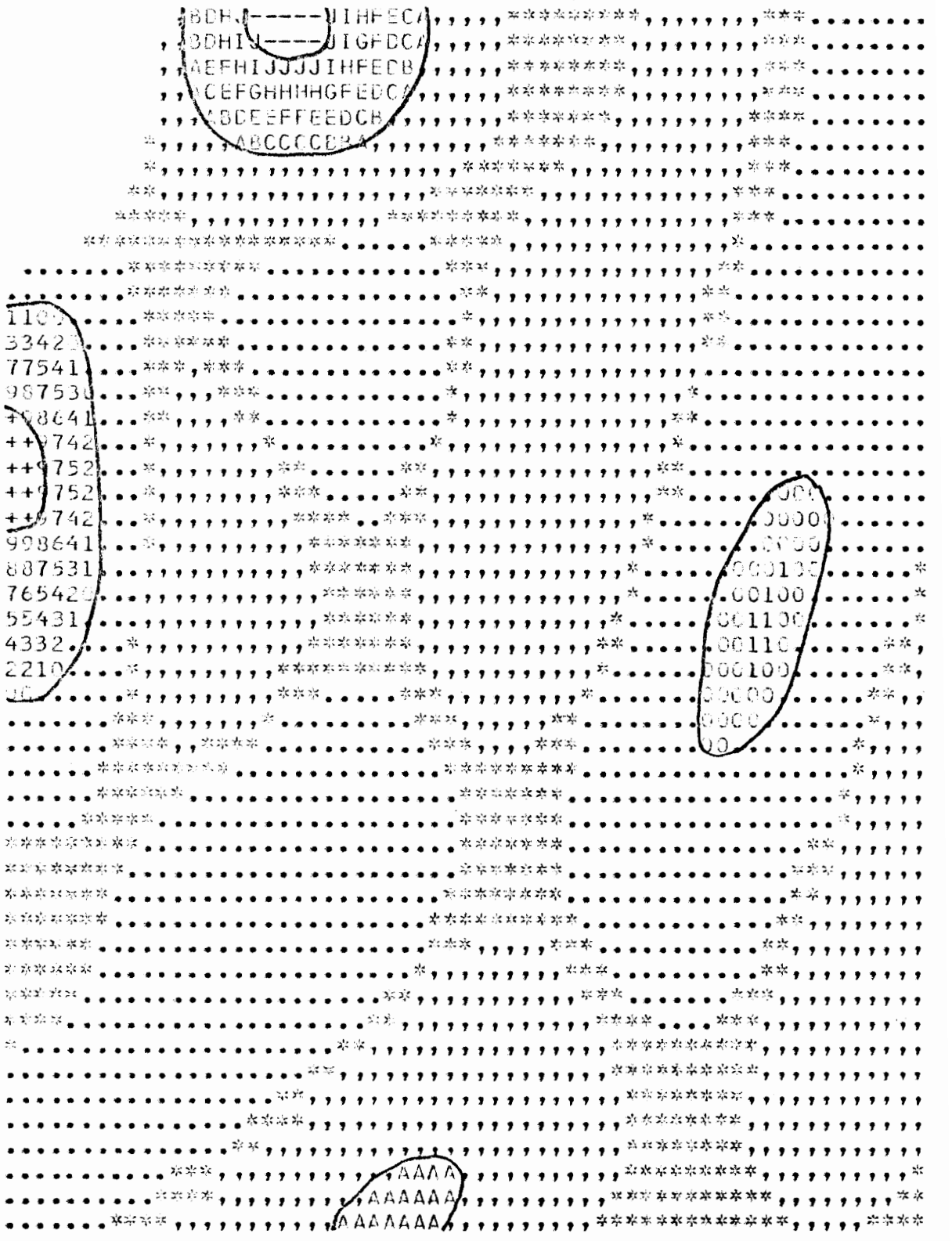

DILATATIONAL STRESS, INVARIANT, ISOPACHICS MAP NO. 7

M = 3.0 SCALE FACTOR = 0.264

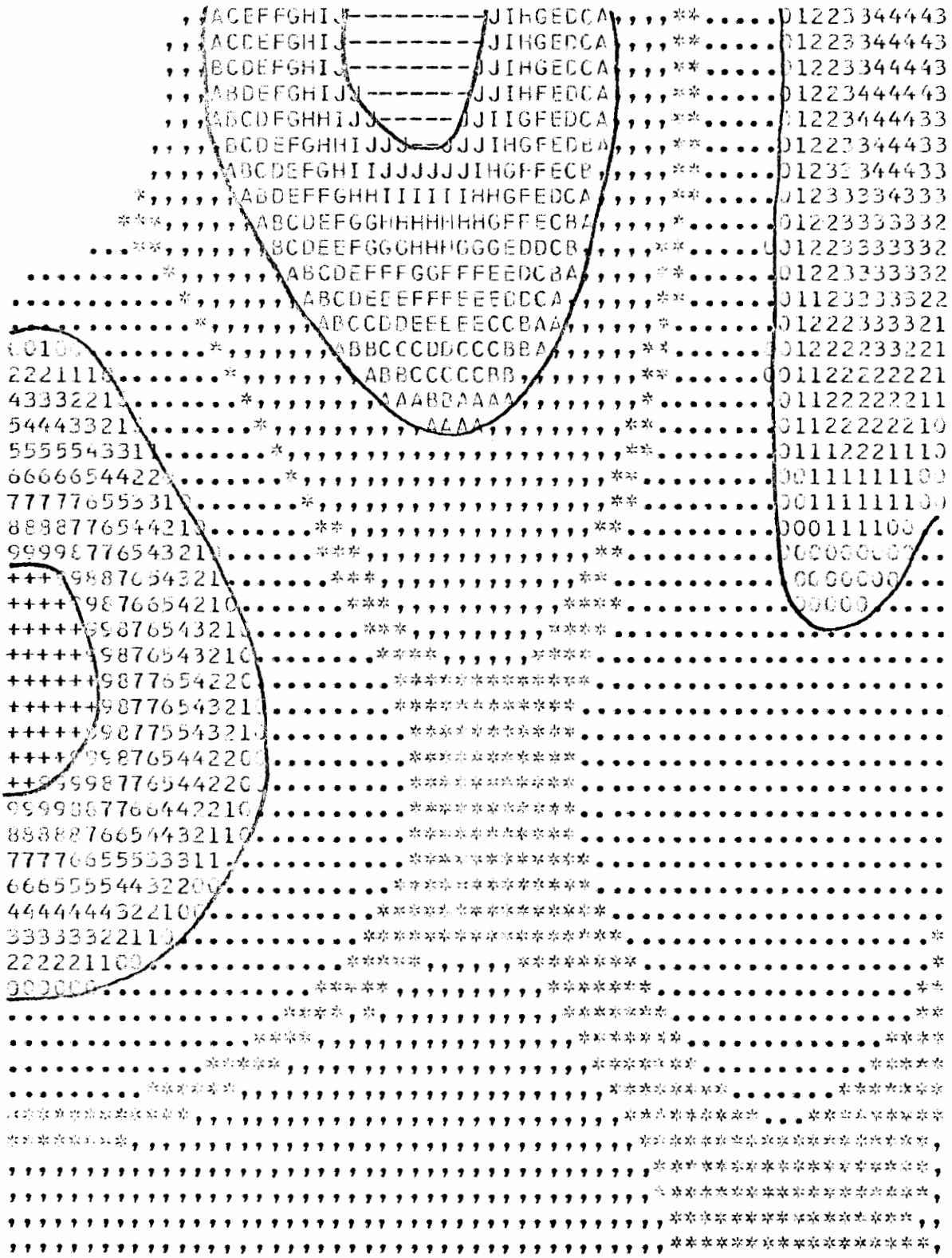

STRESS INVARIANT 2 MAP NO. 8

M = 0.0 SCALE FACTOR = 0.204

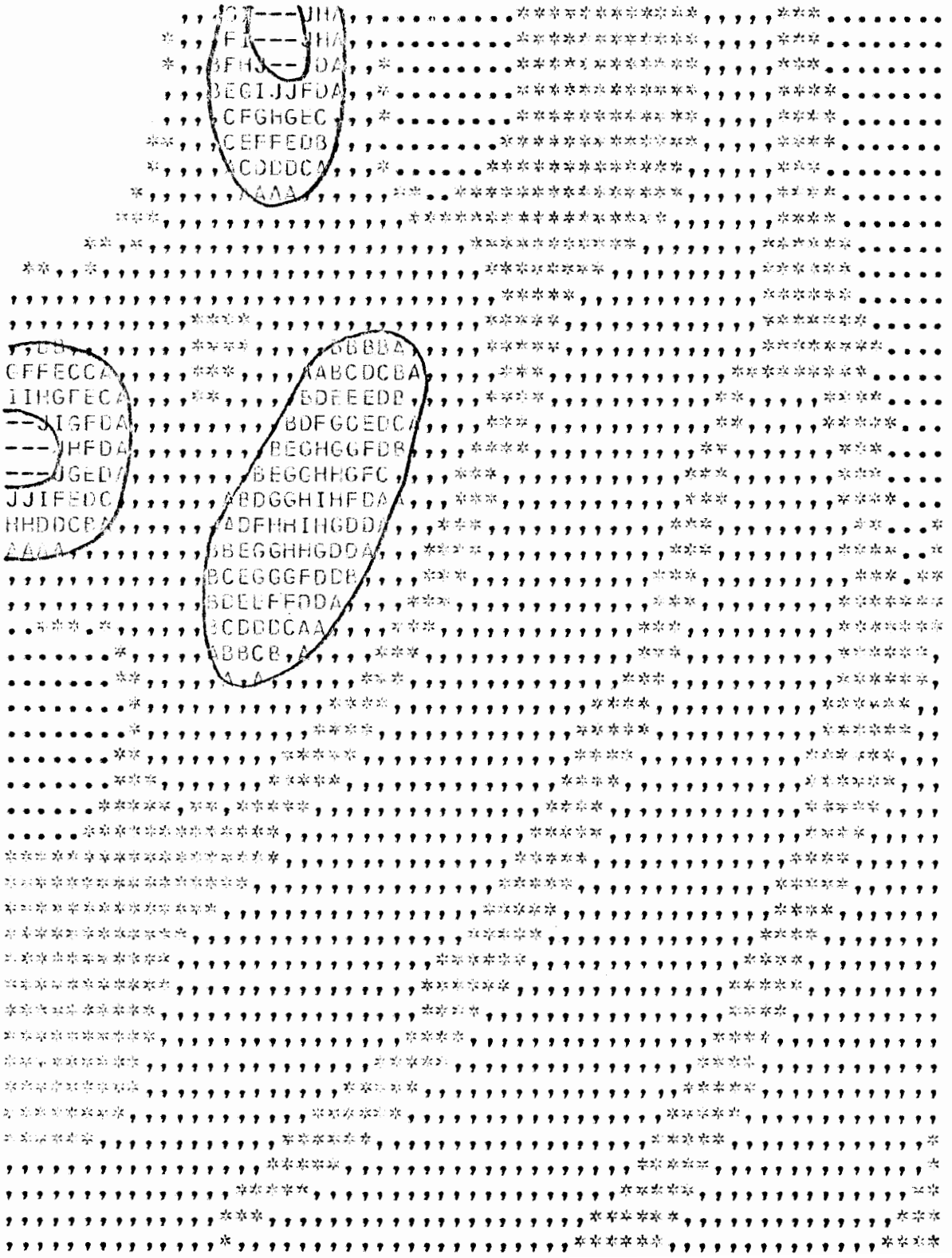

PRINCIPAL NORMAL STRESS(PLUS), INVARIANT MAP NO. 9

M = 0.0 SCALE FACTOR = 0.697

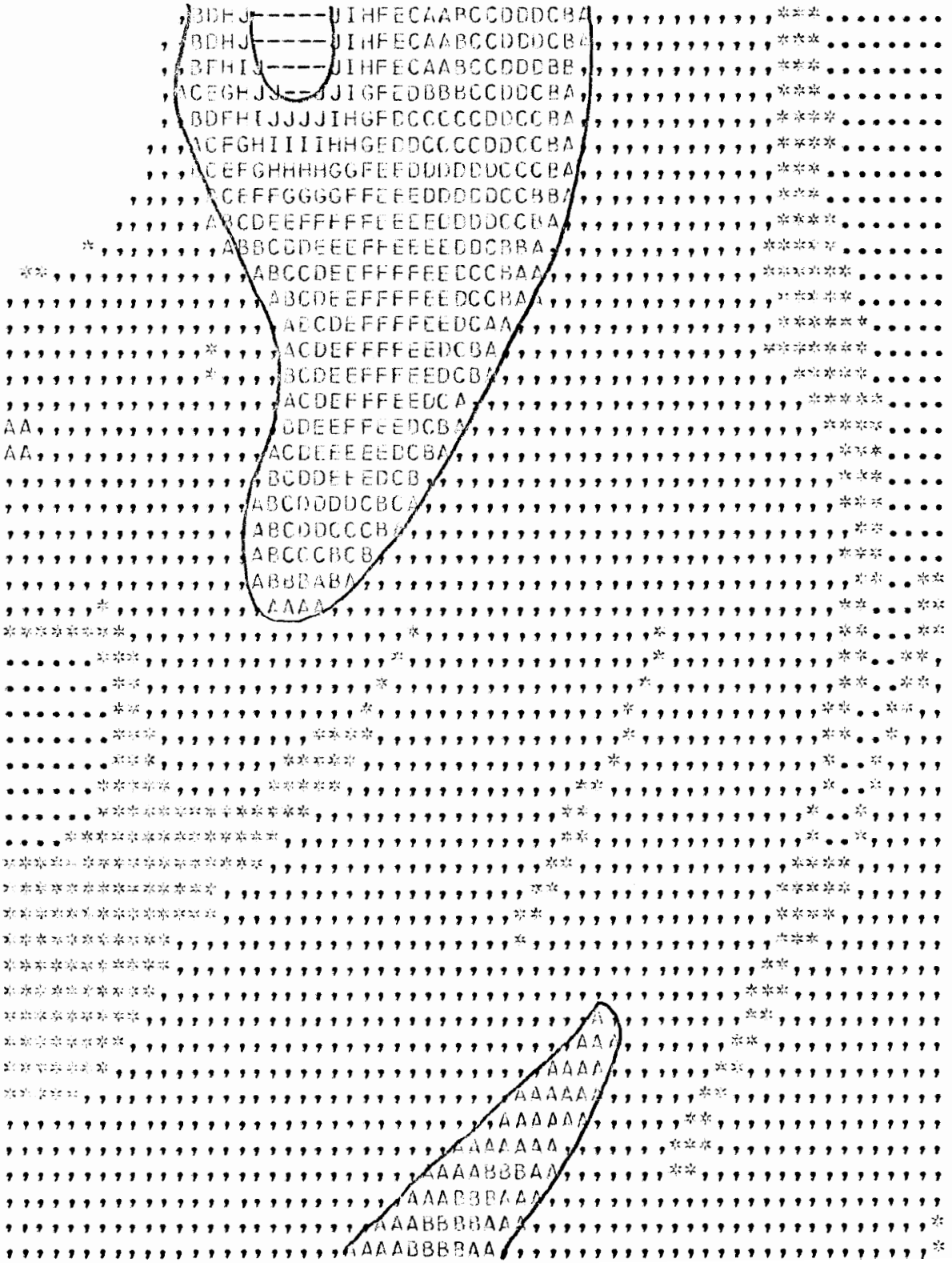

PRINCIPAL NORMAL STRESS(MILUS), INVARIANT MAP NO. 10

M = 0.0 SCALE FACTOR = 0.697

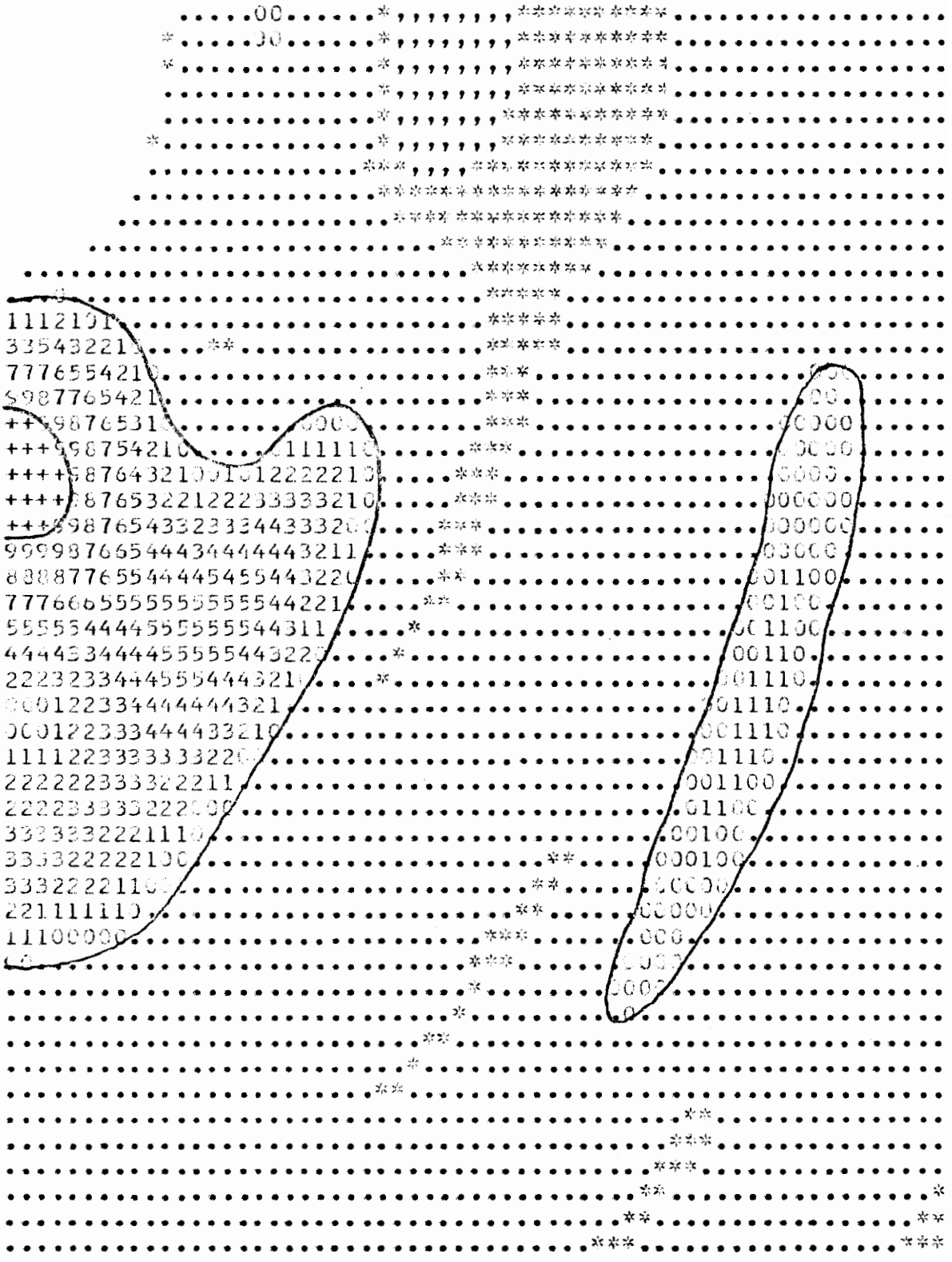

PRINCIPAL SHEAR STRESS, INVARIANT, ISOCHROMATICS MAP NO. 11

M = 0.0 SCALE FACTOR = 0.492

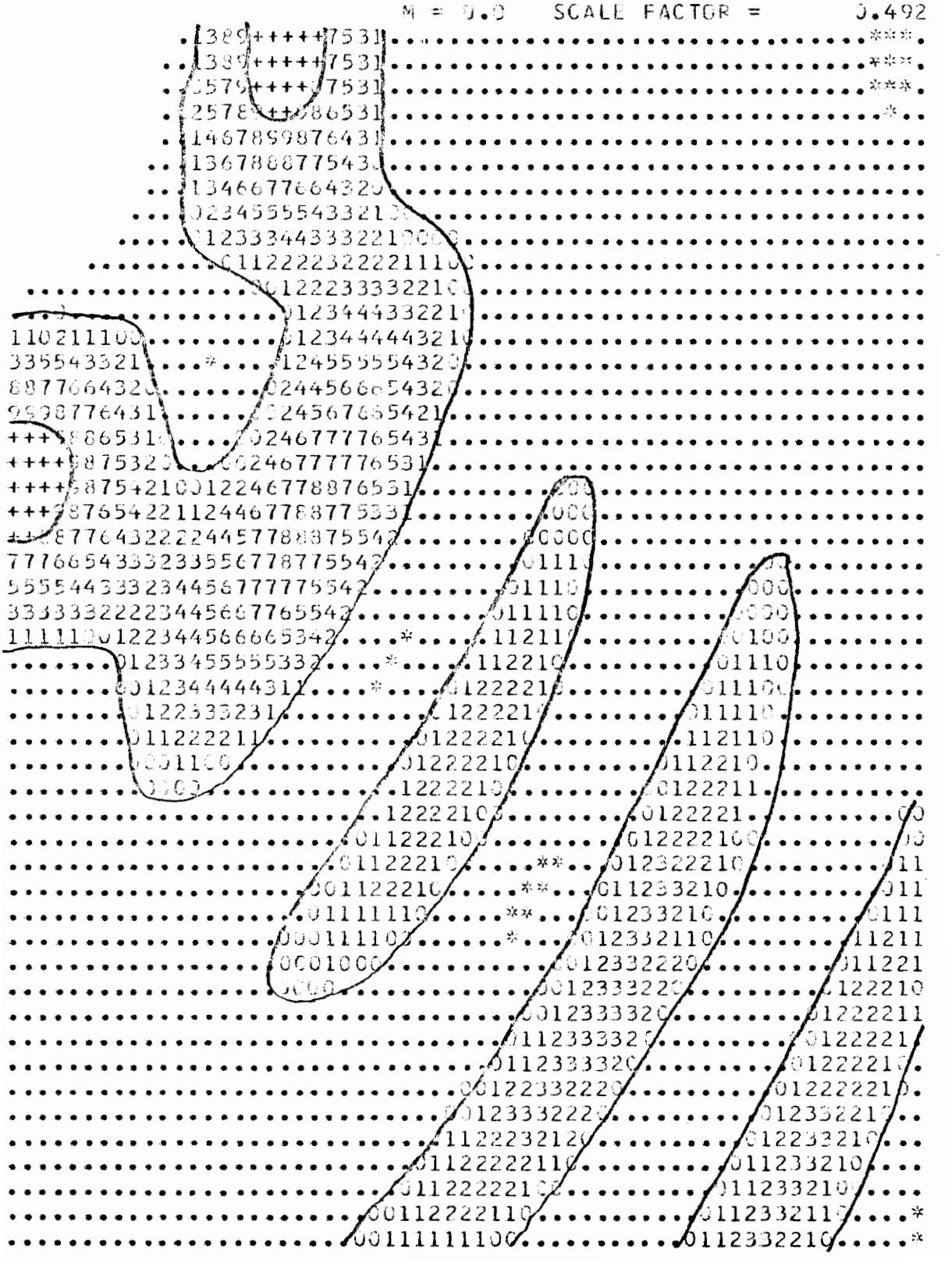

PRINCIPAL DIRECTION, INVARIANT, ISOCLINICS MAP NO. 12

M = 0.0 SCALE FACTOR = 0.785

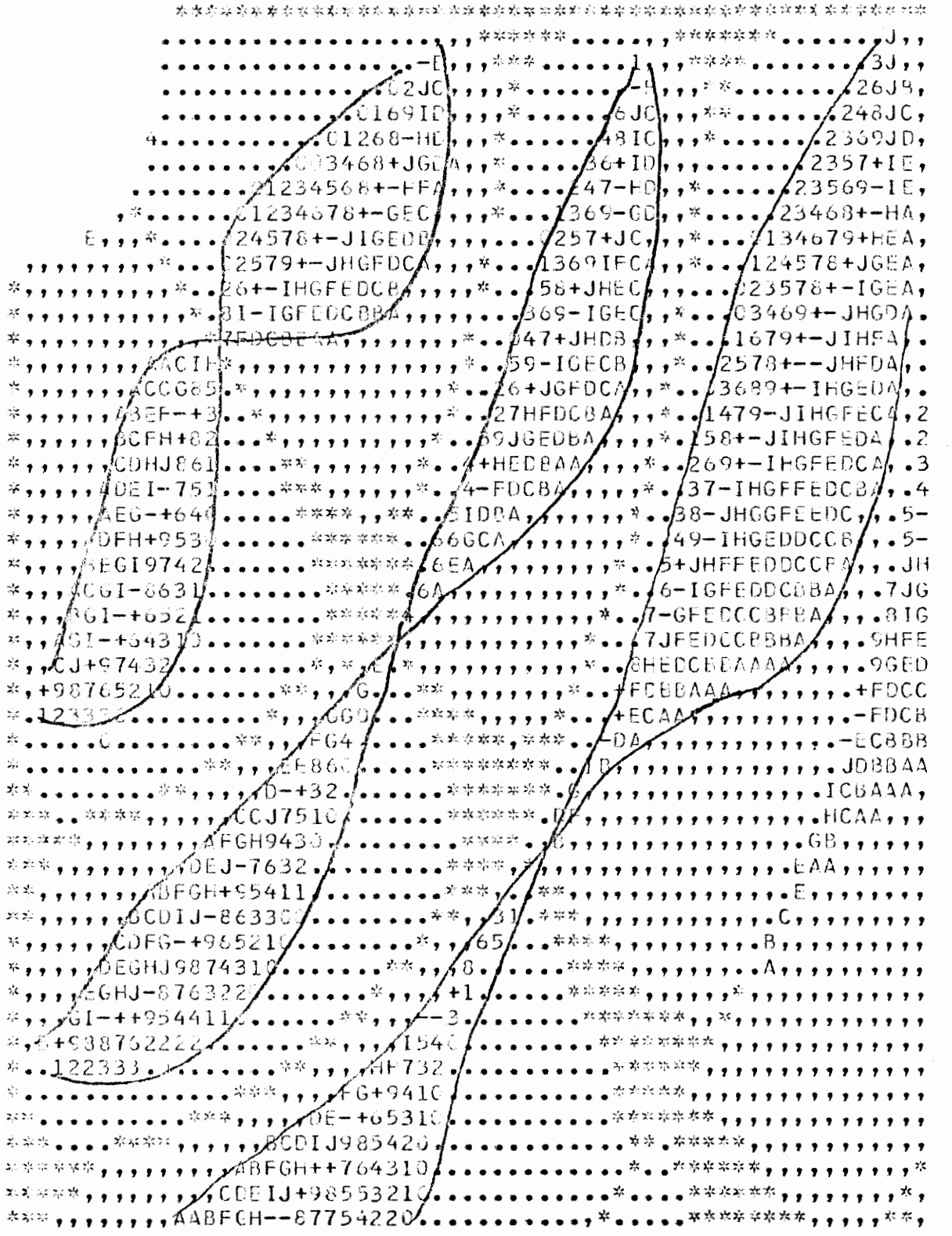

X COMPONENT OF DISPLACEMENT MAP NO. 13

M = 0.0 SCALE FACTOR = 0.802

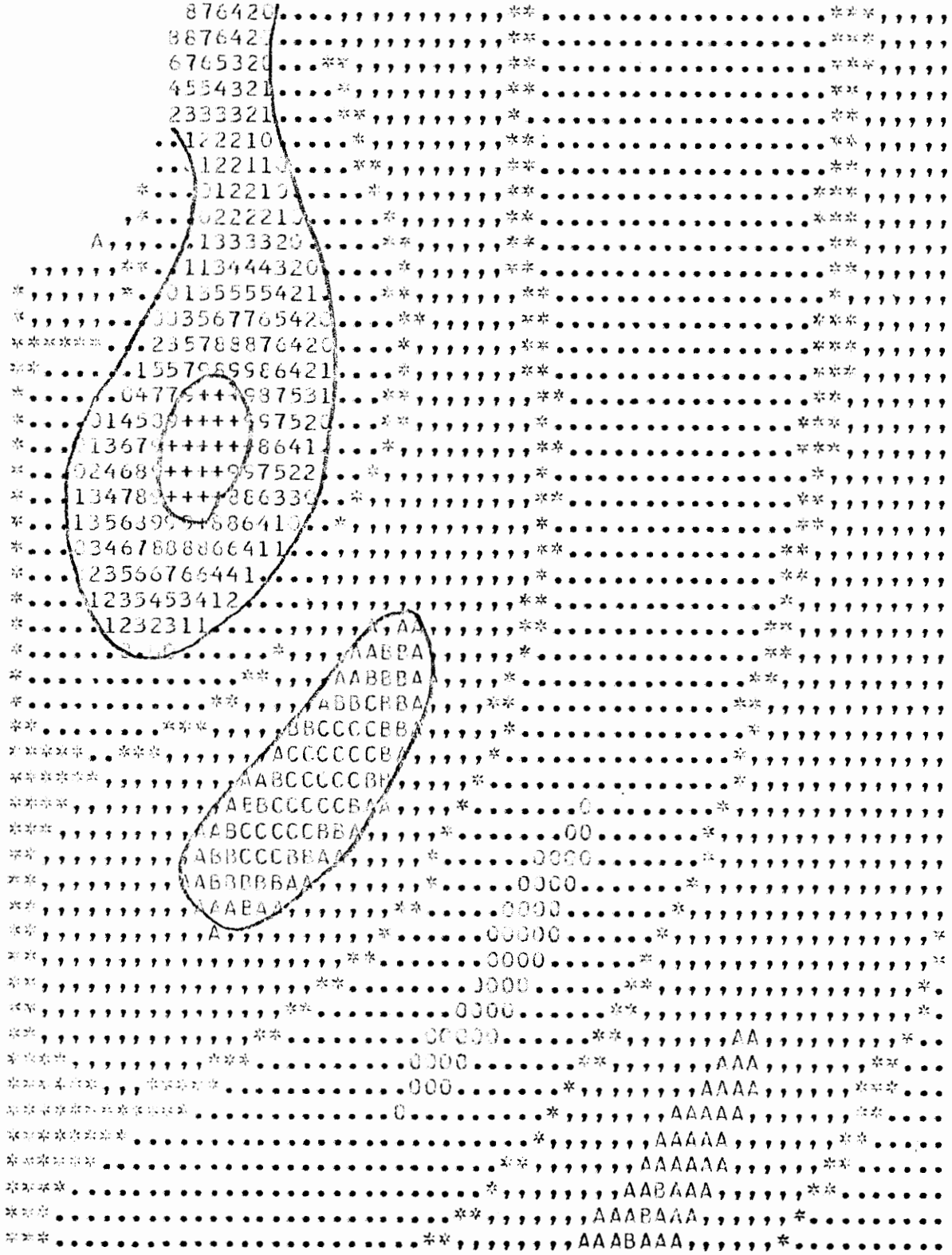

Y COMPONENT OF DISPLACEMENT MAP NO. 14

M = 0.0 SCALE FACTOR = 0.302

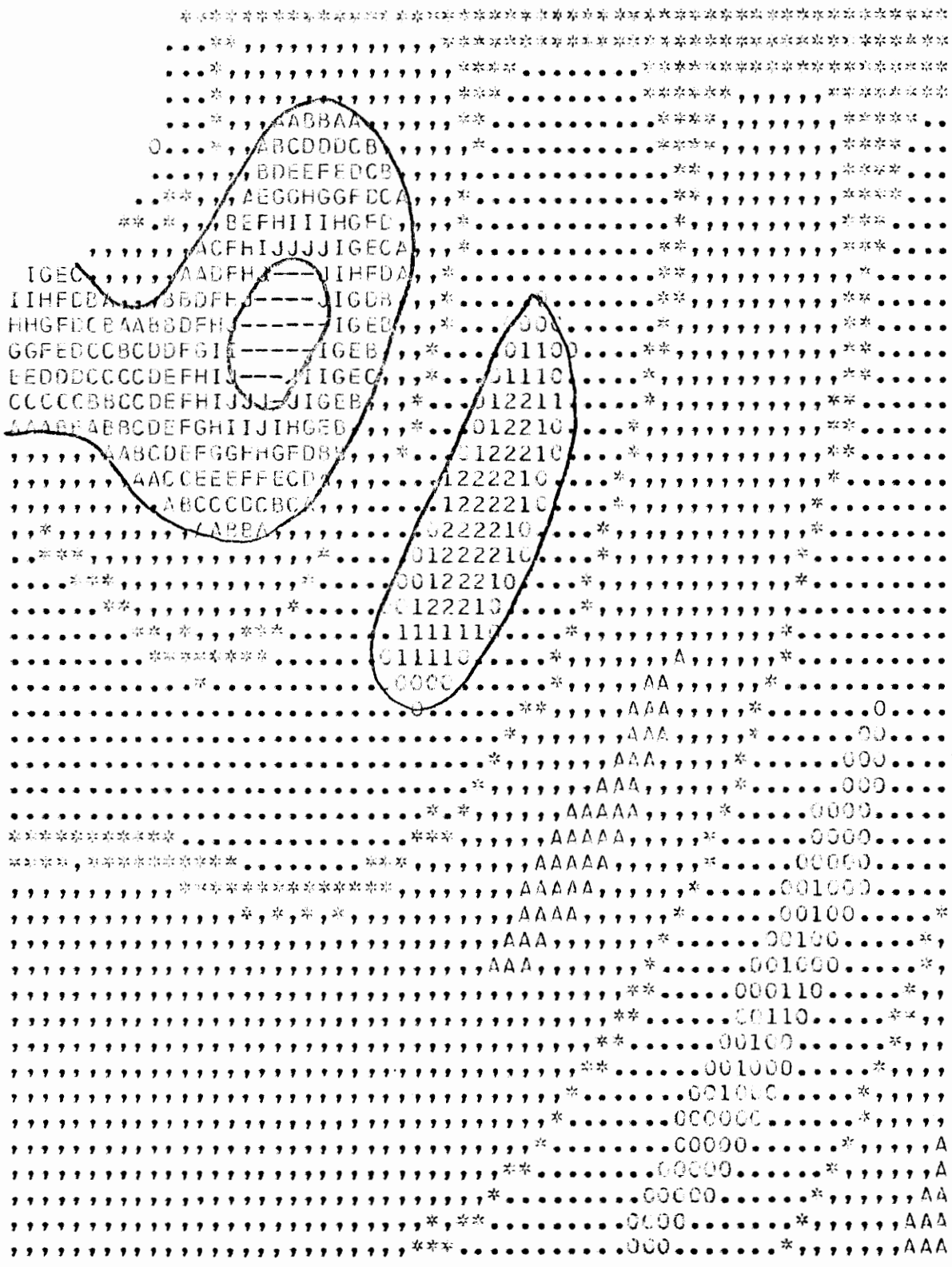

MODULUS OF DISPLACEMENT MAP NO. 15

M = 2.0 SCALE FACTOR = 1.034

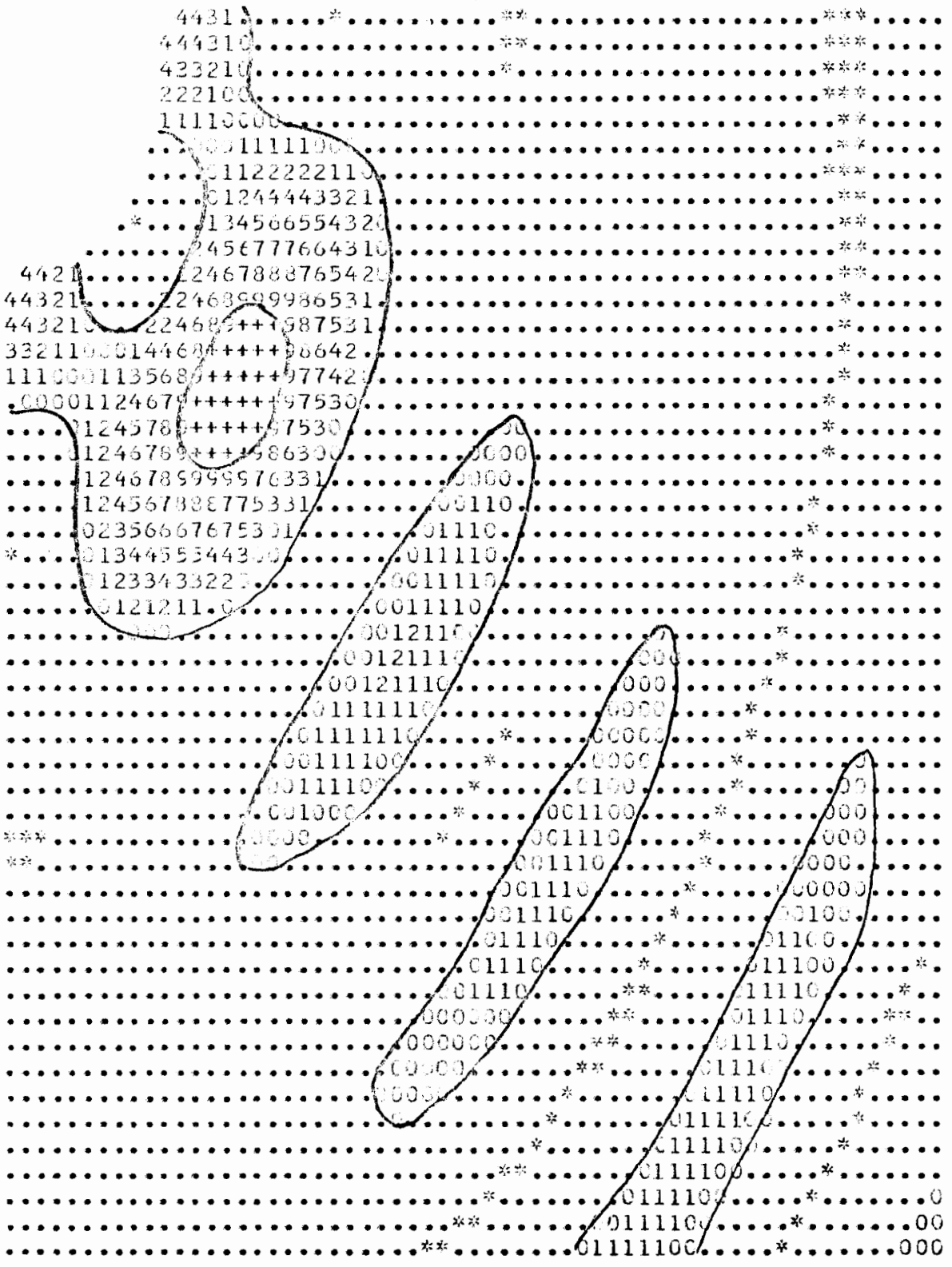

The dilatational stress is of interest from the point of view of experimental methods. Due to the Poisson effect transverse strain ε_{ZZ} and transverse displacement W will be generated [20, p. 233]

$$\frac{\partial W}{\partial Z} = \varepsilon_{ZZ} = \frac{-\nu}{E}[\sigma_{xx} + \sigma_{yy}]$$

where ν = Poisson's ratio

E = Young's Modulus

It is suggested that time lapse Holography could detect spatial variations in the transverse or out of plane displacement which is proportional to the dilatational stress. The Holographic patterns would be the isopachics. Plots 16, 17, 18, 19, 20, 21, 22, 23, 24, 25, 26 are the isopachics for the following values of m: .00, .01, .02, .03, .04, .05, .10, .20, .30, .40, .50. For these plots each character has a spatial separation (Δs) of .20 inch.

The use of Holography as an experimental method seems appropriate since:

a) The disturbance is a standing wave

b) The frequency of the vibration is relatively large (kilo Hertz range). This is because the in-plane stiffness of thin plates is relatively large compared to the bending stiffness. In summary, the frequency f is given by:

$$f = \frac{C_{S\gamma}}{2\pi \hat{R}} \text{ Hz}$$

where: C_S = shear wave speed

$$= \frac{E}{2(1 - \nu)\rho}$$

$$\hat{R} = \frac{a}{1 + m} \quad ; \quad a = \text{semi-major axis}$$

$$m = \frac{a - b}{a + b} \quad ; \quad b = \text{semi-minor axis}$$

and

$$\gamma = N\,C\left[1 + \frac{1}{2N\sqrt{1 - C^2}} + O(m^2)\right] \quad ; \quad N = 4,6,8,\ldots$$

$$\gamma = 2.349\sqrt{1 - 0.234\,m^2 + O(m^2)} \quad ; \quad N = 2$$

$$C = C_R/C_S$$

C_R = Rayleigh wave speed

Hence:

$$f = \frac{1 + m}{a}\frac{NC_R}{2\pi}\left[1 + O(m^2) + O\left(\frac{1}{N}\right)\right]\text{Hz}$$

c) The Holograms would detect the isopachics which (as can be seen from plots 16 to 26) are extremely sensitive to small changes in m.

The disturbance could be generated by applying the periodic surface traction

$$\sigma_{RR} \propto \text{Cos}(N\theta)\ \text{Cos}(ft) \quad ; \quad N = 2,4,6,\ldots$$

on any of the j-surfaces (refer to page 39).

$$R_o = \frac{j\pi a}{\sqrt{\delta\gamma}(1+m)} \quad ; \quad j = 4,5,6,\ldots$$

This would generate traveling P-waves which would intersect the elliptical void at grazing incidence and perhaps resonate the free vibration to such an extent that it could be detected. For the case of a slit the incident P-waves would generate evanescent Py surface waves [25], [26], [27], [28], [29, p. 24]. The actual response could be more complicated than suggested here and it might be difficult to sort out and identify the various types of wave behavior. As an aid in detecting the wave it should be noted that the isopachics are separated approximately by

$$\Delta x = \frac{\pi a}{\sqrt{\delta}(1 + m)\gamma(m)}$$

which is proportional to the semi-major axis a.

The dilatational stress concentrations suggest that the standing wave could create or contribute to fracture or microcracks in materials that fail in tension. The number and shape of the stress concentrations for large m suggest that the fractures might be analogous to scabbing.[1] This term originally coined by Hopkinson is used to describe "the interference between an incident (traveling) wave and its reflected counterpart." [23, p. 125] The results here are for standing waves which tend to be nearly dilatational as the eccentricity is increased and tend to be confined to the X-axis. Photographs of scabbing in [23, pp. 125, 128] compare favorably with the dilatational stress concentrations and suggest multiple scabbing; a series of

---

[1]Also called spalling, especially in modern terminology.

parallel cracks. Also see [24, p. 186].

It is observed that for m > 0 that there is very little dilatational stress in a large region near the elliptical void. This is because as m increases, the order of the Bessel function that dominates the solution also increases. The higher order Bessel functions do not reach their peak values until larger arguments are reached.

The following is a table of the values of Z when $J_N(Z)$ has its maximum value:

N	Z
0	0
2	3.1
4	5.4
6	7.6
8	9.6

This explains why the perturbed eigenvectors are large. Near the boundary the higher order Bessel functions are small and hence the coefficients of these Bessel functions must be large in order to satisfy the boundary conditions at each order of perturbation.

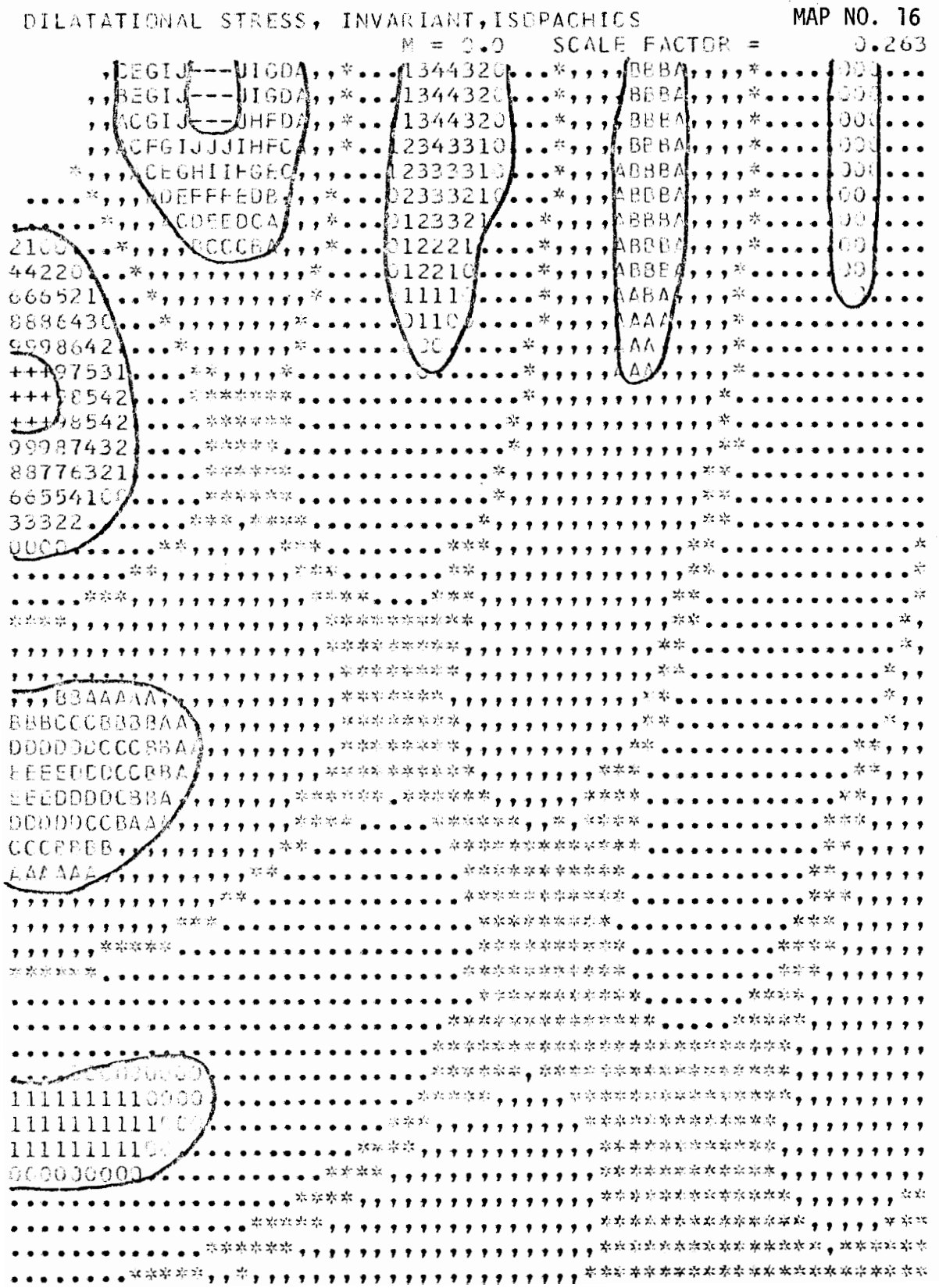
DILATATIONAL STRESS, INVARIANT, ISOPACHICS
MAP NO. 16
M = 0.0
SCALE FACTOR = 0.263

DILATATIONAL STRESS, INVARIANT, ISOPACHICS MAP NO. 17

M = 0.010 SCALE FACTOR = 0.299

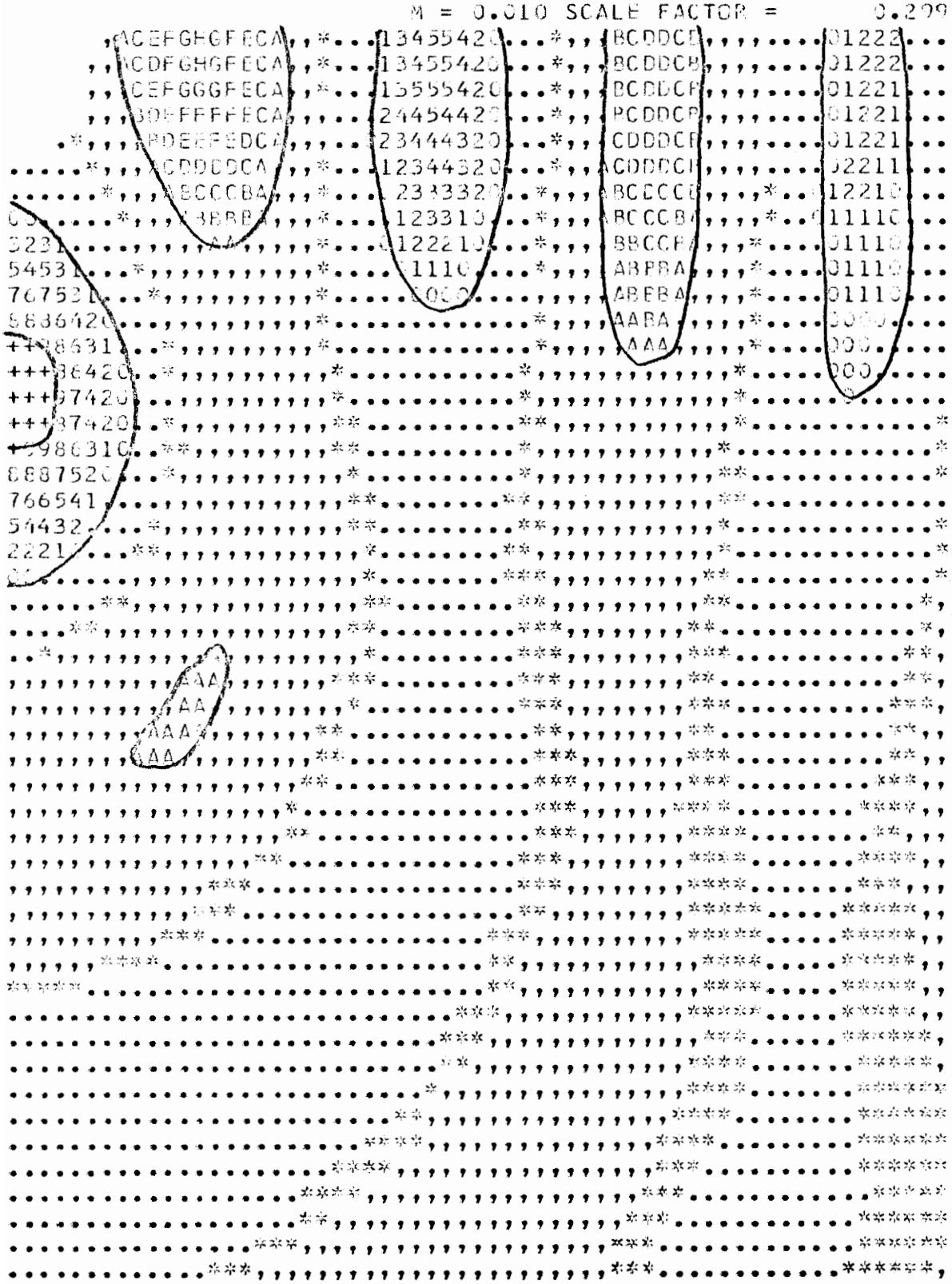

DILATATIONAL STRESS, INVARIANT, ISOPACHICS MAP NO. 18

N = 0.020 SCALE FACTOR = 0.342

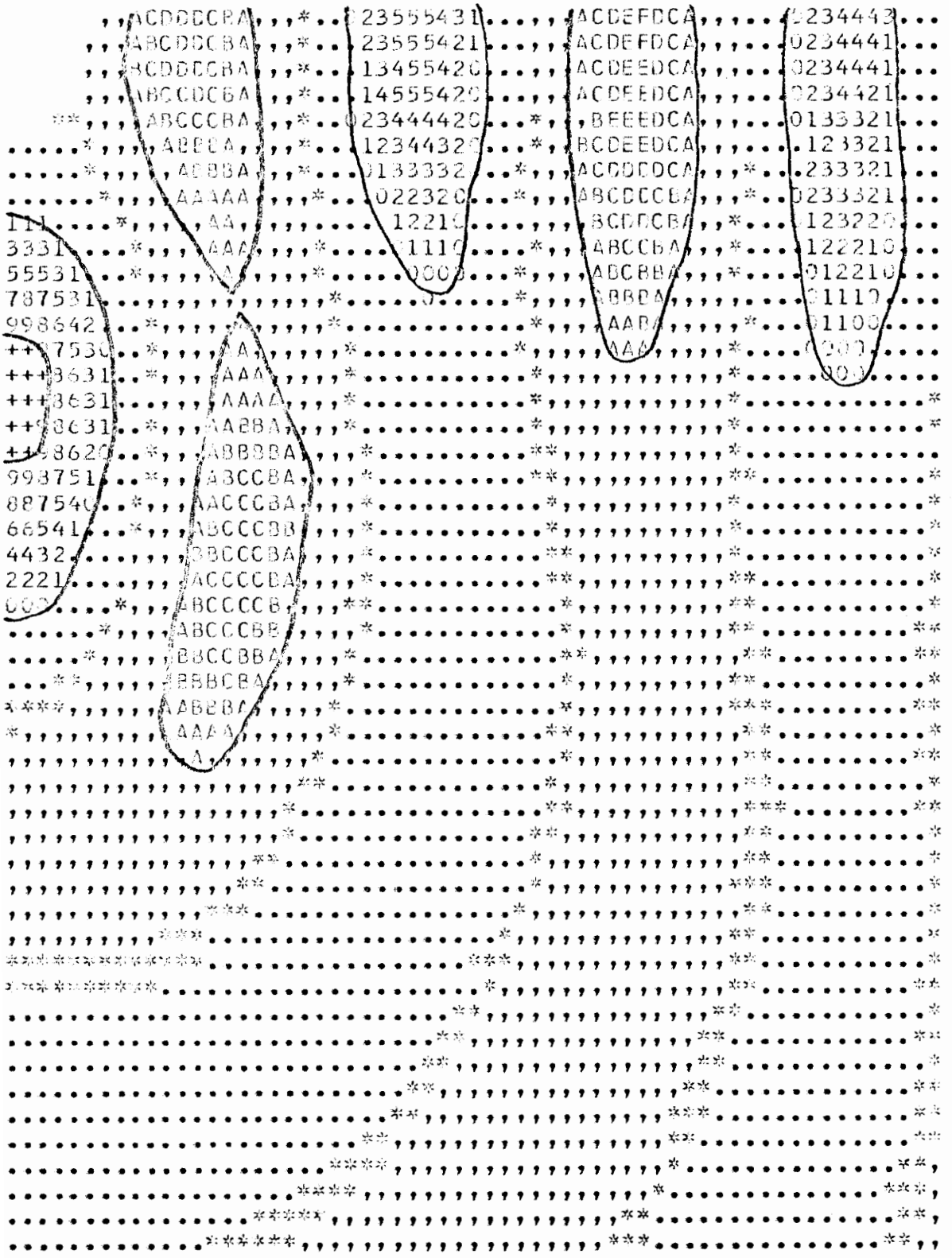

DILATATIONAL STRESS, INVARIANT, ISOPACHICS MAP NO. 19

A = 3.030 SCALE FACTOR = 0.400

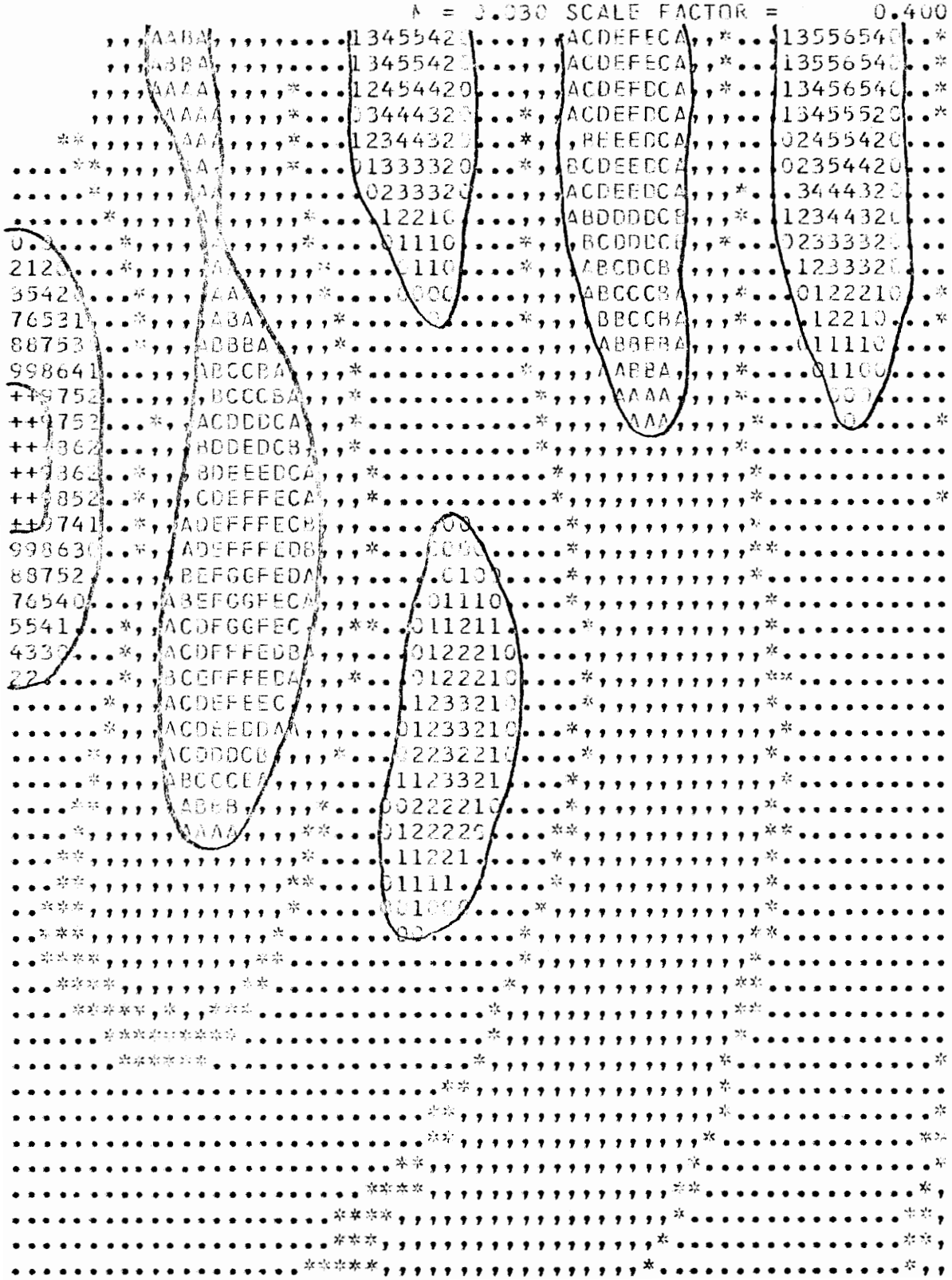

DILATATIONAL STRESS, INVARIANT, ISOPACHICS MAP NO. 20

M = 0.040 SCALE FACTOR = 0.477

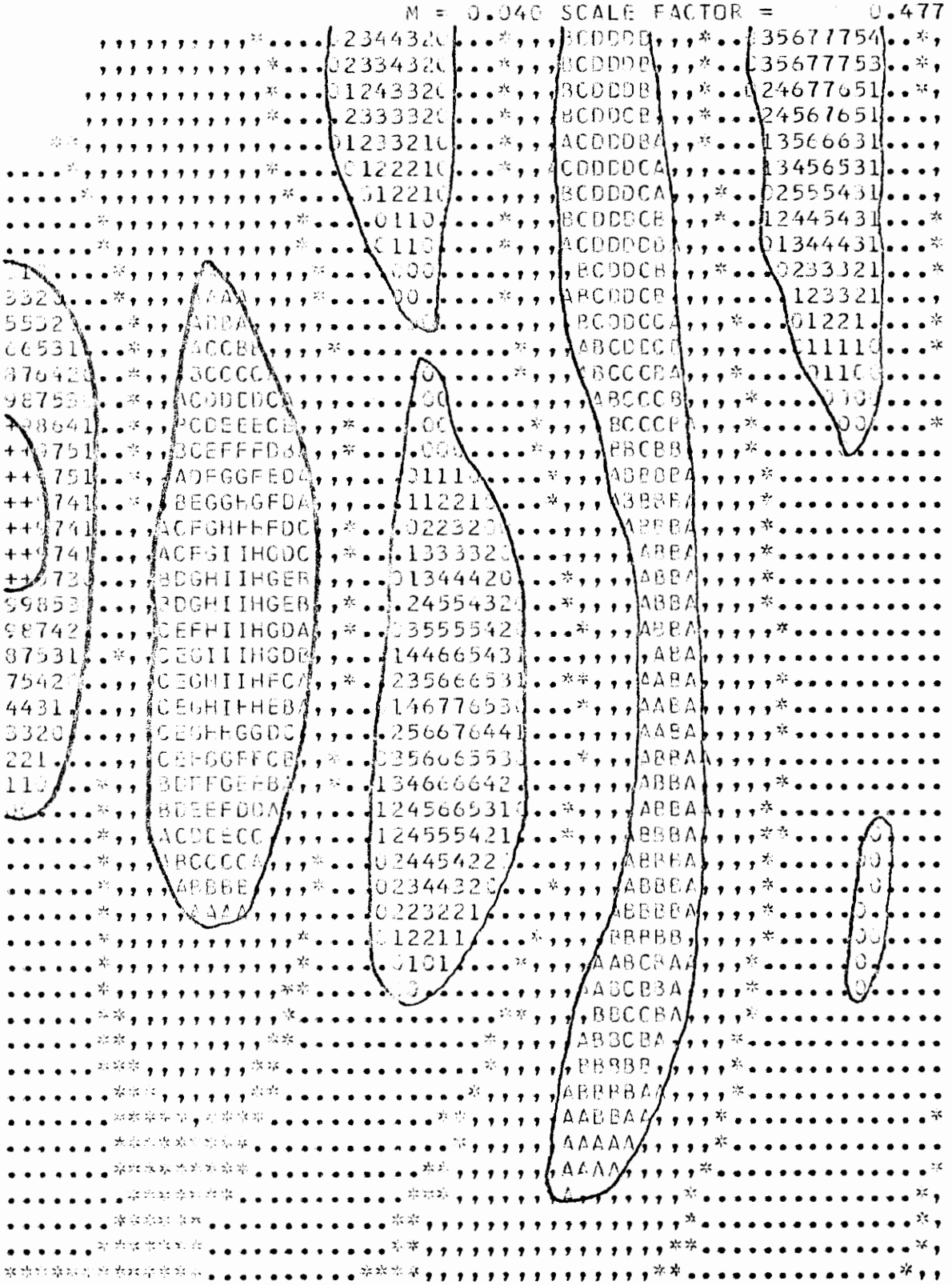

DILATATIONAL STRESS, INVARIANT, ISOPACHICS MAP NO. 21

M = 0.050 SCALE FACTOR = 0.585

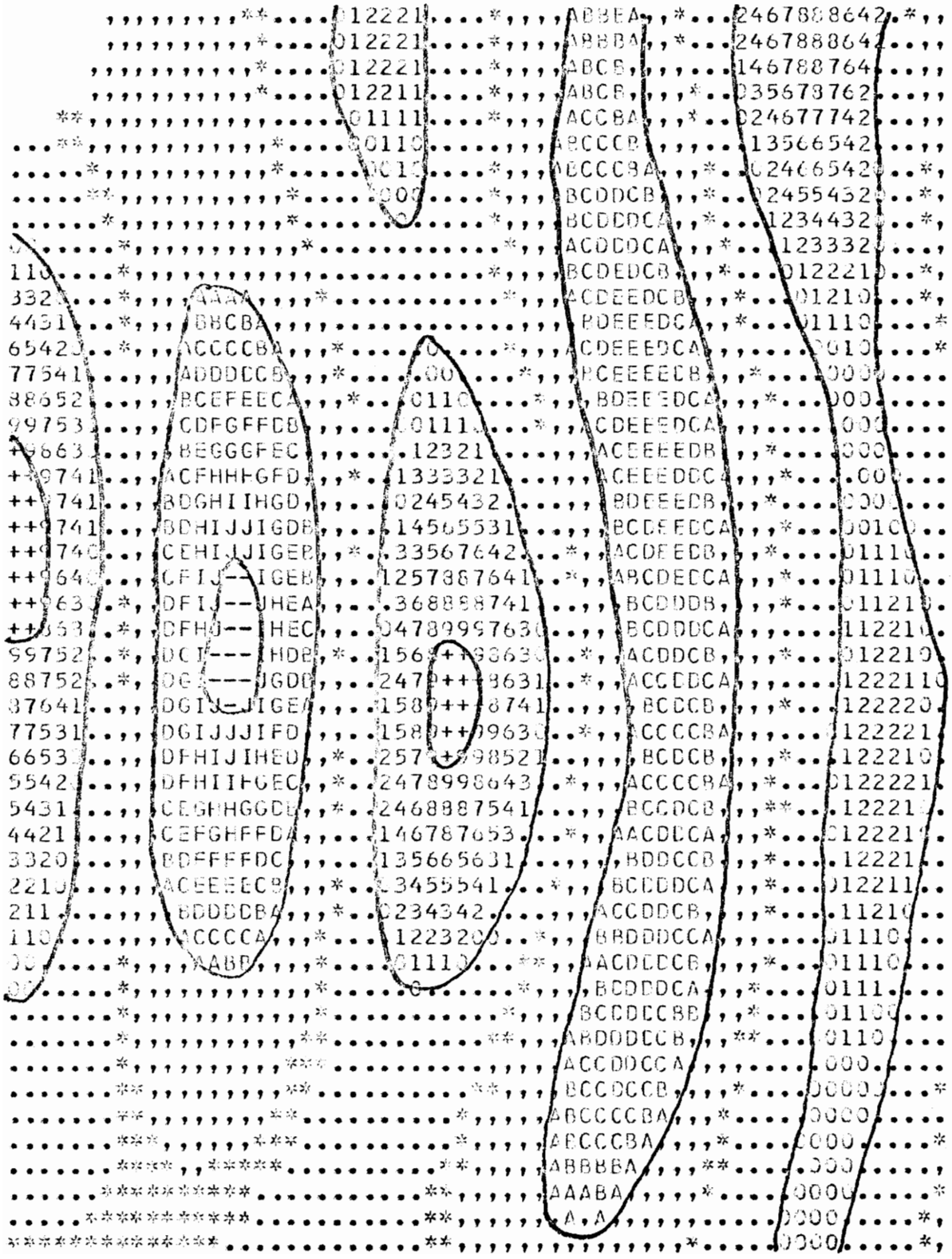

DILATATIONAL STRESS, INVARIANT, ISOPACHICS MAP NO. 22

M = 0.100 SCALE FACTOR = 10.537

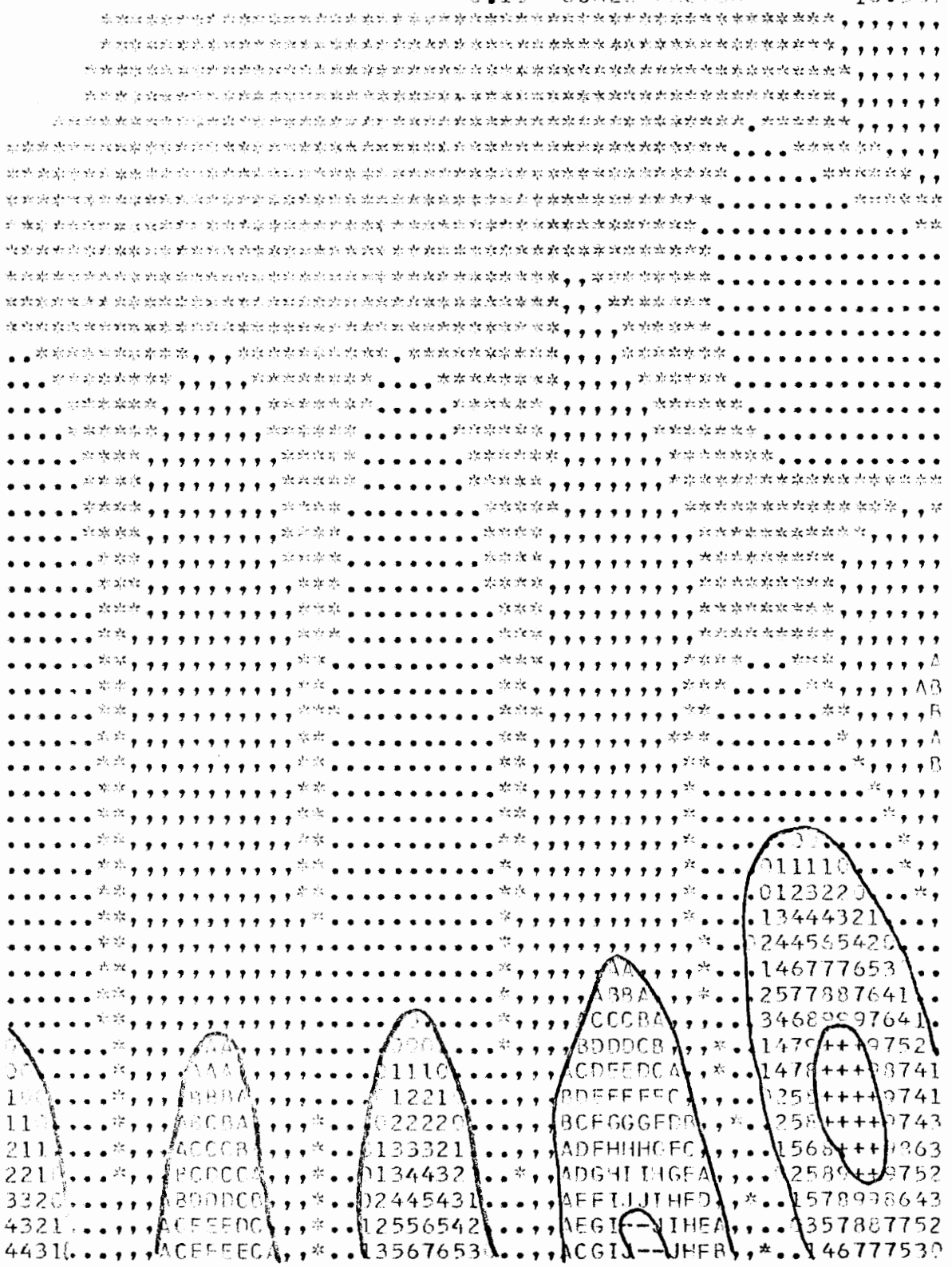

DILATATIONAL STRESS, INVARIANT, ISOPACHICS MAP NO. 23

N = 0.200 SCALE FACTOR = 491.151

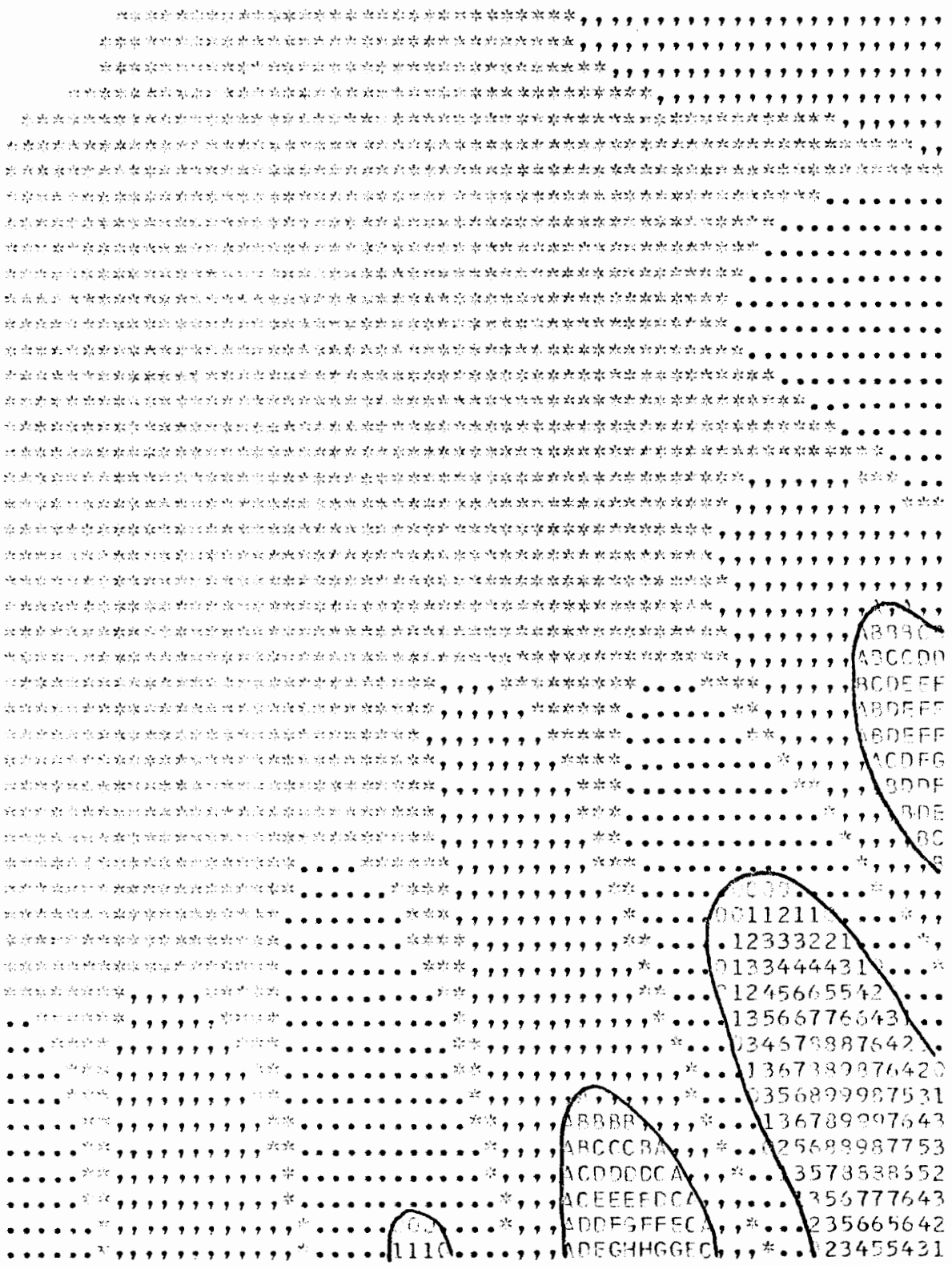

DILATATIONAL STRESS, INVARIANT, ISOPACHICS MAP NO. 24

M = 0.300 SCALE FACTOR = 3750.067

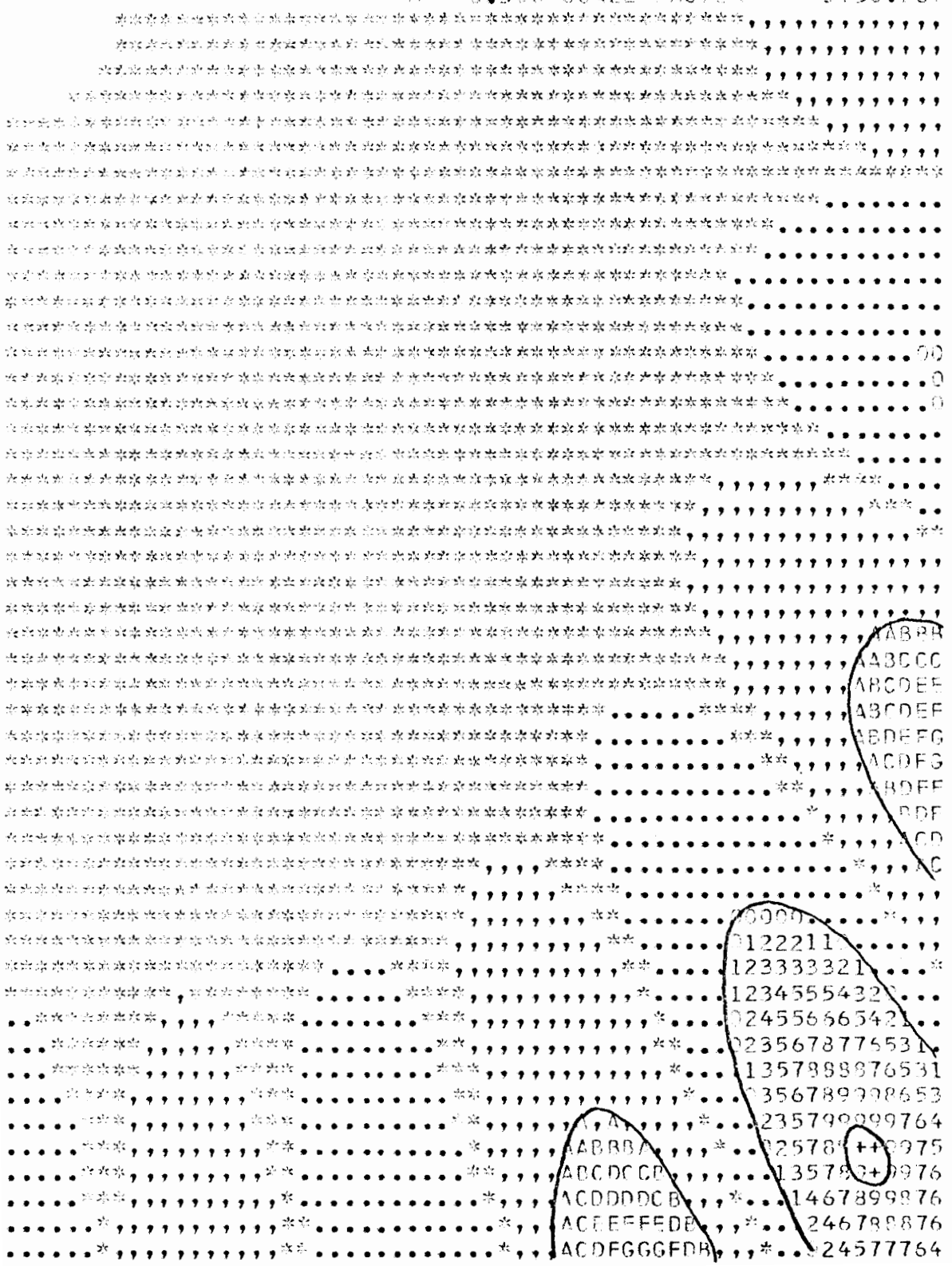

DILATATIONAL STRESS, INVARIANT, ISOPACHICS MAP NO. 25

M = 0.400 SCALE FACTOR = 12277.000

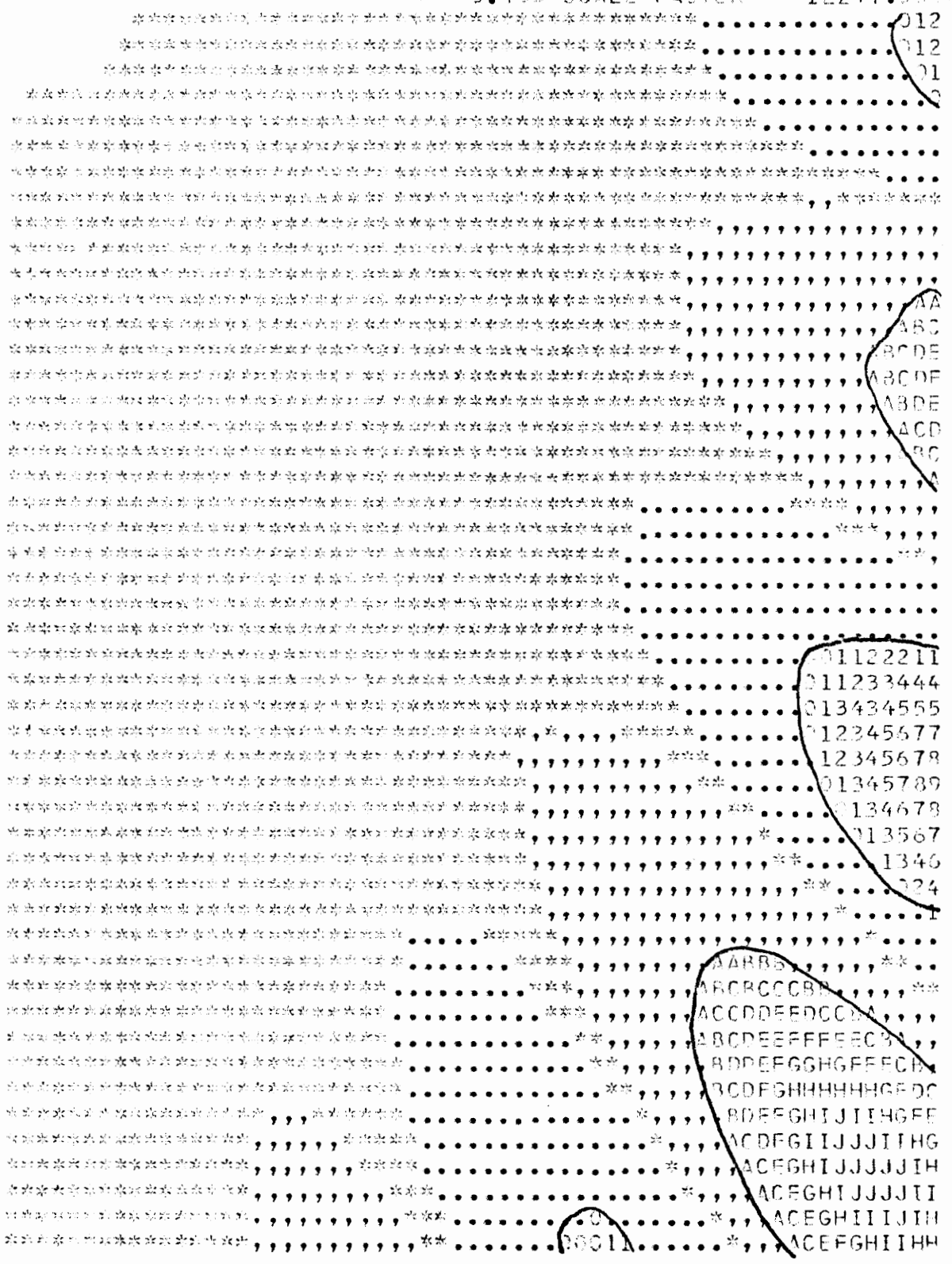

DILATATIONAL STRESS, INVARIANT, ISOPACHICS MAP NO. 26

N = 0.500 SCALE FACTOR = 1966.210

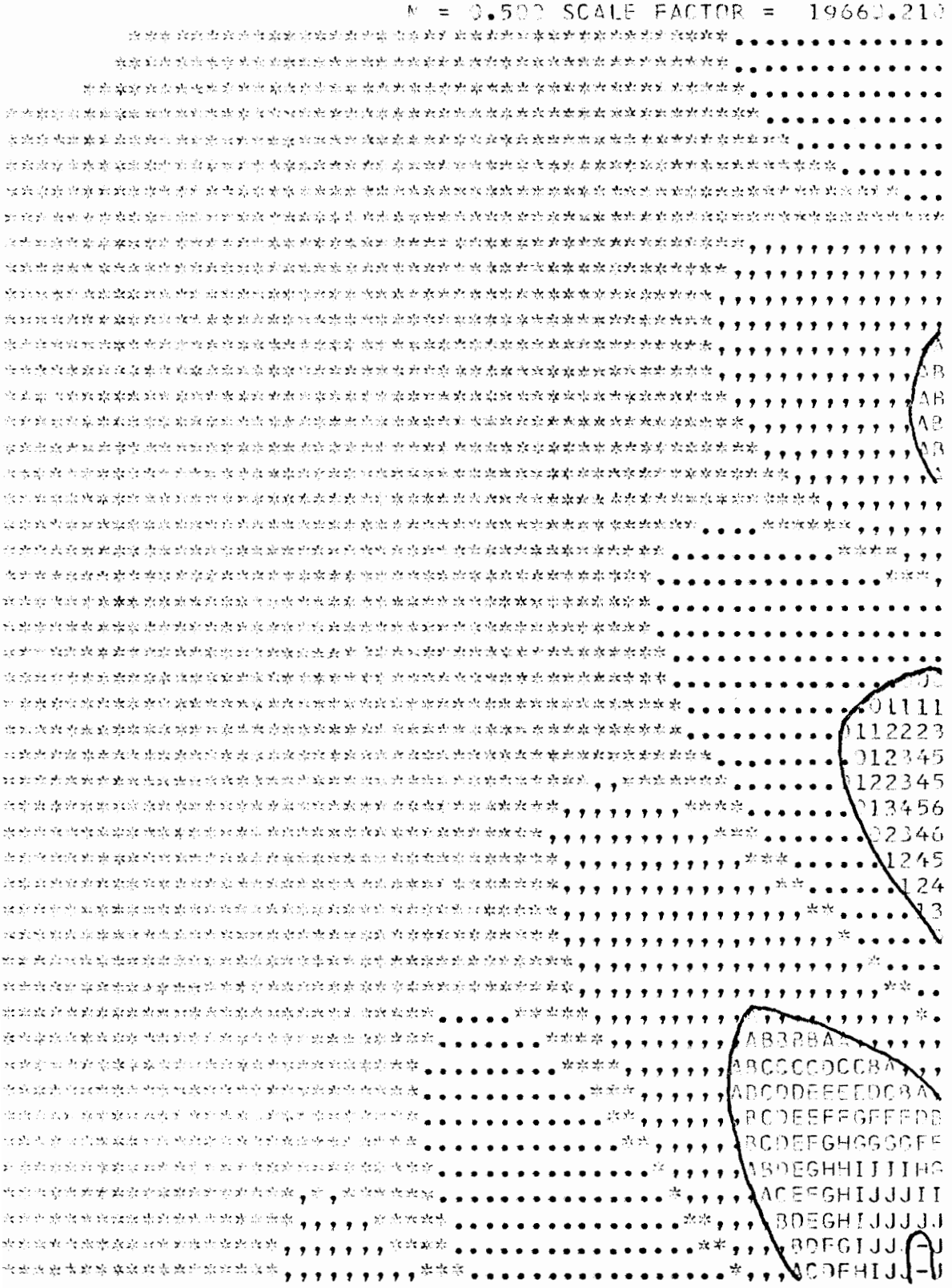

3.10 Summary

The combined use of the Kutta conformal mapping function and the Bessel function addition formula enabled a representation of solutions of the reduced wave equation appropriate for boundary conditions on an ellipse. The boundary conditions were then satisfied by both perturbation (for small m) and numerical (for arbitrary m) methods.

The eigenvalue was found to be slowly varying in m (see page 100), whereas the eigenvector was found to be fast varying in m (see page 102). For the case of a circle, the results of Viktorov were extended (see page 53), the location of turning points were found and it was shown that the tendency is to have nearly repeated eigenvalues and eigenvectors. This renders numerical solution of the eigenvector for large m to be difficult by any method. A modification of the Lanczos method was used to improve the accuracy of Gauss-Jordan reduction and enable a solution for larger m than would otherwise be possible. It was felt that separation of variables is not a numerically efficient technique for the case of a slit to calculate the eigenvector.

Contour plots of stresses, invariants and displacements were presented for the case of a circle. It was shown that for this simplified case that dilatational stress concentrations occur some distance from the boundary and are related to the properties of the $J_2(x)$ Bessel function (see page 112).

Contour plots of the dilatational stress (see pages 137 to 147) were plotted for various values of m. It was shown that numerous dilatational stress concentrations occur as narrow bands which correlate

well with the experimental observation of the appearance of micro-cracks or voids ahead of a main crack. It is noted that as $m \to 1$ the solution tends to be a standing dilatational wave at grazing incidence (see page 73).

The experimental techniques to generate and detect waves with the properties predicted in this chapter (see page 133) is discussed.

Chapter 3 Literature Cited

1. Love, A. E. H., A Treatise on the Mathematical Theory of Elasticity, 1927.

2. Sokolnikoff, I. S., Mathematical Theory of Elasticity, McGraw-Hill, 1965.

3. Watson, G. N., A Treatise on the Theory of Bessel Functions, Cambridge, 1922.

4. Whittaker, E. T., and Watson, G. N., A Course of Modern Analysis, Cambridge Univ. Press, 1969.

5. Mow, C. C., and Pao, Y. H., "The Diffraction of Elastic Waves and Dynamic Stress Concentrations," Rand Corp., R-482-PR, April, 1971.

6. Abramowitz, M. and Stegun, I. A., Handbook of Mathematical Functions, Dover, 1965.

7. Nayfeh, A. H., Perturbation Methods, Wiley, 1973.

8. Langer, R. E., "The Solutions of the Mathieu Equation with a Complex Variable and at Least One Parameter Large," Transac. Amer. Math. Soc., 36 (1934), pp 637-695.

9. Roberts, S. B., "The Eigenvalue Problem for Two Dimensional Regions with Irregular Boundaries," J. App. Mech., Vol. 34, No. 3, Sept., 1967, pp 618-621, series E.

10. Lin, C. C., "On a Perturbation Theory Based on the Method of Characteristics," J. of Math. & Phy., Vol. 33, July, 1954, pp 117-134.

11. Segal, L. A., "Application of Conformal Mapping to Boundary Perturbation Problems for the Membrane Equation," Archive for Rat. Mech. and Anal., Vol. 8, No. 3, 1961, pp 228-237.

12. Wilkinson, J. H., The Algebraic Eigenvalue Problem, Clarendon Press, 1965.

13. Wilkinson, J. H., "The Calculation of the Eigenvectors of Codiagonal Matrices," Computer J., Vol. 1, pp 90-96, (1958).

14. Wilkinson, J. H., "The Calculation of Eigenvectors by the Method of Lanczo," Computer J., Vol. 1, (1958), pp 148-152.

15. Van Ness, J. E., "Inverse Iteration Method for Finding Eigenvectors," IEEE Trans. Auto. Control, Feb. 1969, pp 63-66.

16. Parlett, B., "The Development and Use of Methods of LR Type," SIAM Rev., 1964, Vol. 6, pp 275-295.

17. Ralston, A., A First Course in Numerical Analysis, McGraw-Hill, 1965.

18. Lanczos, C., "An Iteration Method for the Solution of the Eigenvalue Problem of Linear Differential and Integral Operators," Journal of Research of the National Bureau of Standards, Vol. 45, p 255.

19. Meirovitch, L., Analytical Methods in Vibrations, 1971, The Macmillan Co.

20. Fung, Y. C., Foundations of Solid Mechanics, Prentice-Hall, 1965.

21. Dally, J. W., and Riley, W. F., Experimental Stress Analysis, McGraw-Hill, 1965.

22. Viktorov, I. A., "Rayleigh-Type Waves on a Cylindrical Surface," Soviet Physics Acoustics, V. 4, 1958, pp 131-136.

23. Rinehart, J. S., and Pearson, J., Behavior of Metals Under Impulsive Loads, American Soc. for Metals, 1954; Dover, 1965.

24. Kolsky, H. Stress Waves in Solids, Oxford Univ. Press, 1953.

25. Goodier, J. N., and Bishop, R. E. D., "A Note on Critical Reflections of Elastic Waves at Free Surfaces," J. of App. Phy., Vol. 23, No. 1, Jan., 1952, pp 124-126.

26. McNiven, H. D., and Mengi, Y., "Critical Angles Associated with the Reflection-Refraction of Elastic Waves at an Interface," The J. Acoust. Soc. of Am., Vol. 44, No. 6, May, 1968, pp 1658-1663.

27. Fu, C. Y., "Studies on Seismic Waves: I. Reflection and Refraction of Plane Waves," Geophysics, Vol. XI, No. 1, Jan., 1946, pp 1-9.

28. Henneke, E. G., II, "Reflection-Refraction of a Stress Wave at a Plane Boundary Between Anisotropic Media," J. Acous. Soc. of Am., Vol. 51, No. 1 (Part 2), 1972, pp 210-217.

29. Ewing, E., Jardetzry, W. S., and Press, F., Elastic Waves in Layered Media, McGraw-Hill (1957).

CHAPTER 4

SUMMARY OF RESULTS AND CONCLUSIONS

Table of Contents

4.1 Observations and Objectives

This thesis was motivated by the observation that microcracks[1] appear in the neighborhood of a main crack and that solutions of the wave equation are capable (see page 1) of exhibiting concentrations which would cause fatigue and perhaps nucleate the microcracks. Furthermore, the coalescence of microcracks is one mechanism of crack propagation; and the mathematics here plays the role of homogeneous solutions in the study of unsteady crack propagation which involves nonhomogeneous wave equations. The nonhomogeneous terms come from differentiating the superimposed static solution with respect to time.

The objectives of this thesis were to investigate the possibility that continuum mechanics could predict the origin of the microcracks and as a necessary preliminary to the study of unsteady crack propagation. In this respect it is important to note that the eigenvalue is inversely proportional to the semi-major axis which would be a function of time for the unsteady problem.

---

[1]Pictures from Freudenthal, Chapter 1, [3] show that the microcracks tend to be equally spaced. This suggests a rational rather than random cause.

4.2 New Techniques

The method of the Dual Pair (Chapter 2) enables an investigation into the possible existence of solutions having mixed boundary conditions. This application of the technique apparently has not been attempted before and shows that eigensolutions do exist. The application of the theory of integral equations suggests the type of wave functions (see page 30) in which to construct an analytical solution and assess further properties; in particular, the behavior at infinity.

The method of Generalized Separation of Variables (Chapter 3) enables a representation of the solution of the wave equation appropriate for boundary conditions on an ellipse provided the eccentricity is not large. This is a new technique which permits a single representation of all order perturbations in the eccentricity parameter and leads to a system of simultaneous equations nonlinear in both eigenvalue and eccentricity parameter.

Numerical techniques were developed for the solution of generalized eigenvalue problems which are nonlinear in the eigenvalue and tend to have nearly repeated eigenvalues (see pages 89, 96, 99).

4.3 New Results

The results of Viktorov are extended to include a simple formula (page 50) for the second order term in the expansion of the eigenvalue for Rayleigh type waves on the surface of a cylindrical cavity. The location of the turning points are found and it is shown that only for Rayleigh type eigenvalues do turning points not occur and then only for the interior problem (pages 51, 52). The five smallest eigenvalues are plotted (page 53) vs. N and it is shown that the Rayleigh type root is the fundamental. Also, there are a few eigenvalues, which as a function of N, tend to be repeated.

Perturbation methods were applied numerically to obtain a third order solution in the eccentricity parameter m. It was found that the eigenvalue is slowly varying in m but the eigenvector is fast varying in m (see graphs on pages 100, 102, and equations page 70). It is shown that the loss of machine precision prevents carrying the perturbation solution to higher orders.

Numerical procedures for the solution of generalized eigenvalue problems for large m were discussed for the case in which the roots tend to be nearly repeated. See page 77 for properties of the coefficient matrix.

It was argued that any of a number of methods can be used to calculate the eigenvalue. However, the calculation of the eigenvector presents special problems since the tendency is to have nearly repeated eigenvalues which preclude the utility of several well known methods. Of the methods studied it is shown that the iterative use of

Gauss-Jordan reduction (page 99) followed by a modification of the Lanczos method (page 89) is best suited for the determination of both eigenvalue and eigenvector. As a bonus, a precise criterion (page 96) of the solvability and rank is provided as a function of machine precision. The advantages of this modification of the Lanczos method are stated on page 91.

The case $m \to 1$ presents special problems which are discussed on pages 73, 74.

By proper reinterpretation of the mapping function (page 41) and the range on ξ the solution for the regions interior and exterior to the elliptical boundary can be obtained simultaneously. It was then found that the eigenvalue is continuous at $m = 1$ which tends to support the conclusion (page 101) that $\gamma(m) = \frac{1}{m}\gamma\left(\frac{1}{m}\right)$.

By observing the symmetry of the differential operators (page 47) the solution for Mode II in which:

$$\phi = \text{odd in both } x,y$$

$$\psi = \text{even in both } x,y$$

can be obtained from the Mode I computer programs by letting

$$\delta \leftarrow \frac{1}{\delta}$$

$$\gamma \leftarrow \sqrt{\delta}\,\gamma$$

$$\phi \leftrightarrow \psi$$

Contour curves of stresses, invariant quantities, and displacements for the case of a circular boundary are presented and certain

features pointed out. In particular, it is shown why the principal directions can be discontinuous at isotropic points (page 113, 114). This is used as an elementary example to demonstrate that in the solution of

$$[G\{m,\gamma(m)\}]\ \{V(m)\} = 0$$

in which G is analytic in both m and γ that $\{V(m)\}$ can be discontinuous as a function of m if the eigenvalues are repeated (page 66). This explains the difficulty in computing the eigenvector for large m.

Contour curves of the dilatational stress (pages 137-147) are presented for several values of eccentricity parameter. The curves show finite stress concentrations away from the boundary. For the case of a circular boundary the stress concentrations can be related quite simply to the properties of the Bessel functions (page 112). This substantiates our initial observations (page 1). For the case of an elliptical boundary a simple correlation of the location of the stress concentrations to the mathematics is not available. The location, orientation, and shape of the dilatational stress concentrations for $m > 0$ agree qualitatively with photographs [1.3] of microcracks in solid propellant.

Results pertinent to experimental verification are summarized on pages 133,5.

4.4 Conclusions

It is concluded that standing waves whose wave length is the same order of magnitude as the semi-major axis could theoretically cause microcracks in materials that fail in tension.

The method of separation of variables is computationally inefficient for large eccentricity.

4.5 Suggested Further Work

1. The study of the perturbed circle boundary is incomplete with respect to N (the angular periodicity) and the eigenvector. Special attention should be given to the possibility of branching (page 75).

2. The case of a slit has not been solved satisfactorily. This could be accomplished by

   a. evaluating the integral (page 30) suggested by the Dual Pair
   b. considering the degenerate case (page 73) of generalized separation of variables
   c. use elements of the theory of Muskhelishivi and Vekua to obtain a representation in terms of Volterra integral equations (appendix).
   d. constructing approximate analytic solutions for large eigenvalues by the methods of C. C. Lin [3.10], Segal [3.11], and Nayfeh [3.7].

3. The results for Mode II could be obtained easily (see page 156), and might yield shear concentrations.

4. Experimental verification should be attempted.

5. Investigate unsteady fracture as a nonhomogeneous wave problem in which the homogeneous solution is now known.

6. Investigate how knowledge of these waves can influence the design of engineering materials so as to avoid microcracks, and in geophysical exploration to generate underground fractures.

4.6 Comments

The results of this thesis are interpreted as an explanation of the origin of microcracks. However, there may be other explanations. It is hoped that the reader will form his own conclusions and be cautious not to perpetuate any possible fallacies or incorrect conclusions. To this end it is important to distinguish between fact and fiction: between results, intepretations, conclusions, and conjectures. Each of these is important in judging the evidence and as a clue to suggest new areas of research.

Some of the main results and conclusions of this thesis are the questions which are raised (rather than answered), and the mathematical developments capable of answering some--but not all--of these questions. In particular, unsteady crack growth is an area in which little is known.

APPENDIX A

In this appendix it is shown that the problem (in-plane vibration) can be reduced to an integral equation analogous to the Muskhelishvili boundary value problem [1].

The advantages of this approach are:

i) the formulation is valid for arbitrary plane multiple connected regions

ii) the kernel of the integral equation is continuous

iii) an asymptotic expansion for large eigenvalues can easily be constructed

iv) for the case of an elliptic boundary the use of Cauchy integrals and the properties of the conformal mapping function greatly simplify the formulation [2, pp. 312, 313].

The disadvantages are:

i) the remote boundary condition is not automatically satisfied and must be included in a numerical solution

ii) by the nature of the formulation it is difficult to deduce or compute some properties of the solution

iii) integration of the kernel is required

For the case of an elliptic boundary, the disadvantages seemed to outweigh the advantages as compared to the method of Generalized Separation of Variables. Numerical solution was therefore not attempted. However this method is still of interest for application to general boundaries and for some of the properties of the formulation.

The analysis, here, is similar to that of I. N. Vekua [3] and P. N. Vekua [4] but differs in the following:

i) symmetry conditions

ii) the analysis is applied to elliptic boundaries

iii) employs dependent variables suggested by the elasticity of the problem rather than generalized B.V.P. (otherwise, the system tends not to be of the normal type, (see [4])).

iv) it is observed that the singular part of the solution is an exact differential.

1. Problem Statement

In terms of the complex variables:

$Z = X + iY$ $\quad$ (X,Y) = Cartesian coordinates

$\Phi = \phi + i\psi$ = Complex potential

$U = u + iv$ = Complex displacement
$(u, v) = (X, Y)$
components of
displacement

$= 2 \frac{\partial \overline{\Phi}}{\partial \overline{Z}}$

The equations governing in-plane vibration can be written quite concisely as:

a. Field Equations: $[\nabla^2 + \delta\gamma^2]\phi = 0$

$$[\nabla^2 + \gamma^2]\psi = 0$$

b. Boundary Conditions:

$$\frac{\partial^2 \phi}{\partial Z^2} \frac{dZ}{ds} + \frac{1 - \delta}{4} \gamma^2 \phi \frac{d\overline{Z}}{ds} = 0 \text{ on } S \qquad (1)$$

where $\delta = (C_2/C_1)^2$; $C_{1,2}$ = wave speeds

$= \frac{1 - 2\nu}{2 - 2\nu}$; ν = Poisson's ratio

γ = eigenvalue to be determined

ds = differential arc length

S = union of all boundaries

By analogy with fluid mechanics: ϕ = velocity potential

ψ = stream function

c. Symmetry Conditions

The symmetry conditions for Mode I displacements

$$u(X,Y) = u(X,-Y) = -u(-X,Y)$$

$$v(X,Y) = -v(X,-Y) = v(-X,Y)$$

can be expressed compactly by

$$\overline{\Phi}[\pm Z, \pm\overline{Z}] = \Phi[Z,\overline{Z}]$$

using the notation [5, p. 94].

2. Derive Boundary Condition as Line Integral

It is not necessary, but may be instructive to derive the boundary condition as a line integral of the surface traction since the dominant part of the boundary condition turns out to be an exact differential.

This derivation follows [2, p. 270] with the exception that

$$U = u + iv$$

is the complex displacement, and not the Airy stress function. Define

$$f(t) = i \int_{to}^{t} [T_1 + i\, T_2]\, ds \qquad (3)$$

where s = arc length

$T_{1,2}$ = Cartesian components of the stress tensor

t = boundary value of $Z = X + iY$

Substituting $T_\alpha = \sigma_{\alpha\beta}\, n^\beta \quad ; \quad \alpha,\beta = 1,2$

$$\sigma_{\alpha\beta} = 2\mu\, \varepsilon_{\alpha\beta} + \lambda\Delta\delta_{\alpha\beta}$$

$$n^1 = \cos(X^1, n) = \frac{dX^2}{ds}$$

$$n^2 = \cos(X^2, n) = -\frac{dX^1}{ds}$$

into (3) gives

$$f(t) = i\mu \int_{to}^{t} \left[-2\, \frac{\partial U}{\partial \bar{Z}}\, \frac{d\bar{Z}}{ds} + \frac{1-\delta}{\delta}\, D\, \frac{dZ}{ds}\right] ds \tag{4}$$

Substituting $U = 2\, \frac{\partial \bar{\Phi}}{\partial \bar{Z}}$

$$\Delta = \nabla^2\phi = -\delta\gamma^2\phi$$

into (4) gives

$$f(t) = -4i\mu \int_{to}^{t} \left[\frac{\partial^2 \bar{\phi}}{\partial \bar{Z}^2}\, \frac{d\bar{Z}}{ds} + \frac{1-\delta}{4}\, \gamma^2\phi\, \frac{dZ}{ds}\right] ds \tag{5}$$

We observe that the integrand of (5) is the same as the complex conjugate of (1). The utility of the integrated form is that the dominant part (most singular) is a total derivative. To see this, integrate the field equation:

$$\nabla^2\Phi = -\gamma^2[\alpha\Phi - \beta\bar{\Phi}] \tag{6}$$

where $\alpha = (1+\delta)/2$

$\beta \quad (1-\delta)/2$

to get

$$\Phi(Z,\bar{Z}) = \bar{\Phi}_1(\bar{Z}) + \Phi_2(Z)$$

$$- \varepsilon Z \int_{Z_0}^{\bar{Z}} [\alpha\bar{\Phi}_1(t) - \beta\bar{\Phi}_2(t)]dt$$

$$- \varepsilon\bar{Z} \int_{Z_0}^{Z} [\alpha\Phi_2(t) - \beta\Phi_1(t)]dt + O(\varepsilon^2) \qquad (7)$$

where $\varepsilon = \gamma^2/4$

Z_0 = reference point in the region

$\Phi_{1,2}$ are two arbitrary analytic functions

By substitution of (7) into (5) one obtains

$$f(t) = -4i\mu \int_{t_o}^{t} [\{\bar{\Phi}_2''(\bar{Z}) - \varepsilon\bar{\Phi}_2'(\bar{Z}) + \varepsilon\beta Z\bar{G}''(\bar{Z})\} \frac{d\bar{Z}}{ds}$$

$$+ \beta\varepsilon\{\bar{G}'(\bar{Z}) + G'(Z)\} \frac{dZ}{ds} + O(\varepsilon^2)]ds$$

where $G'(Z) \equiv \Phi_1(Z) + \Phi_2(Z)$

Noting that the combination

$$Z\,\bar{G}''(\bar{Z})d\bar{Z} + \bar{G}'(\bar{Z})dZ = d[Z\bar{G}'(\bar{Z})]$$

is a total derivative.

We obtain

$$f(t) = -4i\mu[\overline{\Phi}_2'(\overline{Z}) + \varepsilon\beta\{Z\overline{G}(\overline{Z}) + G(Z)\}$$

$$- \varepsilon\overline{\Phi}_2(\overline{Z}) + O(\varepsilon^2)]\Big|_{Z=t_o}^{t}$$

Now $\overline{U} = 2\frac{\partial\Phi}{\partial\overline{Z}}$

and $\phi = \overline{G}' - \overline{\Phi}_2 + \Phi_2 + O(\varepsilon)$

Hence $\overline{U} = 2\Phi_2' + O(\varepsilon)$

From elasticity we have the requirement that the wave solution must be superimposed on any static solution. Hence, a zero eigenvalue must correspond to only a trivial (rigid body motion) solution, and

$$\lim_{\varepsilon \to 0} U(Z,\overline{Z};\varepsilon) = 0$$

This suggests letting

$$\phi_2'(Z) \equiv \varepsilon\beta H(Z)$$

which then gives

$$\frac{f(t)}{-4i\mu\varepsilon\beta} = G(t) + t\,\overline{G}'(\overline{t}) + \overline{H}(\overline{t})$$

$$+ O\left(\frac{\varepsilon}{1-\delta}\right)$$

$$+ \text{arbitrary constant} \qquad (8)$$

The parameter $\delta \equiv (C_2/C_1)^2 = \frac{\mu}{\lambda + 2\mu} = \frac{1 - 2\nu}{2 - 2\nu}$

is restricted to the range: $0 \leq \delta < \frac{1}{3}$

on physical grounds if: $\frac{1}{4} < \nu \leq \frac{1}{2}$

We thus have the result that the representation (7) and the substitutions:

$$\Phi_1(Z) = - \Phi_2(Z) + G'(Z)$$

$$\Phi_2(Z) = \varepsilon\beta \, H(Z)$$

result in a boundary value problem which is of the Muskhelishvili type [1]:

$$G(t) + t \, \overline{G}'(\overline{t}) + \overline{H}(\overline{t}) = \varepsilon F(t;\varepsilon) \qquad (9)$$

where: $F(t;\varepsilon)$ is due to the higher order terms in the field equation. It is noted that the problem is nonlinear in the eigenvalue $\varepsilon \equiv \gamma^2/4$ and will require iteration of a technique which solves the linearized problem.

There are several techniques available for the solution of (9) for an assumed value of ε. For general boundaries, use the method of Sherman [2, p. 314]. For the case of a region exterior to an elliptical boundary, considerable simplification results by applying the technique in [2, p. 292]. Defining

$$Z = \hat{R} \left[\frac{1}{\zeta} + m\zeta\right] \qquad \text{(mapping function)}$$

$$g(\zeta) = G(Z(\zeta))$$

$$h(\zeta) = H(Z(\zeta))$$

$$f(\sigma) = F(t(\sigma);\varepsilon) \quad ; \quad \sigma = \text{boundary value of } \zeta$$

results in

$$g(\zeta) = \frac{\varepsilon\zeta}{2\pi i}\int_C \frac{f(\sigma)}{\sigma(\sigma - \zeta)}\, d\sigma \tag{10}$$

$$h(\zeta) = \frac{\varepsilon\zeta(\zeta^2 + m)}{1 - m\zeta^2}\, g'(\zeta) + \frac{\varepsilon}{2\pi i}\int_C \frac{\sigma}{\sigma - \zeta}\, d\sigma \tag{11}$$

where C = unit circle $|\sigma| = 1$

$g'(\pm 1) = 0$ if $m = 1$.

Since: $f(\sigma)$ is of the form:

$$f(\sigma) = i\int_{\sigma_o}^{\sigma} S(\sigma)\sqrt{w'(\sigma)\bar{w}'(\sigma)}\, d\sigma$$

The interchange of the order of integration gives on the boundary $\zeta = e^{i\eta}$, $\xi = 1$

$$g(e^{i\eta}) = \frac{\varepsilon e^{i\eta}}{2\pi}\int_o^{2\pi} (\eta - \theta)\, S(e^{i\theta})\sqrt{w'\bar{w}'}\, d\theta$$

Since $S(\sigma)$ is linear in $g(\sigma)$ and $h(\sigma)$, the kernel of the integral equation is continuous. It is concluded that a solution procedure has been presented which reduces the exterior ellipse problem to the solution of an integral equation having a continuous kernel.

It now remains to include the higher order terms in the wave equation. These terms will then specify $f(\sigma)$ and $S(\sigma)$.

3. Represent Solution to Wave Equation by Fractional Integrals

In the last section an approximate representation (7) of the solution of the field equation (6) was employed in order to demonstrate a solution procedure.

In this section an exact representation of the solution of (6.) is employed in order to specify $F(t)$, $f(\sigma)$, and $S(\sigma)$ and thereby enable a solution to be obtained.

Following I. N. Vekua [3, p. 57] the solution of the reduced wave equation

$$[\nabla^2 + \lambda^2]\phi = 0$$

can be expressed by

$$\phi(Z,\bar{Z}) = \phi_0(Z) - \int_{Z_0}^{Z} \phi_0(t) \frac{\partial}{\partial t} J_0\{\lambda\sqrt{\bar{Z}(Z - t)}\}dt$$

where $\phi_0(Z)$ is analytic in the region

Z_0 is any reference point in the region

This representation does not automatically satisfy our symmetry conditions. However, it can be modified. As an example which automatically satisfies the symmetry conditions, we will take

$$\Phi(Z,\overline{Z}) = \overline{\Phi}_1(\overline{Z}) + \Phi_2(Z)$$

$$+ \frac{1}{2} \sum_{j=1}^{2} \sum_{n=1} (-1)^n \varepsilon^n \left[\frac{Z^n}{n!} \int_{\overline{Z}_j}^{\overline{Z}} \frac{\{\overline{Z} - t\}^{n-1}}{(n-1)!} \{a_n \Phi_1(t)\right.$$

$$\left. - b_n \overline{\Phi}_2(t)\} dt + \frac{\overline{Z}^n}{n!} \int_{Z_j}^{Z} \frac{\{Z - t\}^{n-1}}{(n-1)!} \{a_n \Phi_2(t)\right.$$

$$\left. - b_n \Phi_1(t)\} dt \right] \qquad (12)$$

where $\varepsilon = \gamma^2/4$

$$a_n = \frac{1 + \delta^n}{2} \quad ; \quad b_n = \frac{1 - \delta^n}{2}$$

$\phi_k(Z)$ = analytic in D ; $k = 1,2$

The j-summation provides the proper symmetry provided

$$\overline{\phi}_k[\pm Z] = \phi_k[Z] \quad ; \quad k = 1,2$$

$$Z_1 = -Z_2 = \text{real constant}$$

It can be shown that:

$$\Phi = \phi + i\psi$$

$$[\nabla^2 + \delta\gamma^2]\phi = 0 \quad ; \quad [\nabla^2 + \gamma^2]\psi = 0$$

or what is equivalent, that Φ satisfies (6)

Using $\Phi_1 = -\Phi_2 + G'$

$$\Phi_2' = \varepsilon\, b_1\, H \quad ; \quad \Phi_2(Z) = \varepsilon\, b_1 \int_{Z_o}^{Z} H(\alpha)d\alpha$$

and substituting (12) into (5) gives:

$$G(t) + t\,\bar{G}'(\bar{t}) + \bar{H}(\bar{t}) = \varepsilon F(t;\varepsilon)$$

where: $$F(t) = \int_{t_o}^{t} S(Z(s), \bar{Z}(s))ds$$

and:

$$S = Z\,\overline{H(Z)}\,\frac{d\bar{Z}}{ds} + \frac{Z^2}{2}\left[(1+\delta)\overline{G'(Z)} - \varepsilon\int_{Z_o}^{Z}\bar{H}(\alpha)d\alpha\right]\frac{d\bar{Z}}{ds}$$

$$+ \frac{dZ}{ds}\sum_{j=1}^{2}\delta\,\mathrm{Re}\left[\bar{Z}\int_{Z_j}^{Z}\frac{2\,J_1\{\gamma\sqrt{\delta\bar{Z}(Z-t)}\}}{\gamma\sqrt{\delta\bar{Z}(Z-t)}}\,G'(t)dt\right]$$

$$+ \frac{\gamma}{4}\frac{d\bar{Z}}{ds}\sum_{j=1}^{2}\int_{Z_j}^{Z}\left\{\frac{Z-t}{\bar{Z}}\right\}^{1/2}J_1\{\gamma\sqrt{\bar{Z}(Z-t)}\}\int_{Z_o}^{t}H(\tau)d\tau dt$$

$$+ \gamma\sum_{j=1}^{2}\int_{\bar{Z}_j}^{\bar{Z}}\left\{\frac{Z}{\bar{Z}-t}\right\}^{3/2}J_3\{\gamma\sqrt{Z(\bar{Z}-t)}\}\int_{\bar{Z}_o}^{t}\bar{H}(\tau)d\tau dt$$

$$- \frac{1}{(1-\delta)\gamma}\frac{d\bar{Z}}{ds}\sum_{j=1}^{2}\int_{Z_j}^{Z}\left\{\frac{Z-t}{\bar{Z}}\right\}^{1/2}\left[J_1\{\gamma\sqrt{\bar{Z}(Z-t)}\}\right.$$

$$\left. + \delta^{3/2}\,J_1\{\gamma\sqrt{\delta\bar{Z}(Z-t)}\}\right]G'(t)dt$$

$$+ \frac{1}{(1-\delta)\gamma}\frac{d\bar{Z}}{ds}\sum_{j=1}^{2}\int_{\bar{Z}_j}^{\bar{Z}}\left\{\frac{Z}{\bar{Z}-t}\right\}^{3/2}\left[J_3\{\gamma\sqrt{Z(\bar{Z}-t)}\}\right.$$

$$+ \delta^{3/2} J_3\{\gamma\sqrt{\delta Z(\bar{Z} - t)}\}]\bar{G}'(t)dt$$

This lengthy formula discouraged further efforts by this method. It is of interest to note that

$$S = Z \bar{H} \frac{d\bar{Z}}{ds} + \frac{1 + \delta}{2} Z^2 \bar{G}' \frac{d\bar{Z}}{ds}$$

$$+ 2\delta \frac{dZ}{ds} \mathrm{Re}[\bar{Z} G]$$

$$- \frac{1 + \delta^2}{1 - \delta} \frac{d\bar{Z}}{ds} \sqrt{\bar{Z}} \sum_{j=1}^{2} \int_{Z_j}^{Z} (Z - t)^{3/2} G'(t)dt$$

$$+ O(\varepsilon) .$$

This simplification might be useful for the investigation of creeping waves, i.e., low frequency.

Appendix A Literature Cited

1. Muskhelishvili, N. I., Some Basic Problems of the Mathematical Theory of Elasticity, Noordhoff, 1963.

2. Sokolnikoff, I. S., Mathematical Theory of Elasticity, McGraw-Hill, 1956.

3. Vekua, I. N., New Methods for Solving Elliptic Equations, North-Holland, 1967.

4. Vekua, N. P., Systems of Singular Integral Equations, Noordhoff, 1967.

5. Muskhelishvili, N. I., Singular Integral Equations, Noordhoff, 1946.

6. Sneddon, I. N., Mixed Boundary Value Problems in Potential Theory, Interscience, 1966.

LITERATURE CITED

Chapter 1

1. Van Elst, H. C., "The Intermittent Propagation of Brittle Fracture," Personal Communication, Dynamic Crack Conf., Lehigh Univ., July, 1972.

2. Dvorak, G. J., Dynamic Crack Conf., Lehigh Univ., July, 1972.

3. Freudenthal, A. M., Columbia Univ. Tech. Report No. 28, June, 1965, Figures 2a, b.

4. Koterazawa, R., et al., "Fractographic Study of Fatigue Crack Propagation," ASME J. Eng. Mat. & Tech., Vol. 95, Series H, No. 4, Oct., 1973.

5. Born, M., and Wolf, E., Principles of Optics, Pergamon, 1970.

6. Fung, Y. C., Foundations of Solid Mechanics, Prentice-Hall, 1965.

7. Sokolnikoff, I. S., Mathematical Theory of Elasticity, Noordhoff, 1963.

8. Viktorov, I. A., "Rayleigh-Type Waves on a Cylindrical Surface," Soviet Physics Acoustics, V. 4, 1958, pp. 131-136.

Chapter 2

1. Fung, Y. C., Foundations of Solid Mechanics, Prentice-Hall, 1965.

2. Ewing, E., Jardetzky, W. S., and Press, F., Elastic Waves in Layered Media, McGraw-Hill (1957).

3. Yoffe , E. H., "The Moving Griffith Crack," Phil. Mag., 42, 739 (1951).

4. Sternberg, E. and Eubanks, R. A., "On Stress Functions for Elastokinetics and the Integration of the Repeated Wave Equation," Q. J. App. Math., 15 (1957) 149-153.

5. Mow, C. C., and Pao, Y. H., "The Diffraction of Elastic Waves and Dynamic Stress Concentrations," Rand Corp., R-482-PR, April, 1971.

6. Born, M. and Wolf, E., Principles of Optics, Pergamon, 1970.

7. Sommerfeld, A., Optics, Academic Press, 1967.

8. Smirnov, V. I., A Course of Higher Mathematics, Vol. IV, p 680, Addison Wesley, 1964.

9. Kleinman, R. E., and Roach, G. F., "Boundary Integral Equations for the Three-Dimensional Helmholtz Equation," SIAM Review, Vol. 16, No. 2, April, 1974, p 214.

10. Kelvin, Popular Lectures, Vol. I, Macmillan, 1891.

11. Musgrave, M. J. P., Crystal Acoustics, Holden-Day, 1970.

12. Born, M., and Huang, K., Dynamical Theory of Crystal Lattices, Oxford, 1954.

13. Titchmarsh, E. C., Theory of Fourier Integrals, Oxford, 1937.

14. Busbridge, I. W., "Dual Integral Equations," Proc. London Math. Soc., 44 (1938), 115.

15. Tranter, C. J., Integral Transforms in Mathematical Physics, Methuen & Co., 1951.

16. Williams, W. E., "The Reduction of Boundary Value Problems to Fredholm Integral Equations of the Second Kind," ZAMP, Vol. XIII, 1962, pp 133, 151.

17. Roberts, J. A., "Approximate Methods for the Solution of Certain Dual Fourier-Bessel Series Relations," North Carlina State Univ., Ph.D. Thesis, 1964; Univ. Microfilms, Ann Arbor, Mich., 65-2825.

18. Fichter, W., "Some Solutions for a Narrow Plate Containing a Central Longitudinal Crack," M. S. Thesis, V.P.I., 1966.

19. Hartranft, R. J. and Sih, G. C., "An Approx. Three-Dimensional Theory of Plates with an Application to Crack Problems," Lehigh Univ., 1972, unpublished.

20. Sneddon, I. N., Mixed Boundary Value Problems in Potential Theory, Interscience, 1966.

21. Tranter, C. J., "A Further Note on Dual Integral Equations and an Application to the Diffraction of Electromagnetic Waves," Q. J. Mech. and App. Math., Vol. VII, p 3 (1954).

22. Magnus, W. and Oberhettinger, F., "Formula and Theorems for the Functions of Mathematical Physics," Chelsea, 1949.

23. Watson, G. N., Theory of Bessel Functions.

24. Gray, A., Mathews and MacRobert, Bessel Functions, Macmillan & Co. (1931).

25. Tamarkin, J. D., "On Fredholm's Integral Equations Whose Kernel Are Analytic in a Parameter," Ann. of Math. 28 (1927), pp 122-152.

26. Filon, "On a Quadrature Formula for Trigonometric Integrals," Proc. Royal Soc. of Edinburgh, Vol. 49 (1928), pp 38-47.

27. Cochran, J., Analysis of Linear Integral Equations, McGraw-Hill, 1972.

28. Lovitt, W. V., Linear Integral Equations, Dover, 1950.

29. Kerkhof, F., Personal communication, Dynamic Crack Conf., July, 1972, Lehigh Univ.

30. Irwin, G. R., "Fracture Mechanics," Proc. First Symp. on Navel Struc. Mech., Pergamon, 1960.

31. Kolsky, H. and Rader, D., "Stress Waves and Fracture," Fracture, Vol. 1, Chap. 9, Academic Press, 1969.

32. Broberg, B., "On the Speed of a Brittle Crack," J. App. Mech., p 546, Sept., 1964.

33. Sih, G. C., "Dynamic Aspects of Crack Propagation," Inelastic Behavior of Solids, pp 607-639.

34. Mott, N. F., Engineering, Vol. 165, p 16, 1948.

35. Roberts, D. K., and Wells, A. A., "The Velocity of Brittle Fracture," Engineering, Vol. 178, p 820, 1954.

Chapter 3

1. Love, A. E. H., A Treatise on the Mathematical Theory of Elasticity, 1927.

2. Sokolnikoff, I. S., Mathematical Theory of Elasticity, McGraw-Hill, 1965.

3. Watson, G. N., A Treatise on the Theory of Bessel Functions, Cambridge, 1922.

4. Whittaker, E. T., and Watson, G. N., A Course of Modern Analysis, Cambridge Univ. Press, 1969.

5. Mow, C. C., and Pao, Y. H., "The Diffraction of Elastic Waves and Dynamic Stress Concentrations," Rand Corp., R-482-PR, April, 1971.

6. Abramowitz, M. and Stegun, I. A., Handbook of Mathematical Functions, Dover, 1965.

7. Nayfeh, A. H., Perturbation Methods, Wiley, 1973.

8. Langer, R. E., "The Solutions of the Mathieu Equation with a Complex Variable and at Least One Parameter Large," Transac. Amer. Math. Soc., 36 (1934), pp 637-695.

9. Roberts, S. B., "The Eigenvalue Problem for Two Dimensional Regions with Irregular Boundaries," J. App. Mech., Vol. 34, No. 3, Sept., 1967, pp 618-621, series E.

10. Lin, C. C., "On a Perturbation Theory Based on the Method of Characteristics," J. of Math. & Phy., Vol. 33, July, 1954, pp 117-134.

11. Segal, L. A., "Application of Conformal Mapping to Boundary Perturbation Problems for the Membrane Equation," Archive for Rat. Mech. and Anal., Vol. 8, No. 3, 1961, pp 228-237.

12. Wilkinson, J. H., The Algebraic Eigenvalue Problem, Clarendon Press, 1965.

13. Wilkinson, J. H., "The Calculation of the Eigenvectors of Codiagonal Matrices," Computer J., Vol. 1, pp 90-96, (1958).

14. Wilkinson, J. H., "The Calculation of Eigenvectors by the Method of Lanczo," Computer J., Vol. 1, (1958), pp 148-152.

15. Van Ness, J. E., "Inverse Iteration Method for Finding Eigenvectors," IEEE Trans. Auto. Control, Feb. 1969, pp 63-66.

16. Parlett, B., "The Development and Use of Methods of LR Type," SIAM Rev., 1964, Vol. 6, pp 275-295.

17. Ralston, A., A First Course in Numerical Analysis, McGraw-Hill, 1965.

18. Lanczos, C., "An Iteration Method for the Solution of the Eigenvalue Problem of Linear Differential and Integral Operators," Journal of Research of the National Bureau of Standards, Vol. 45, p 255.

19. Meirovitch, L., Analytical Methods in Vibrations, 1971, The Macmillan Co.

20. Fung, Y. C., Foundations of Solid Mechanics, Prentice-Hall, 1965.

21. Dally, J. W., and Riley, W. F., Experimental Stress Analysis, McGraw-Hill, 1965.

22. Viktorov, I. A., "Rayleigh-Type Waves on a Cylindrical Surface," Soviet Physics Acoustics, V. 4, 1958, pp 131-136.

23. Rinehart, J. S., and Pearson, J., Behavior of Metals Under Impulsive Loads, American Soc. for Metals, 1954; Dover, 1965.

24. Kolsky, H. Stress Waves in Solids, Oxford Univ. Press, 1953.

25. Goodier, J. N., and Bishop, R. E. D., "A Note on Critical Reflections of Elastic Waves at Free Surfaces," J. of App. Phy., Vol. 23, No. 1, Jan., 1952, pp 124-126.

26. McNiven, H. D., and Mengi, Y., "Critical Angles Associated with the Reflection-Refraction of Elastic Waves at an Interface," The J. Acoust. Soc. of Am., Vol. 44, No. 6, May, 1968, pp 1658-1663.

27. Fu, C. Y., "Studies on Seismic Waves: I. Reflection and Refraction of Plane Waves," Geophysics, Vol. XI, No. 1, Jan., 1946, pp 1-9.

28. Henneke, E. G., II, "Reflection-Refraction of a Stress Wave at a Plane Boundary Between Anisotropic Media," J. Acous. Soc. of Am., Vol. 51, No. 1 (Part 2), 1972, pp 210-217.

29. Ewing, E., Jardetzry, W. S., and Press, F., Elastic Waves in Layered Media, McGraw-Hill (1957).

IN-PLANE VIBRATION OF A PLATE HAVING AN ELLIPTICAL HOLE OF ARBITRARY ECCENTRICITY

by

Robert F. Cooke

(ABSTRACT)

The in-plane vibration of a plate with an elliptic hole is studied. It is shown that standing waves whose wave length is the same order of magnitude as the size of the hole are theoretically capable of causing microcracks which have been observed experimentally.

Several approaches were used including reduction of the mixed boundary value problem to a Fredholm equation, and to a matrix eigenvalue problem. Contour curves of various stresses and displacements were obtained numerically.

A new technique was developed for the solution of the wave equation appropriate for boundary conditions on an elliptical surface.